Pharmacometrics of dolutegravir and tenofovir: A quantitative approach to characterise drug-drug interactions, pharmacogenetics and optimise treatment

by

Aida Nakayiwa Kawuma

A Thesis Presented for the Degree of

DOCTOR OF PHILOSOPHY

in the Division of Clinical Pharmacology

Department of Medicine

UNIVERSITY OF CAPE TOWN

January 2023

Primary supervisor: A/Professor Paolo Denti

1st Co-supervisor: Doctor Roeland E. Wasmann

2nd Co-supervisor: Professor Gary Maartens

Contributions to the field

This thesis includes some of the following contributions to the field of pharmacometrics and clinical pharmacology.

Full-length original articles

1. **Kawuma, A.N.**, Walimbwa, S.I., Pillai, G.C., Khoo, S., Lamorde, M., Wasmann, R.E. & Denti, P. 2021. Dolutegravir pharmacokinetics during co-administration with either artemether/lumefantrine or artesunate/amodiaquine. *Journal of Antimicrobial Chemotherapy*. 76(5):1269–1272. https://doi.org/10.1093/jac/dkab022

2. **Kawuma, A.N.**, Wasmann, R.E., Dooley, K.E., Marta, B., Maartens, G., Denti, P. (2022). Population pharmacokinetic model and alternative dosing regimens for dolutegravir co-administered with rifampicin. *Antimicrobial agents and Chemotherapy*. https://doi.org/10.1128/aac.00215-22

3. **Kawuma, A.N.**, Wasmann, R.E., Dooley, K.E., Maartens, G., Denti, P. (2022). Drug-drug interaction between rifabutin and dolutegravir: a population pharmacokinetic model. *British Journal of Clinical Pharmacology*. https://doi.org/10.1111/bcp.15604

4. **Kawuma, A.N**, Wasmann, R.E., Sinxadi, P., Venter, F., Sokhela, S., Chandiwana, N., Wiesner, L., Maartens, G., Denti, P. (2022) Population Pharmacokinetics of Tenofovir given as either Tenofovir disoproxil fumarate or tenofovir alafenamide. ***(Submitted to Clinical Pharmacology and Therapeutics: Pharmacometrics and Systems Pharmacology)***

The author has also contributed to the following articles.

5. Griesel, R., **Kawuma, A.N**., Wasmann, R., Sokhela, S., Akpomiemie, G., Venter, W.D.F., Wiesner, L., Denti, P., et al. (2022). Concentration-response relationships of dolutegravir and efavirenz with weight change after starting antiretroviral therapy. *British Journal of Clinical Pharmacology*. 88(3):883–893. https://doi.org/10.1111/bcp.15177

6. Cindi, Z, **Kawuma, A.N**., Maartens, G., Bradford, Y., Venter, F., Sokhela, S., Chandiwana, N., Wasmann, R.E., Denti, P., Wiesner, L., Ritchie, M.D., Haas, D.W., Sinxadi, P. (2022). Pharmacogenetics of dolutegravir plasma exposure among Southern Africans living with HIV. *Journal of Infectious Diseases.* https://doi.org/10.1093/infdis/jiac174

7. Perumal, P., Arodola-Oladoyinbo, O., Naidoo, A., **Kawuma, A.N**., Naidoo, K., Gengiah, T.N., Chirehwa, M., Padayatchi, N., Denti, P. (2022). Altered Drug Exposures of First-Line Tuberculosis Drugs in a Moxifloxacin-Containing Treatment Regimen. *International Journal of Tuberculosis and Lung Disease.* https://doi.org/10.5588/ijtld.21.0702

8. Griesel, R., Sinxadi, P., **Kawuma, A.N**., Joska, J., Simiso Sokhela, S., Akpomiemie, G., Venter, F., Denti, P., Haas, D.W., Maartens, G. (2022) Pharmacokinetic and pharmacogenetic associations with dolutegravir neuropsychiatric adverse events in an African population. *Journal of Antimicrobial Chemotherapy*. https://doi.org/10.1093/jac/dkac290

9. Zinhle C., **Kawuma, A.N**., Maartens, G., Bradford, Y., Sokhela, S., Chandiwana, N., Venter, F.W.D., Wasmann, R.E., Denti, P., Wiesner, L., Ritchie, M.D., Haas, D.W., Sinxadi, P. (2022) Pharmacogenetics of tenofovir clearance among Southern Africans living with HIV. ***(In press at Pharmacogenetics and Genomics)***

Scientific conference abstracts

- **Kawuma, A.N**., Wang, X., Boffito, M., Maartens, G., Pillai, C., Denti, P. Dolutegravir population pharmacokinetics in co-administration with rifampicin. 28th Population Approach Group Europe (PAGE), Stockholm, Sweden, 11– 14 June 2019

- **Kawuma, A.N.,** Wasmann, R.E., Dooley, K.E., Marta, B., Maartens, G., Denti, P. Rifabutin changes dolutegravir's half-life but not area under the curve when co-administered. 29th Population Approach Group Europe (PAGE), Virtual conference 2 – 3 and 6 – 7 September 2021.

- **Kawuma, A.N**, Nalule, L.C., Denti, P., Aarons, L., Pillai, C., and the Pharmacometrics Africa Team. An online Clinical Pharmacology and Pharmacometrics training course in Africa: Results of a proof-of-concept implementation. 3rd Word Conference on Pharmacometrics (WCOP), Cape Town, South Africa, 29th March – 1st April 2022

- **Kawuma, A.N**, Wasmann, R.E., Sinxadi, P., Venter, F., Sokhela, S., Chandiwana, N., Wiesner, L., Maartens, G., Denti, P. Population Pharmacokinetics of Tenofovir given as either Tenofovir disoproxil fumarate or tenofovir alafenamide. 30th Population Approach Group Europe (PAGE), Ljubljana, Slovenia 28th June – 01st July 2022.

Declaration of work

I, **Aida Nakayiwa Kawuma**, hereby declare that the work on which this dissertation/thesis is based is my original work (except where acknowledgements indicate otherwise) and that neither the whole work nor any part of it has been, is being, or is to be submitted for another degree in this or any other university. **Chapters 4, 5, 6** and **8** of the thesis have been published or are under review in an international journal and contents remain unchanged from the printed versions except where formatting was required to maintain consistency in the thesis. All co-authors gave their written consent to include the publications as part of a PhD.

I empower the university to reproduce for research either the whole or any portion of the contents in any manner whatsoever.

Student Name: Aida Nakayiwa Kawuma

Date: 30th January 2023

Student Number: KWMAID001

Declaration on the Inclusion of Publications in a PhD Thesis

"I confirm that I have been granted permission by the University of Cape Town's Doctoral Degrees Board to include the following publication(s) in my PhD thesis, and where co-authorships are involved, my co-authors have agreed that I may include the publication(s):"

1. Kawuma, A.N., Walimbwa, S.I., Pillai, G.C., Khoo, S., Lamorde, M., Wasmann, R.E. & Denti, P. 2021. Dolutegravir pharmacokinetics during co-administration with either artemether/lumefantrine or artesunate/amodiaquine. *Journal of Antimicrobial Chemotherapy*. 76(5):1269–1272. https://doi.org/10.1093/jac/dkab022

2. Kawuma, A.N., Wasmann, R.E., Dooley, K.E., Marta, B., Maartens, G., Denti, P. (2022). Population pharmacokinetic model and alternative dosing regimens for dolutegravir co-administered with rifampicin. *Antimicrobial agents and Chemotherapy.* https://doi.org/10.1128/aac.00215-22

3. Kawuma, A.N., Wasmann, R.E., Dooley, K.E., Maartens, G., Denti, P. (2022). Drug-drug interaction between rifabutin and dolutegravir: a population pharmacokinetic model. *British Journal of Clinical Pharmacology*. https://doi.org/10.1111/bcp.15604

4. Kawuma, A.N, Wasmann, R.E., Sinxadi, P., Venter, F., Sokhela, S., Chandiwana, N., Wiesner, L., Maartens, G., Denti, P. (2022) Population Pharmacokinetics of Tenofovir given as either Tenofovir disoproxil fumarate or tenofovir alafenamide. (Submitted, in review)

Signature: Signed by candidate **Date:** ___30th January 2023___

Student Name: Aida Nakayiwa Kawuma

Student Number: KWMAID001

Acknowledgements

I would like to express my sincere gratitude to:

The Lord God, who gave me courage, grace, and determination to undertake a PhD in the continually changing field of Pharmacometrics.

Pharmacometrics Africa NPC, for the financial support for this PhD.

My supervisor, Professor Paolo Denti, for overseeing my research and his expert guidance during all the stages of this degree, from proposal development to the analyses of data and publication of papers – for his enthusiasm, invaluable advice, ideas and feedback.

My co-supervisor, Dr Roeland Wasmann, for his timely feedback, advice, and encouragement. It would have been difficult for me to conclude this PhD without his guidance.

My co-supervisor, Professor Gary Maartens, for his valuable input about the clinical implications of my research and how to translate this to a wider clinical audience, and for providing the data that I used for my projects.

Professor Colin Pillai, for all the academic and non-academic discussions we had and particularly his encouragement when I ran into challenges – for opening doors of opportunity for me.

All present and past colleagues at the pharmacometrics unit of the University of Cape Town. I appreciate your willingness to help me work through challenging analyses.

My parents, Professor Medi Ally Kawuma and Mrs Caroline Nassozi Kawuma, who showed me the value of education and who have always encouraged me to push further.

My sister, Davina Philomena Kawuma, for being my rock – for listening to me cry, for letting me know it will be ok, for watching the boys when I couldn't and for encouraging me.

My sons, Emmanuel Tendo Tusiime and Elijah Sinza Tusiime, who inspire me daily.

My husband, Moses Tusiime, without whose love and support I couldn't have done this. For his patience, encouragement and listening to me endlessly talk about pharmacometrics terms that he hardly understood – for walking this journey with me.

Special thanks are also due to the Infectious Diseases Institute, Makerere University, College of Health Sciences, ViiV Healthcare for graciously providing data that I worked with, and the Division of Clinical Pharmacology, University of Cape Town.

Computations were performed using facilities provided by the University of Cape Town's ICTS High-Performance Computing team: https://ucthpc.uct.ac.za/

Abstract

Pharmacometrics of dolutegravir and tenofovir: A quantitative approach to characterise drug-drug interactions, pharmacogenetics and optimise treatment

Africa houses more than 50% of the 37 million people estimated to be living with HIV (PLWH) and although great strides have been made in increasing access to antiretroviral therapy, there is still a high incidence of new HIV infections. In sub-Saharan Africa, co-infections of HIV, tuberculosis and malaria are common because the three pandemics overlap considerably. Treatment of these co-infections is often challenging because of the increased risk of drug-drug interactions. Dolutegravir-based regimens are now the preferred first-line option for the management of HIV. Therefore, many African countries have transitioned most PLWH from efavirenz to dolutegravir-based regimens. A fixed-dose combination pill of dolutegravir, tenofovir, and lamivudine constitutes one of the most widely used regimens in Africa.

In this thesis, we employ population pharmacokinetic modelling to improve HIV treatment using data from healthy volunteers and PLWH who may or may not be co-infected with tuberculosis. We characterise dolutegravir's pharmacokinetics, pharmacogenetics, and its drug-drug interaction with the antituberculosis drugs, rifampicin and rifabutin and with the antimalarial drugs, artemether-lumefantrine and artesunate-amodiaquine. We also describe the pharmacokinetics of tenofovir when dosed as either tenofovir disoproxil fumarate or tenofovir alafenamide in South Africans living with HIV.

We found that rifampicin increases dolutegravir clearance more than twofold leading to a reduction in its exposure to warrant twice-daily dosing of dolutegravir when co-administered. However, we demonstrate that a simpler regimen of 100 mg once daily (as opposed to 50 mg twice daily) may be sufficient to achieve desired targets. We found that rifabutin decreased dolutegravir's volume of distribution, but without an overall change in its area under the

concentration-time curve. The interaction between dolutegravir and artemether-lumefantrine or artesunate-amodiaquine was not clinically significant, and no dose adjustment is required when these are co-administered. Lastly, we demonstrate in a cohort of African subjects that polymorphisms within the *UGT1A* locus affect dolutegravir exposure, as has been shown with other populations. For tenofovir, we developed a joint model describing its pharmacokinetics when given either as tenofovir disoproxil fumarate or tenofovir alafenamide.

In conclusion, by employing pharmacometric techniques, we were able to analyse data pooled from different studies, use sparsely sampled data, and run simulations to test and inform alternative dosing scenarios.

Table of Contents

List of Tables

List of Figures

Abbreviations and acronyms

AIC	Akaike Information Criterion
ART	Antiretroviral therapy
$AUC_{0–24}$	The 24-hour area under the concentration-time curve
BLQ	Below the limit of quantification
BOV	Between-occasion variability
CCR5	Chemokine receptor 5
CI	Confidence Interval
CL	Clearance
C_{max}	Maximum plasma concentration
C_{min}	Minimum plasma concentration
COVID-19	Coronavirus disease
CXCR4	Chemokine receptor 4
CYP	Cytochrome
DNA	Deoxyribonucleic acid
F	Oral bioavailability
FDC	Fixed dose combination
FFM	Fat-free mass
FOCE-I	First-order conditional estimation with eta-epsilon interaction
GOF	Goodness of fit
HIV	Human immunodeficiency virus
INSTI	Integrase strand transfer inhibitors
K_a	Absorption rate constant
LLOQ	Lower limit of quantification
MTT	Mean transit time
NCA	Noncompartmental analysis
NN	Number of absorption transit compartments
NONMEM	Non-linear mixed-effects modelling
NNRTI	Non-nucleoside reverse transcriptase inhibitors
NRTI	Nucleoside reverse transcriptase inhibitors
OFV	Objective function value
PD	Pharmacodynamics
PI	Protease inhibitors
P-gp	P-glycoprotein
PsN	Perl-speaks-NONMEM
PXR	Pregnane X receptor
Q	Intercompartmental clearance
RNA	Ribonucleic acid
SIR	Sampling importance resampling
TAF	Tenofovir alafenamide
TDF	Tenofovir disoproxil fumarate
TFV-DP	Tenofovir diphosphate

TBW	Total body weight
T_{max}	Time to maximum plasma concentration
UGT1A1	UDP Glucuronosyltransferase Family 1 Member A1
V	Volume of distribution
V_c	Volume of distribution of the central compartment
V_p	Volume of distribution of the peripheral compartment
VPC	Visual predictive check
WHO	World Health Organization

Chapter 1 Introduction and literature review

1.1 Global disease burden of HIV

In 2020, it was estimated that about 37 million people were living with human immunodeficiency virus (HIV) globally, with more than 50% in Africa. Although 84% of these are aware of their status and over 70% are receiving antiretroviral therapy (ART), the number of new HIV infections remains high. In 2020, there were approximately 1.5 million new HIV infections (UNAIDS, 2021). In sub-Saharan Africa, the majority (63%) of these new infections were among women and girls who disproportionately suffer the burden of HIV. In recognition of the sustained threat of HIV, the Joint United Nations Programme on HIV/AIDS (UNAIDS) has set an ambitious target aimed at ending the epidemic by 2030. The 95-95-95 targets aim at ensuring that "*95% of people living with HIV are diagnosed, of whom 95% are on treatment, and of whom 95% are virally suppressed.*" Unfortunately, the COVID-19 pandemic has slowed the gains made in achieving these targets, especially in Africa. Lockdowns and other instituted restrictions in many countries disrupted HIV testing, diagnosis, and delivery of treatment. A report by The Global Fund to Fight AIDS, Tuberculosis and Malaria that collated data from 502 health facilities across more than 30 African and Asian countries highlighted this. They report that compared to the same period in 2019, they saw a 41% and 37% decline in HIV testing and referrals for diagnosis or treatment, respectively during the first COVID-19 lockdowns in 2020 (The Global Fund, 2021). Moreover, with COVID-19 disrupting services aimed at HIV prevention, there is an increased risk of new HIV infections especially for vulnerable and marginalized populations. Strict lockdowns meant that inequalities that perpetuate HIV infection were exacerbated. With the COVID-19 pandemic came increased cases of domestic violence and sexual violence, millions of girls out of school, and an increase in teenage pregnancies (UNAIDS, 2022), all of which have been associated with an increased risk to HIV. Also, marginalized populations; many of whom rely on informal employment in

low and middle-income countries were especially affected by the economic slowdown caused by the pandemic and this has plunged many into poverty. Poverty compels individuals, especially women into risky behaviour such as sexual trade and teenage marriages, which inevitable increase the risk to HIV (Mufune, 2015). According to the 2022 UNAIDS global AIDS update, over the last 10 years, regions including Eastern Europe, Central Asia, the Middle East, North Africa and Latin America have all registered increases in annual HIV infections (UNAIDS, 2022).

1.2 HIV disease

HIV attacks the immune system, particularly CD4+ cells, which include T helper cells, macrophages, and dendritic cells. HIV is a retrovirus, and its genome consists of two identical single strands of ribonucleic acid (RNA), which encode three essential structural genes i.e., the *gag*, *pol* and *env* genes. The *gag* gene is responsible for the production of the viral outer core membrane protein, the capsid protein, and the nucleocapsid. The *pol* gene is responsible for the enzymes; reverse transcriptase, protease, and integrase, while the *env* gene is responsible for coding the viral envelope glycoproteins (surface protein gp120 and transmembrane protein gp41). Each of the surface proteins and viral enzymes is responsible for a crucial step in the HIV infection process. Reverse transcriptase transcribes viral RNA to pro-viral DNA while integrase inserts the double-stranded pro-viral DNA into the genome of the host cells. The protease enzyme cleaves proteins into smaller fragments required by the virus. As detailed below in section 1.3, ART has been developed to target the different stages of the life cycle of the virus, mostly by targeting the different enzymes (reverse transcriptase, protease, and integrase) (Palmisano & Vella, 2011).

1.2.1 Infection of a host cell

Infection of a host cell is a complex process characterised by protein-protein interactions. For the virus to enter a host cell, its surface protein, gp120 binds to a CD4 receptor and a complementary co-receptor, chemokine receptor 5 (CCR5) or chemokine receptor 4 (CXCR4) found on the surface of the host cell (Seitz, 2016). Once gp120 binds to CD4, the virus can insert into the host cell plasma membrane via the gp41 transmembrane protein causing the fusion of the cell membrane with the viral envelope.

Once fusion is complete, the virus releases its genome into the host cell cytoplasm. Here the HIV reverse transcriptase enzyme is activated and transcribes HIV single-strand RNA into double-stranded pro-viral DNA, which is transported to the nucleus and inserted into the DNA of the host cell via the integrase enzyme. Integration of pro-viral DNA into a host cell genome completes the HIV infection process and the establishment of a persistent infection by irreversibly transforming the host cell into a virus producer. The pro-viral genome can then be replicated together with and as part of the host cell genome. Viral proteins are transported to and assembled in proximity to the cell membrane.

Infection with the virus gradually destroys one's immune system and as a consequence, an infected individual becomes increasingly immunodeficient. Therefore, this weakened defence makes an infected individual more prone to a variety of infections and some types of cancer that they would otherwise have been able to fight off with a healthy immune system (Deeks et al., 2015).

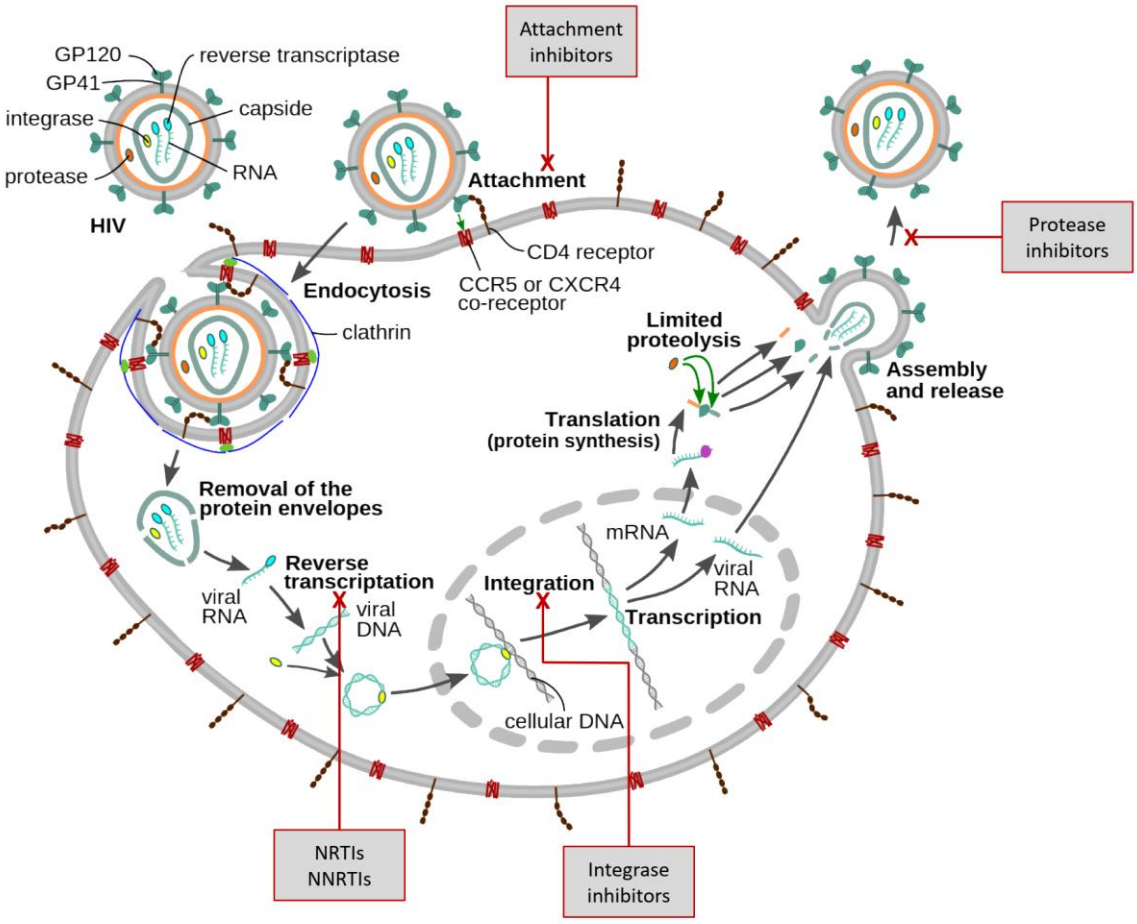

Figure 1.1 HIV virion structure, infection, and replication

(Figure was adapted from Jmarchn - Own work, CC BY-SA 3.0)
https://commons.wikimedia.org/w/index.php?curid=58188472

1.2.2 HIV-1 versus HIV-2

HIV-1 infection is the most common type of HIV and accounts for most of the global acquired immune deficiency syndrome (AIDS) pandemic. Conversely, HIV-2 is less common and predominantly causes infection in West Africa in countries such as Senegal, Guinea-Bissau, Cote d'Ivoire, Nigeria, Mali, and Sierra Leone. Although the routes of transmission of HIV-2 and HIV-1 are similar, the infectivity is lower for HIV-2 compared to HIV-1 (Campbell-Yesufu & Gandhi, 2011).

1.2.3 AIDS

Infection with HIV leads to progressive depletion of the immune system, leading to an immune system that cannot fight or fend off disease and infections. This is the underlying cause of AIDS, a collection of infections and symptoms arising due to a deficiency in the immune system. The presence of certain infections is used as an indicator of different stages of AIDS. If left untreated, individuals infected with HIV will progress to AIDS within 8 or 10 years of the infection. Treatment with antiretroviral therapy is essential in depleting viral load and improving the CD4+ cell count, which then slows the progression to AIDS (Barry, Mulcahy & Back, 1998).

1.3 HIV treatment

Strategies to treat HIV were introduced in 1987. However, these often resulted in treatment failure because drugs or drug combinations were used that were not potent enough to suppress viral replication. In 1995, highly active antiretroviral therapy (ART) was introduced, and this consisted of a combination of three or more drugs potent enough to stop replication. Since then, treatment outcomes have improved markedly, leading to an increase in life expectancy for people living with HIV (PLWH) (Piacenti, 2006). For example, a study in California found that between 2011 and 2016, PLWH with a CD4 cell count of 500 cells/μL or more who started ART had a life expectancy of 57.4 years comparable to 64.2 years among healthy adults (difference, 6.8 years; 95% CI, 5.0 – 8.5 years) at the age of 21 years (Marcus et al., 2020). Because more people are surviving longer with HIV, it is now recognized as a chronic illness (Deeks, Lewin & Havlir, 2013).

ART aims to provide rapid and sustained viral suppression and therefore prevent transmission, and opportunistic infections, and maintain optimal health (Saag et al., 2020). Antiviral agents are classified according to their mechanisms of action which target specific steps within the

HIV replication cycle. The key tenet of ART is the use of a potent combination of antiviral drugs capable of suppressing replication, usually with different mechanisms of action. Suppressing viral replication prevents the virus from developing resistance. The most widely used agents can be grouped into:

- Integrase strand transfer inhibitors (INSTIs) inhibit the integrase enzyme responsible for integrating viral DNA into the host chromosome. Examples include bictegravir, dolutegravir, raltegravir, and elvitegravir.
- Nucleoside (or nucleotide) reverse transcriptase inhibitors (NRTIs) consist of drugs that are analogues of endogenous nucleotides used as building blocks for DNA. They inhibit the reverse transcriptase enzyme and stop chain elongation of proviral DNA. Examples include abacavir, emtricitabine, lamivudine, zidovudine, and tenofovir.
- Non-nucleoside reverse transcriptase inhibitors (NNRTIs) also inhibit the reverse transcriptase enzyme but at a site different from the NRTIs and include efavirenz, nevirapine, and rilpivirine.
- Protease inhibitors (PIs) such as lopinavir, ritonavir, atazanavir and darunavir work by inhibiting HIV-1 protease, the enzyme responsible for cleaving proteins into smaller fragments required by the virus.

Most first-line regimens for treatment-naïve patients include two NRTIs plus one INSTI or NNRTI (Saag et al., 2020). Viral load is the most important marker used to monitor treatment efficacy (Piacenti, 2006).

Although effective, ART is a lifelong therapy and possesses challenges, including adverse drug reactions, drug-drug interactions (DDI), the need to maintain life-long adherence to treatment, and the development of resistance and clinical failure. In special and often neglected populations, including pregnant women, young children, and those with co-morbidities for

whom research is limited, these challenges pose an even greater risk (Desai, Iyer & Dikshit, 2012) (Esté & Cihlar, 2010).

1.4 Drug-drug interactions

Drug-drug interactions (DDI) can be defined as the influence of one drug on another. Colloquially**,** the drug causing the DDI is called the perpetrator while the drug affected by the DDI is referred to as the victim drug. DDI can broadly be categorized as either pharmacokinetic or pharmacodynamic DDI. Pharmacodynamic interactions usually constitute antagonism or synergism of a drug by another at the same site of action. On the other hand, pharmacokinetic interactions can occur through several different mechanisms including reduced/ altered absorption of a drug, displacement from binding sites, and the induction or inhibition of drug-metabolizing enzymes and/or drug transporters. In this thesis, the analysis focused on characterising drug-drug interactions of the pharmacokinetic kind.

1.4.1 Drug-drug interactions among PLWH

The HIV scourge overlaps considerably with other infectious diseases including tuberculosis and malaria, leading to a considerable number of co-infections in sub-Saharan Africa (Vitoria et al., 2009). The treatment of PLWH and co-infected with tuberculosis is particularly challenging. First-line tuberculosis treatment consists of a rifampicin-based regimen (World Health Organization, 2022). Rifampicin is a potent inducer of a variety of drug-metabolizing enzymes and transporters including cytochromes P450 (CYP) enzymes such as CYP2B6, CYP3A4, UDP-glucuronosyltransferase 1A (UGT1A1) and P-glycoprotein. The consequence is that many antiretroviral drugs need a dose adjustment or cannot be used when concomitantly administered with rifampicin (Food and Drug Administration, 2013). For example, in the case of dolutegravir, which constitutes the preferred first-line HIV regimen (dolutegravir, tenofovir,

and emtricitabine or lamivudine). Because of rifampicin's induction of UGT1A1, which is responsible for dolutegravir metabolism, current treatment guidelines recommend the dolutegravir dose be adjusted to counter this interaction (World Health Organization, 2018). Implementing dose adjustments is often challenging in a high-burden and resource-limited setting with high patient-health care provider ratios. Usually, treatment is provided under programmatic conditions with co-formulated, fixed-dose combination pills and stockouts are likely to occur of the single formulations of dolutegravir. Also, reduced compliance/adherence to the twice-daily regimen could pose a challenge. Adherence studies have shown that, especially for ART-naïve individuals starting treatment, once-daily dosing is associated with better adherence compared to twice-daily dosing (Nachega et al., 2014).

In addition, the burden of non-communicable diseases has significantly increased across Africa, with cancers and cardiovascular diseases leading the way. While the success of HIV treatment has decreased the frequency of AIDS-related comorbidities and opportunistic infections, HIV-associated comorbidities are becoming more common because of an increase in life expectancy (Deeks, Lewin & Havlir, 2013). This comorbidity often requires polypharmacy and thus poses a potential risk for drug-drug interactions.

1.5 Pharmacology of dolutegravir

Dolutegravir is a second-generation INSTI that is indicated for the treatment of HIV-1 (Shah, Schafer & Desimone, 2014). It was first approved for use in 2013 by the United States Food and Drug Authority for both ART-naïve and ART-experienced but INSTI-naïve individuals. To exert its inhibitory effect, dolutegravir binds to magnesium in the active site of the integrase enzyme. It is recommended for adults, including pregnant women, and children aged 4 weeks or older who weigh at least 3 kg. Adults are dosed at 50 mg once daily or 50 mg twice daily when co-administered with strong metabolic inducers such as rifampicin. Dosing in pediatrics

is weight based and ranges from 5 mg once daily (using dispersible tablets) for those weighing between 3 – 6 kg to 40 mg once daily (using a film-coated tablet) for those weighing between 14 – 20 kg. For children weighing more than 20 kg, the 50 mg (film-coated tablet) once-daily adult dose is used (TIVICAY (ViiV Healthcare), 2020). Dolutegravir presents many advantages that have supported its use in low and middle-income countries and in 2019 the World Health Organization (WHO) recommended dolutegravir-based regimens (replacing efavirenz-based regimens) as the preferred first-line option for PLWH. Compared to efavirenz, dolutegravir causes more rapid viral suppression after initiation of ART (World Health Organization, 2018). In addition, compared to efavirenz, dolutegravir has a lower risk for drug-drug interactions, a more tolerable side effect profile and is less prone to developing resistance (high genetic barrier). For high-burden, low-income countries, dolutegravir is mostly available within a fixed-dose combination pill consisting of dolutegravir 50 mg, tenofovir disoproxil fumarate 300 mg, and lamivudine 300 mg taken once daily (World Health Organization, 2018).

1.5.1 Absorption

Dolutegravir is rapidly absorbed after oral administration. Peak plasma concentrations are achieved within about 1-hour post-dose. Moreover, food increases its absorption. Taking dolutegravir with a low, moderate, or high-fat meal increases its AUC by 33%, 41%, and 66%, respectively (Song et al., 2012). Treatment guidelines do not give a preference on whether dolutegravir should be taken with/without food (TIVICAY (ViiV Healthcare), 2020) because regardless of whether it is taken under fed or fasted conditions, trough concentrations remain above the desired target.

1.5.2 Distribution

Dolutegravir is more than 99% bound to human plasma proteins. It has a reported apparent volume of distribution of approximately 17.4 L (TIVICAY (ViiV Healthcare), 2020). The dolutegravir free fraction in plasma was estimated to be 1.10% in healthy subjects, 0.5% in moderate hepatic impairment, and 1.01% in subjects with severe renal impairment. For PLWH, only 0.49% is estimated to be unbound. Dolutegravir crosses the blood-brain barrier and distributes into the central nervous system (CNS). After a dose of 50 mg once daily, it was found in the cerebrospinal fluid (CSF) at an average steady-state concentration of 0.018 mg/L (at 2 weeks). However, compared with a median steady-state plasma concentration at the same time (3.36 mg/L), concentrations in the CSF are low, with CSF-plasma ratios of 0.52% (range, 0.12%–0.66%) (Letendre et al., 2014). Dolutegravir is also present in breastmilk, and seminal fluid, and transfers across the placenta (Imaz et al., 2016; Schalkwijk et al., 2016; Dickinson et al., 2020).

1.5.3 Metabolism and elimination

Dolutegravir is primarily metabolized by UGT1A1 with CYP3A4 playing a minor role. In addition, dolutegravir is a substrate of the efflux drug transporters P-glycoprotein and breast cancer resistance protein (BCRP) (Reese et al., 2013a; Mercadel et al., 2014). Dolutegravir has an oral clearance of 1.0 L and a terminal half-life of approximately 14 hours. Therefore, steady-state concentrations should be achieved after about 3 days of dosing. After an oral dose of 20 mg, approximately 31.6% of dolutegravir is excreted in the urine while 64% is excreted unchanged in the faeces (Castellino et al., 2013). Considering that CYP3A4 only plays a minor role in dolutegravir elimination, first-pass metabolism is expected to be low after oral dosing. Weight, age, and smoker status have been reported to affect dolutegravir clearance while gender was reported to affect bioavailability. However, these effects are not considered

clinically relevant because they all lead to a less than 30% change in dolutegravir exposure and, even though concentrations are reduced, these are still maintained above the target 90% inhibitory (IC90) and effective (EC90) concentrations (Zhang et al., 2015).

1.5.4 Dolutegravir drug-drug interactions

Dolutegravir neither induces nor inhibits the major drug-metabolizing enzymes or transporters and therefore, is less prone to cause DDIs. However, there are a few exceptions. Dolutegravir inhibits the renal organic cation transporter 2 (OCT2), causing a decrease in the secretion of creatinine in the urine. Therefore, for drugs such as dofetilide and metformin whose excretion depends on transport by OCT2, dolutegravir co-administration may change exposure significantly. A DDI study showed that dolutegravir co-administration led to a 79% and 66% increase in metformin AUC and C_{max}, respectively (Song et al., 2016).

Dolutegravir is susceptible to interactions with polyvalent cations (including iron, calcium, zinc, and magnesium), which can cause chelation complexes that limit absorption when co-administered. Therefore, the guidance recommends giving dolutegravir either 2 hours before or 4 hours after antacids (Patel et al., 2011). This interaction is similar to the other INSTIs, which show clinically significant interactions when co-administered with antacids (Krishna et al., 2016).

Since dolutegravir is a substrate of UGT1A1 and CYP3A4, drugs that either induce or inhibit these enzymes can potentially affect dolutegravir exposure. Moderate to strong inducers including rifampicin, carbamazepine, etravirine, efavirenz, and ritonavir-boosted fosamprenavir or tipranavir have been shown to reduce plasma concentrations significantly enough to warrant dose adjustment when co-administered with dolutegravir. Current guidelines for dolutegravir co-administration with either rifampicin or carbamazepine recommend 50 mg twice daily as opposed to 50 mg once daily (World Health Organization, 2019).

1.5.5 Adverse events

Compared to other antiretroviral drugs, dolutegravir is well tolerated and has relatively few side effects. Nevertheless, as dolutegravir is rolled out in different populations across the globe and post-marketing surveillance data builds up, we may see previously unreported or an increase in previously reported side effects.

The most common adverse events (AEs) associated with dolutegravir are neuropsychiatric, with insomnia being the most frequently reported. Others include sleep disturbances, dizziness, and painful paresthesia. A paper by Hoffman *et al.* compared rates of discontinuation caused by adverse events in patients initiated on INST1s (dolutegravir, raltegravir or elvitegravir/cobicistat) and reported that discontinuation rates for patients with neuropsychiatric events within 12 and 24 months, were estimated at 5.6% and 6.7% for dolutegravir, and less than 3% for either elvitegravir (0.7% and 1.5%) or raltegravir (1.9% and 2.3%) (Hoffmann et al., 2017). Similar findings of dolutegravir intolerance were reported by van den Berk *et al.* where dolutegravir treatment was stopped in 62 out of 387 (16.0%) patients (Ait Moha & Van den Berk, 2016). It has been suggested that CNS toxicity due to dolutegravir may be a class effect. However, CNS toxicity is seen less frequently with either raltegravir or elvitegravir.

More recently, there is mounting evidence that dolutegravir causes altered glucose metabolism leading to severe hyperglycemia and complications such as diabetic ketoacidosis (Kamal & Sharma, 2019; Ntem-Mensah et al., 2019; Lamorde et al., 2020). The cause of this side effect is hypothesized to involve chelation of magnesium by dolutegravir (and other INSTIs), altering glucose transport via the GLUT 4 receptor and leading to insulin resistance. INSTIs mechanism of action is believed to involve binding to magnesium to prevent HIV from integrating into the host cell DNA. Although this side effect appears to be uncommon, healthcare providers must be aware of it. Thus, regular monitoring of plasma glucose levels may be warranted for

individuals on dolutegravir-based regimens (Hailu, Tesfaye & Tadesse, 2021; Hirigo et al., 2022).

It has also been reported that dolutegravir causes weight gain, especially in women. Two large randomized clinical trials, NAMSAL (The NAMSAL ANRS 12313 Study Group, 2019) and ADVANCE (Venter et al., 2019) showed that weight gain was significantly higher for individuals on a dolutegravir-based ART regimen compared to those on an efavirenz-based regimen. When comparing dolutegravir vs efavirenz groups, The NAMSAL trial reported a median weight gain of 5.0 vs. 3.0 kg and an incidence of obesity of 12.3% vs. 5.4%. The ADVANCE study reported a mean increase in absolute weight of 1.7 kg for the efavirenz group, 3.2 kg in the dolutegravir/tenofovir disoproxil fumarate group and 6.4 kg in the dolutegravir/tenofovir alafenamide group at week 48.

1.5.6 Pharmacodynamics

Antiviral activity

A dolutegravir dose-exposure response relationship for viral load decrease has been described using a sigmoid Emax model (Min et al., 2011). A phase Ia, 10-day monotherapy study in which dolutegravir was dosed at 2, 10, and 50 mg once daily showed that dolutegravir causes a rapid decline in HIV-1 viral RNA. Compared to baseline, a drop (standard deviation) of 2.46 log10 (0.35) HIV-1 RNA copies/mL was observed on day 11. The Emax model reported an *in vivo* EC_{50} of 0.036 μg/mL and demonstrated that the C_{trough} parameter best-predicted reduction of viral load (Min et al., 2011).

Resistance

Compared to raltegravir and elvitegravir, dolutegravir has a high genetic barrier (Cottrell, Hadzic & Kashuba, 2013). This means that the difficulty with which the virus develops

resistance against it is high. One of the key reasons for this is that dolutegravir dissociates slowly from the integrase-DNA wild-type complexes with a mean dissociative half-life of 71 h, compared to 8.8 and 2.7 h for raltegravir and elvitegravir, respectively (Hightower et al., 2011a). This slow dissociation is enabled by dolutegravir's difluorophenyl group which allows it to enter further than other INSTIs into the pocket of the integrase active site. Additionally, at the current dosing of 50 mg daily, dolutegravir has a high inhibitory quotient (C_{trough}/protein adjusted IC90) because it maintains substantially high trough concentrations above the IC90 (Cottrell, Hadzic & Kashuba, 2013).

Dolutegravir's efficacy target

Two exposure targets have been proposed for dolutegravir efficacy. Some recommend targeting trough values above the dolutegravir PA-IC90 of 0.064 mg/L, while others recommend a trough above the EC90 of 0.03 mg /L. The 0.064 mg/L target was found to inhibit HIV-1 in vitro, while the 0.3 mg/L target was derived from a phase IIb study investigating dolutegravir in ART-naïve adults with HIV (Van Lunzen et al., 2012). The study tested doses of 10, 25, and 50 mg and, while all patients were virologically suppressed irrespective of the dosing arm, the value of 0.3 mg/L was the geometric mean of the C_{min} in the 10-mg arm among the 15 patients (out of 53) with drug concentrations available.

1.6 Pharmacology of Tenofovir

In 1993, Balzarini *et al*. reported the antiviral activity of the acyclic nucleoside phosphonate Tenofovir (Balzarini et al., 1993). It was subsequently shown that tenofovir-diphosphate (TFV-DP) a diphosphate metabolite of tenofovir was an analogue of deoxyadenosine-triphosphate and a potent inhibitor of the HIV reverse transcriptase enzyme.

Tenofovir requires phosphorylation intracellularly to TFV-DP, its pharmacologically active form. This sequential phosphorylation involves the conversion of tenofovir to tenofovir monophosphate (TFV-MP) by adenylate kinase 2 (AK2) and conversion of TFV-MP to TFV-DP by different kinases including, creatine kinase muscle, pyruvate kinase muscle and pyruvate kinase liver and red blood cell (Figueroa et al., 2018). It has been suggested that variants of these enzymes necessary for tenofovir activation may lead to a decrease in their activity and subsequent reduction in the formation of TFV-DP (Figueroa et al., 2018). During HIV transcription, TFV-DP competes with deoxyadenosine 5'-triphosphate (the natural substrate) to be inserted into DNA and once incorporated, it blocks the action of HIV reverse transcriptase and stops further replication of viral DNA (Kearney, Flaherty & Shah, 2004). TFV-DP is reported to have a long intracellular half-life in peripheral blood mononuclear cells (PBMC) (Pruvost et al., 2005). After TDF discontinuation, Hawkins *et al*. showed persistent TFV-DP intracellular levels with a median half-life of 150 hours ranging from 60 to more than 175 hours (Hawkins et al., 2005). Tenofovir is eliminated renally, both by active tubular secretion and glomerular filtration. It is not a substrate of cytochrome P450, P-glycoprotein, or multidrug resistance protein type 2 (Ray et al., 2006).

At physiological pH, tenofovir is a dianion and, therefore, has poor membrane permeability and poor oral bioavailability and, therefore, cannot be administered orally (Ray, Fordyce & Hitchcock, 2016). To circumvent this, two lipophilic tenofovir prodrugs have been developed. tenofovir disoproxil fumarate (TDF) and tenofovir alafenamide (TAF). TDF was approved by the United States Food and Drug Administration (FDA) in 2001 and by the European Medicines Agency (EMA) in 2002. TAF was approved by FDA in 2015 and by the Europeans Medicine Agency in 2017.

1.6.1 Tenofovir disoproxil fumarate

TDF is currently used in combination with other antiretroviral agents for the treatment of HIV-1. These combinations include TDF/emtricitabine/efavirenz, TDF/lamivudine/dolutegravir, TDF/emtricitabine/rilpivirine, and TDF/emtricitabine/elvitegravir with cobicistat. TDF given at 300 mg daily has been used widely (for more than 9 million patient-years). In low- and middle-income countries, TDF remains the preferred backbone of HIV combination therapy because of its effective antiviral activity, favourable safety profile, low resistance and its availability within a fixed-dose combination (Estrella, Moosa & Nachega, 2014; Ray, Fordyce & Hitchcock, 2016). After oral administration, TDF is rapidly converted into tenofovir by esterase enzymes in the gut and plasma.

1.6.2 Tenofovir alafenamide

Unlike TDF, TAF is more stable in the plasma because it is selectively cleaved intracellularly. After oral absorption, TAF is rapidly taken up intracellularly where it is converted to tenofovir by Cathepsin A and then to the active form TFV-DP. This rapid uptake of TAF intracellularly reduces plasma tenofovir concentrations while efficiently loading HIV target cells. It concentrates mostly in mononuclear cells such as T-lymphocytes where HIV primarily replicates. This difference in tenofovir levels explains the difference in the safety profile between TDF and TAF.

1.6.3 Tenofovir drug-drug and food interactions

Both TDF and TAF are substrates of P-glycoprotein, BCRP, and ABCB. They are both inhibitors of MRP2. Strong inducers of P-glycoprotein are expected to decrease TAF absorption and subsequently tenofovir plasma concentrations while drugs that inhibit P-glycoprotein may increase TAF absorption and subsequently increase tenofovir concentrations. Therefore, co-administration of TAF with rifampicin and anticonvulsants (oxcarbazepine,

phenobarbital, phenytoin) which strongly induce P-glycoprotein is not recommended. If administered with carbamazepine, guidelines recommend doubling the dose (administered twice daily as opposed to once daily).

1.6.4 Tenofovir side effects.

Several studies have now shown an association between tenofovir and renal dysfunction (Laprise et al., 2012; Scherzer et al., 2012). In one by Laprise *et al.*, the authors report that tenofovir (given as TDF) exposure increased the risk of kidney dysfunction by 63% (hazard ratio of 1.63; 95% confidence interval, 1.26–2.10). After 10 years of exposure to TDF, the cumulative incidence of reduced kidney function signified by a glomerular filtration rate (GFR) <90 mL/min/1.73 m^2 for more than 3 months apart was just over 50% (95% CI, 45.65–59.26) (Laprise et al., 2012).

TAF was developed with the premise that it had the potential for a lower risk of bone and renal toxicity compared to TDF. Indeed, several studies have reported the benefit of TAF over TDF in terms of limiting the number of side effects (Gupta et al., 2019). However, there is some evidence to suggest that this benefit may not be as marked as previously thought. A review of different studies showed that the higher risk of bone and renal toxicity reported for TDF compared to TAF was significant when both TAF and TDF were boosted with either ritonavir or cobicistat. Incidentally, when TDF is boosted, the same dose of 300 mg is maintained while when TAF is boosted, the dose is reduced from 25 mg to 10 mg. On the other hand, when TDF and TAF (both without ritonavir or cobicistat) were compared, there was no difference in efficacy between the two drugs and the TAF safety profile was only marginally better than that of TDF (Hill et al., 2018).

The ADVANCE study, among south Africans living with HIV, enrolled participants in a TAF versus TDF (with either dolutegravir or efavirenz) regimen and showed that weight gain was

greater for participants on the TAF/emtricitabine/dolutegravir regimen compared to the TDF/emtricitabine/dolutegravir regimen, and more so among women.

1.7 Study justification

WHO now recommends dolutegravir-based regimens as the preferred first and second line for the management of HIV. As a result, many African countries have now transitioned most PLWH from efavirenz- to dolutegravir-based regimens. HIV, tuberculosis, and malaria, three of the world's leading causes of morbidity and mortality overlap geographically, leading to a considerable number of co-infections in sub-Saharan Africa. Treatment of these co-infections is often challenging because of the potential for DDI between ART and treatment for tuberculosis and/or malaria. This challenge is especially pronounced in resource-limited, high-burden settings, mostly because treatments are often given under programmatic conditions using fixed-dose combinations. This limitation implies that healthcare providers are unable to liberally switch single agents that may either be the victim or perpetrator drug involved in interactions within a regimen.

As such, there is a need to characterise and better understand the pharmacokinetics and safety of dolutegravir in an African context, especially among patients with comorbidities. This would inform whether dose adjustments are required or whether alternative dosing strategies can be employed. The drug-drug interactions investigated and reported in this thesis are mono-directional, with dolutegravir as the victim drug and the co-administered drugs as the perpetrators of the DDI. Dolutegravir has a low propensity to be the perpetrator for drug-drug interactions because it neither induces nor inhibits drug metabolizing enzymes.

1.8 Objectives

The overall aim of this thesis is to improve and optimise HIV treatment in persons with co-morbidities by employing population pharmacokinetic modelling techniques, using data from PLWH as well as healthy volunteers. Specific objectives include.

1. To describe the population pharmacokinetics of dolutegravir when co-administered with the antimalarial drugs, artemether-lumefantrine or artesunate-amodiaquine, and to characterise the extent of any drug interaction and to provide evidence for the need for dose adjustment.
2. To characterise the population pharmacokinetics of dolutegravir in the presence of rifampicin, describe the extent of the drug interaction, determine factors contributing to variability between individuals and explore alternative dosing scenarios for dolutegravir when co-administered with rifampicin.
3. To characterise the population pharmacokinetics of dolutegravir when co-administered with rifabutin and to describe the extent of the drug-drug interaction.
4. To describe the population pharmacokinetics of dolutegravir among South Africans living with HIV and to show whether genetic polymorphisms affect the levels of exposure.
5. To describe the population pharmacokinetics of tenofovir when administered as either TDF or TAF among South Africans living with HIV.

Chapter 2 Study designs and data description

This chapter describes the different studies from which data used for the thesis is derived. A total of 5 studies carried out in both healthy volunteers and PLWH are highlighted below.

2.1 DOLACT study

DOLACT was a two-way cross-over study that consisted of two (study A and B) open-label, fixed sequence studies enrolling healthy volunteers. **Figure 2.1** represents a schematic of the study. The study was conducted in Uganda by the Infectious Diseases Institute, Makerere University. DOLACT investigated the interaction between dolutegravir (given as 50 mg once daily) and the anti-malarial drugs, artemether-lumefantrine (80/480 mg) or artesunate-amodiaquine (200/540 mg) which are given as 3-day treatment. DOLACT enrolled healthy (no malaria or HIV) consenting adults weighing > 40 kg and willing to sleep under a mosquito bed net and follow study procedures. Pregnant or lactating women and those unwilling to use reliable contraception throughout the study were excluded.

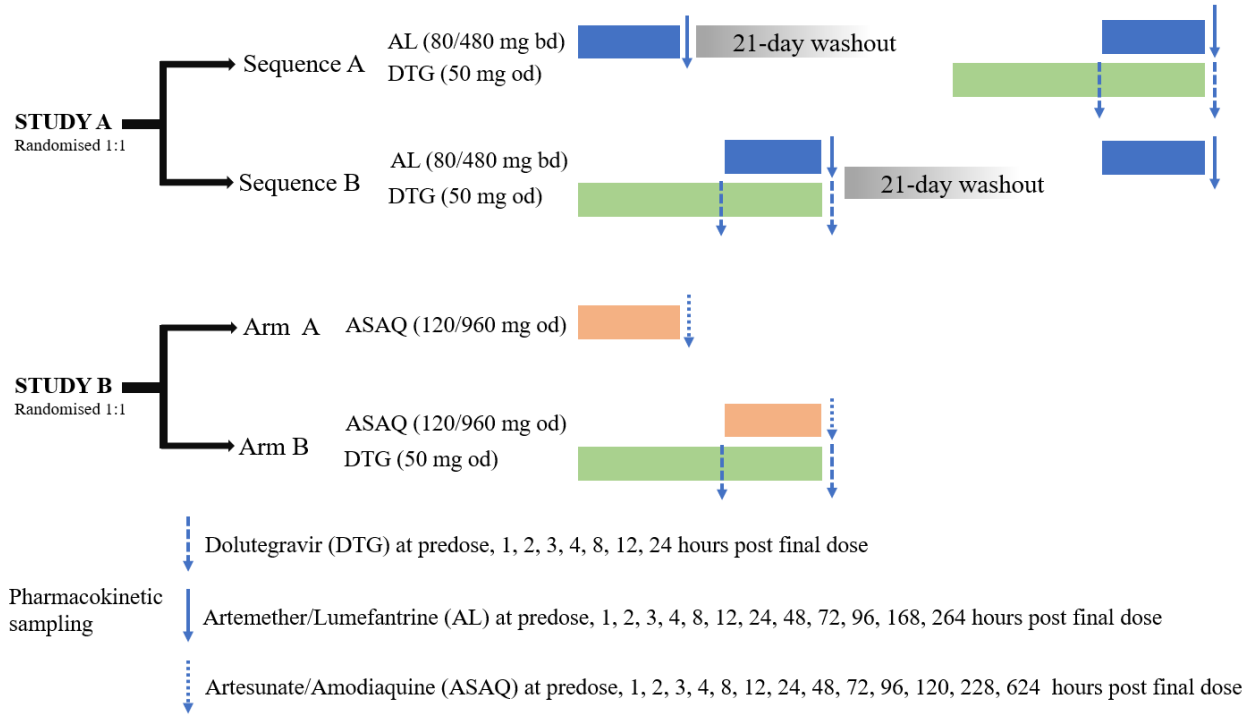

Figure 2.1 DOLACT Study design and pharmacokinetic sampling schedule

Study A (artemether-lumefantrine) was a random sequence, two-way crossover study that randomized participants either to sequence 1 or sequence 2. In sequence 1, participants received oral artemether-lumefantrine (80/480 mg twice daily taken with food) for 3 days (the regimen used for the treatment of uncomplicated malaria). Pharmacokinetic sampling was done at pre-dose (0 h), 1, 2, 3, 4, 8, 12, 24, 48, 72, 96, 168, and 264 h after the final dose. Following a 21-day washout period, participants received dolutegravir 50 mg once daily alone for 6 days with pharmacokinetic sampling at 0, 1, 2, 3, 4, 8, 12, and 24 h post-dose on day 6. They then received 3 days of twice-daily artemether-lumefantrine plus dolutegravir, with pharmacokinetic sampling at 0, 1, 2, 3, 4, 8, 12, 24, 48, 72, 96, 168, and 264 h after the final doses of both drugs. In sequence 2, participants received dolutegravir alone and then a combination of dolutegravir and artemether-lumefantrine with the same pharmacokinetic sampling schedule described for sequence 1, followed by artemether-lumefantrine alone after the 21-day washout period.

Assuming a coefficient of variation of 30%, the effective sample size for study A was calculated at 16 subjects. These would provide a power of >80% to detect a change in AUC outside the bioequivalence limits of 80 to 125% (with the 90% CI for AUC falling within this range for dolutegravir and lumefantrine).

Study B (artesunate-amodiaquine) used a parallel-group design because amodiaquine and its active metabolite N-desethyl-amodiaquine have a long terminal half-life of approximately 9 to 18 days. Participants were randomized to receive artesunate-amodiaquine *"(4 mg/kg artesunate, 10 mg/kg amodiaquine) once daily for 3 days with pharmacokinetic sampling at 0,1, 2, 3, 4, 8, 12, 24, 48, 72, 96, 120, 228, and 624 h after the last dose (arm 1) or dolutegravir for 7 days with pharmacokinetic sampling at 0, 1, 2, 3, 4, 8, 12, and 24 h after the last dose, followed by*

artesunate-amodiaquine once-daily, together with dolutegravir 50 mg once daily for 3 days, with pharmacokinetic sampling after the last dose of both drugs following the sampling schedule for arm 2." For the intensive sampling visits, all study drugs were given after an overnight fast. Drugs were administered with a standard meal with moderate fat content. Dolutegravir was quantified with a validated reversed-phase liquid chromatography (LC)–tandem mass spectrometry (MS) assay. The lower limit of quantification was 0.01 mg/L (Walimbwa et al., 2019).

For Study B, the inclusion of 30 subjects (15 per arm) was estimated to be sufficient to detect an AUC difference of 25% to 30% with a power of at least 80%.

2.2 RADIO study

RADIO was a phase II, open-label, sequential pharmacokinetic study conducted at the St Stephen's Centre in London, UK (Wang et al., 2019). Healthy HIV-negative adults between 18 and 60 years with a body mass index between 18 and 35 kg/m^2 were included. Pregnant and lactating females were excluded as well as individuals with any "clinically significant acute or chronic medical illness, hepatitis B and C, or evidence of organ dysfunction"(Wang et al., 2019). **Figure 2.2** depicts the study design. Participants received 50 mg dolutegravir once-daily (OD) for seven days, then 100 mg dolutegravir OD for seven days, then 600 mg rifampicin OD only for 14 days, followed by 50 mg dolutegravir OD plus 600 mg rifampicin OD for seven days, and lastly 100 mg dolutegravir OD plus 600 mg rifampicin OD for seven days. On the 7th day of each dolutegravir regimen, plasma samples were drawn pre-dose and 2, 4, 8, 12, and 24 hours post-dose. Dolutegravir doses were taken after a standard breakfast (Wang et al., 2019).

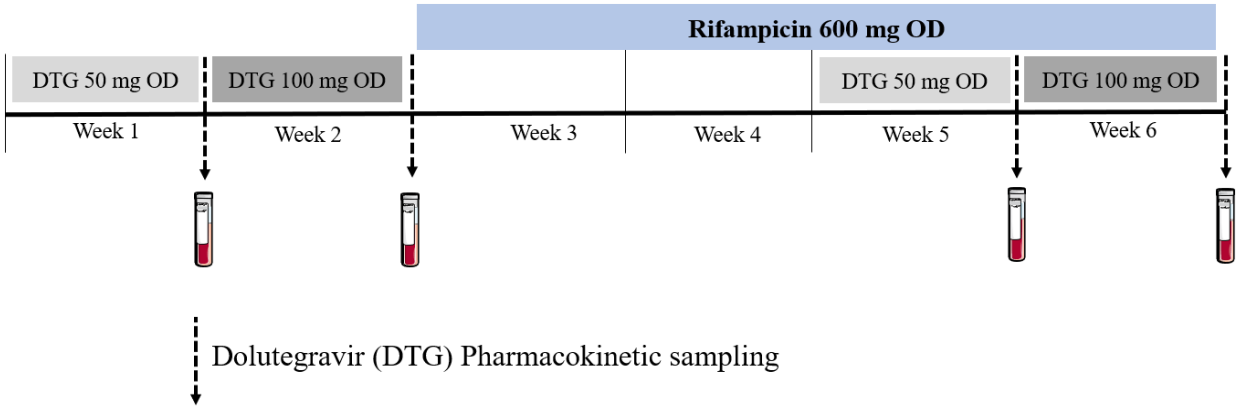

Figure 2.2 RADIO Study design and pharmacokinetic sampling schedule

Sample size estimates for RADIO were based on the following assumptions; a within-subject variability expressed as a coefficient of variation (CV) of 33% (based on previous, similar studies (Dooley et al., 2013)), and an expected withdrawal rate of 30%. Based on these, it was concluded that if 12 subjects completed the study, this would be sufficient to draw relevant conclusions.

2.3 NCT01231542 study

NCT01231542 was a phase I, open-label, two-arm, fixed-sequence crossover study in healthy adults between 18 and 65 years run in Baltimore, Maryland, United States (Dooley et al., 2013). The study design is shown in **Figure 2.3.** For individuals to be included, one had to be negative for HIV, and hepatitis C, and have liver function enzymes >1.5 times the upper limit of normal. The criteria for exclusion were "*creatinine >1.5 mg/dL, haemoglobin ≤12.0 g/dL in men or ≤11.0 g/dL in women, absolute neutrophil count <1250 cells/mm^3, platelets <125,000 cells/mm^3, electrocardiogram with QTc > 450 ms, or evidence of active tuberculosis*."

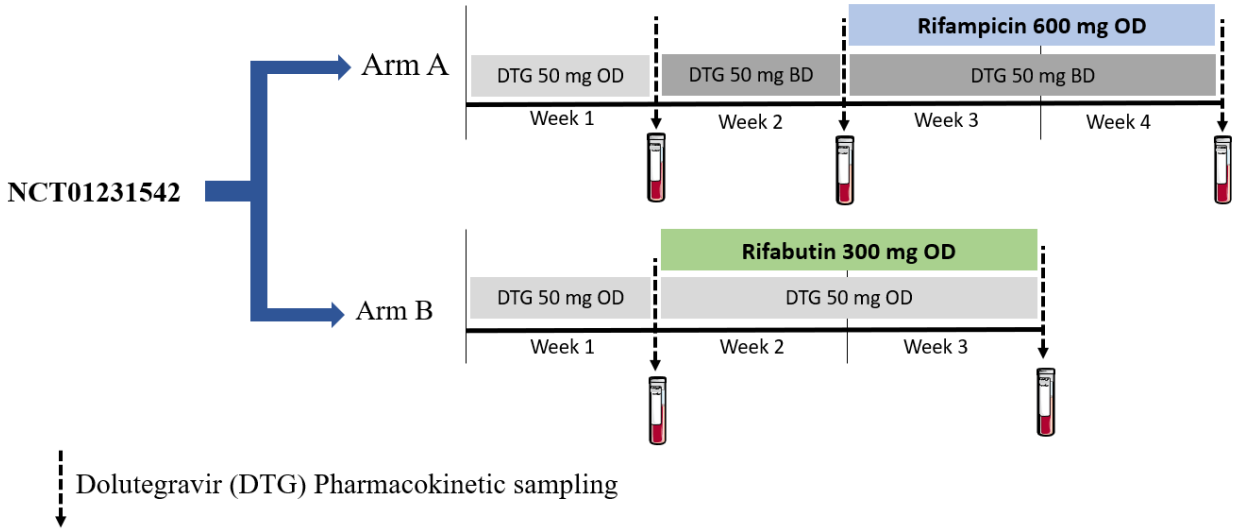

Figure 2.3 NCT01231542 Study design and pharmacokinetic sampling schedule

Arm-A volunteers received 50 mg dolutegravir OD for seven days, then 50 mg dolutegravir twice daily (BD) for seven days, and lastly 50 mg dolutegravir BD with 600 mg rifampicin OD for 14 days. Arm-B volunteers received 50 mg dolutegravir OD for seven days, followed by 50 mg dolutegravir OD with 300 mg rifabutin OD for 14 days.

Steady-state plasma samples were collected pre-dose and 1, 2, 3, 4, 5, 6, 8, and 12 hours post-dose on the last day of each dolutegravir regimen. For the OD regimens, a 24-hour sample was also collected. Dolutegravir doses were taken after an overnight fast (Dooley et al., 2013).

The sample size for NCT01231542 was based on previous dolutegravir pharmacokinetic studies, with the following assumptions: an estimated within-subject variability (CV%) of 33%, an expected withdrawal rate of 20%, and only a difference of 25% or more in exposures deemed to be clinically relevant. With these assumptions, it was estimated that 12 subjects were enough to achieve 10 evaluable subjects in each arm with "*a precision for half the width of the 90% confidence interval (CI) on the log scale for the treatment difference that would be within 26% of the point estimate for the AUC, peak concentration, and trough concentrations*."

2.4 INSPIRING study

International Study of Patients with HIV on Rifampicin ING (INSPIRING) was an open-label, noncomparative, active control, randomized, study among ART-naive adults living with HIV and co-infected with drug-sensitive tuberculosis (Dooley et al., 2020). The study design is shown in **Figure 2.4.**

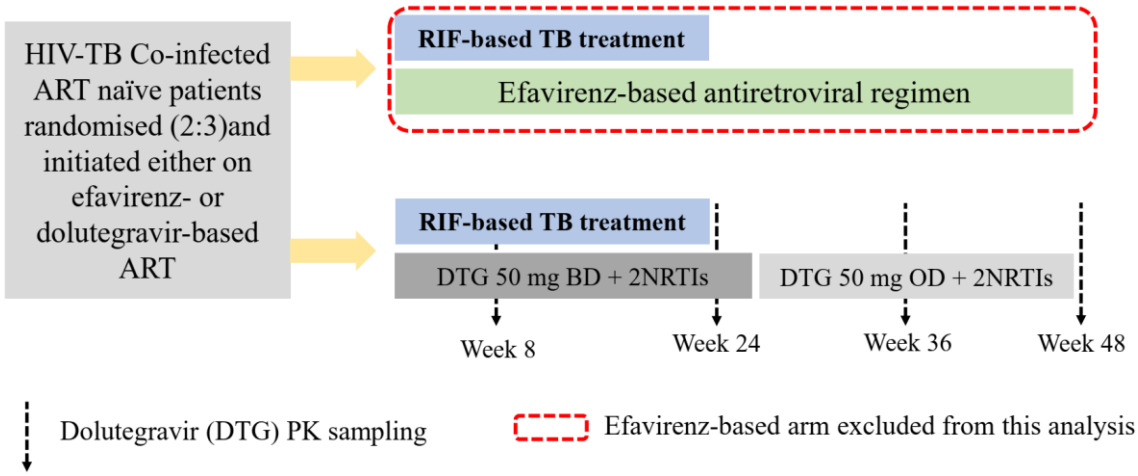

Figure 2.4 INSPIRING Study design

It enrolled adults with culture-proven pulmonary, pleural, or lymph node tuberculosis. Inclusion required an HIV-1 viral load of ≥1000 copies/mL and a CD4+ count of ≥50 cells/mm3. The exclusion criteria included individuals whose primary HIV infection was resistant to NRTI, NNRTI, or PI; those with CNS, miliary, or pericardial tuberculosis; those with hepatitis B; hepatic impairments (Class B or C Child-Pugh score); alanine aminotransferase values that are twice the normal upper limit; haemoglobin less than 7.4 g/dL and a platelet count <50 000/mm^3.

During and after tuberculosis treatment, participants were randomly assigned (3:2) to either a dolutegravir- or efavirenz-based antiretroviral regimen. Together with 2 NRTIs, dolutegravir was dosed at 50 mg twice daily during and for 2 weeks after tuberculosis treatment, then 50

mg OD while efavirenz was dosed at 600 mg once daily. The NRTI backbone was selected by the investigator based on treatment guidelines. For abacavir, this involved testing for human leukocyte antigen-B*5701 before testing for abacavir.

Prior to baseline, participants received rifampicin-based tuberculosis treatment (≤8 weeks), through their local tuberculosis program, which continued throughout the study.

Sparse pharmacokinetic samples were drawn at week 8 (on rifampicin) and week 36 (off rifampicin) pre-dose, 1–3, and 4–12 hours post-dose. A pre-dose sample was also drawn at weeks 24 and 48, on and off rifampicin respectively.

2.5 ADVANCE study

ADVANCE was a phase 3, open-label, randomized (1:1:1 ratio) trial in South Africa in which HIV-positive, ART naïve individuals were assigned to either of three treatment arms, 1) dolutegravir, TAF and emtricitabine; 2) dolutegravir, TDF and emtricitabine; or 3) efavirenz, TDF and emtricitabine. The trial enrolled participants in Johannesburg from February 2017 to May 2018 (Venter et al., 2019).

Individuals ≥ 12 years, with a weight of ≥ 40 kg and viral load ≥ 500 copies/ml were eligible for inclusion in the study. Individuals less than 19 years of age were required to have a creatinine clearance of > 80 mL/min while those ≥ 19 years should have a creatine clearance (calculated with the Cockcroft–Gault formula) of > 60 mL/min. Those excluded include pregnant women, those on current tuberculosis treatment and those treated with any antiretroviral therapy within the past 6 months.

For each of the 3 arms, drugs were administered as TAF (25 mg, Gilead Sciences), co-formulated with emtricitabine (200 mg, Gilead Sciences), dolutegravir (50 mg, ViiV Healthcare); TDF (300 mg), co-formulated with emtricitabine (generic manufacturers), dolutegravir (50 mg, ViiV Healthcare); co-formulated TDF/emtricitabine plus efavirenz (600

mg) (generic manufacturers) as a single daily tablet. For ADVANCE, a sample size of 350 subjects per arm was estimated to have 80% power to show noninferiority in efficacy of the TAF-based regimen compared to a TDF-based regimen or standard of care. (Efavirenz based regime)

Chapter 3 Methodology

This thesis revolves around the application of mathematical and statistical models to analyse data obtained from clinical trials, a methodology that goes under the name of pharmacometrics.

3.1 Pharmacometrics

Pharmacometrics has been defined as "*the science of developing and applying mathematical and statistical methods to (a) characterise, understand, and predict a drug's pharmacokinetic and pharmacodynamic behaviour; (b) quantify the uncertainty of information about that behaviour; and (c) rationalize data-driven decision making in the drug development process and pharmacotherapy. In effect, pharmacometrics is the science of quantitative pharmacology*" (Ette & Williams, 2013). Pharmacometrics applies quantitative models of biology, pharmacology, physiology, and disease progression to describe the pharmacokinetics-and- pharmacodynamics of drugs in relation to their effects and adverse drug reactions in patients (Barrett et al., 2008).

Pharmacokinetics describes the dynamic movements and "*the time course of drug concentration in different body spaces such as plasma, blood, urine and tissues"* (Gabrielsson & Weiner, 2016). It informs us on what the body does to the drug, thus describing drug absorption, distribution, metabolism, and excretion processes. Pharmacodynamics describes the relationship between drug concentration and the effect, both therapeutic and adverse (Southwood, Fleming & Huckaby, 2018). Together pharmacokinetics and pharmacodynamics characterise the relationship between dose and response. In 1999, the FDA recommended the use of a branch of pharmacometrics called population pharmacokinetic modelling to identify differences in the safety and efficacy of drugs among population subgroups (FDA, 1999).

3.2 Population pharmacokinetics

This involves the study of the pharmacokinetics of a drug at a population level, where data from all individuals are evaluated simultaneously and variability among individuals and its sources is quantified (Williams & Ette, 2000). This variability can be measured and accounted for in terms of patient variables including weight, age, sex, or concomitant therapies. Population pharmacokinetics aims to identify and characterise factors that may alter or influence drug disposition and exposure enough to require dose adjustment.

Population pharmacokinetic-pharmacodynamic modelling often employs the use of models to summarize large amounts of pharmacokinetic and/or pharmacodynamic data obtained from sampling individuals within a population. From these models, we can make inferences about the behaviour of a drug in the entire population.

Simply put, models are representations of a "system" that are designed to improve our understanding of the system. Various processes including drug action, physiological changes and disease progression can all be explored and described with models. Models can be descriptive or predictive. Descriptive models characterise/describe a system/observed data while predictive models can be used to explore scenarios outside what is observed by use of simulations (Owen & Fiedler-Kelly, 2014). To be predictive, one needs to be relatively confident that a particular model can be applied to scenarios outside those from which it was developed. For example, a model developed in a paediatric population might be descriptive and predictive within that population. However, if one were to extrapolate to older children/adults, consideration for differences such as enzyme maturation would need to be incorporated into the model to render it more reliable for predicting parameters within this older population.

3.3 Nonlinear mixed-effects modelling

A nonlinear mixed-effects (NLME) model is a hierarchical mathematical framework that allows for the analyses of data from different individuals of a population simultaneously (Mould & Upton, 2012). Often, pharmacokinetic data involves the collection of longitudinal data from the same participants on one or more occasions after either a single or multiple doses. These observations captured from the same individual over time are not independent of each other and therefore require the use of special statistical techniques to take this correlation into account (Twisk, 2013). Mixed-effects modelling is one such technique that takes this correlation into account.

The 'mixed-effects' term denotes the fact that the model is made up of both fixed and random-effects parameters and that during the model building process, these are estimated simultaneously. While random effects vary among individuals, the assumption is that fixed effects remain constant within a population. The 'nonlinear' term suggests that the dependent variable (such as drug concentration) relates to the independent variables (such as time) and model parameters (such as clearance) in a nonlinear way.

NLME models are defined hierarchically and usually comprise three major components i.e., (i) the structural submodel, (ii) the statistical submodel, and (iii) the covariate submodel.

3.3.1 Structural submodel

This describes the central tendency or typical behaviour of the dependent variable across time. For drug concentration data, the structural model aims to describe the typical plasma concentration-time profile of the drug for a population. For pharmacodynamic data, the model describes how drug effect changes over time. (e.g., concentrations of a biomarker).

A structural model can be represented mathematically by **equation 3.1**, based on i individuals and j observations.

$$Y_{ij} = f(\phi_i, x_{ij}) + \varepsilon_{ij}$$

Equation 3.1

Y_{ij} is the prediction of the i^{th} individual at the j^{th} observation. For the i^{th} individual, f denotes a nonlinear function that describes the individual predictions which are dependent on a vector of structural model parameters ϕ_i (such as clearance and volume) and on independent variables (x_{ij}) such as dose and sampling times. ε_{ij} represents residual unexplained variability which represents the deviation of the individual prediction from the observed value. Commonly, the building blocks of structural models consist of "compartments". A "compartment" is defined as a region of the body in which the drug is well mixed and kinetically homogenous (Mould & Upton, 2012).

3.3.2 Statistical submodel

This describes the variability (random effects) around the prediction from the structural model. In population models, variability is classified as level 1 (L1), i.e. inter-individual and inter-occasion variability in the model parameters (e.g. clearance) or as level 2 (L2), i.e. the variability between the model prediction and the observed dependent variable (e.g. drug concentration), this is also referred to as residual unexplained variability (Owen & Fiedler-Kelly, 2014). The L1 random effects describe how much the estimated individual parameters vary from the typical population parameter value. They are generally denoted ETA and assumed to follow a normal distribution with a mean of zero and an estimated variance of ω^2. On the other hand, L2 random effects are usually denoted epsilon with a mean of zero and variance σ^2.

Between-subject variability

The unexplained deviation between individual parameter values and the typical population model parameter is quantified by between-subject variability (BSV). To prevent model parameters from taking on negative, physiologically implausible values, an assumption that they follow a log-normal distribution is made and as such BSV is usually included on model parameters using an exponential relationship.

$$\phi_{ki} = \theta_k \cdot e^{\eta_{ki}} \qquad \eta_k \sim N(0, \omega_k^2)$$

Equation 3.2

Where the k^{th} structural model parameter (ϕ_{ki}) of the i^{th} individual is defined by the typical population parameter value (θ_k) and individual influence ($e^{\eta_{ki}}$). An assumption is made that the random-effects parameters η_{ki} follow a gaussian distribution with a mean of zero and a variance of ω_k^2. Usually, the variance of random-effects parameters is converted to and reported as the coefficient of variation (CV) to ease interpretation. The CV for log-normally distributed parameters can be computed as shown below (Owen & Fiedler-Kelly, 2014; Elassaiss-Schaap & Duisters, 2020)

$$\%CV = \sqrt{e^{\omega_k^2}} \cdot 100$$

Or $$\%CV = \sqrt{e^{\omega_k^2} - 1} \cdot 100$$

Equation 3.3

Between-occasion variability

Pharmacokinetic parameters are generally assumed to be constant within an individual, but in some study designs, subjects are observed over time on more than one visit and pharmacokinetic samples are available on each of these occasions. Possible changes in pharmacokinetic parameters within an individual over time can be quantified with an additional level of variability, called between-occasion variability (BOV). BOV accounts for unexplained

deviations of a parameter value within an individual between different sampling or dosing occasions.

Although the importance of including BOV in population pharmacokinetic analyses has been highlighted before (Karlsson & Sheiner, 1993), the use of BOV remains relatively uncommon and often sub-optimally implemented, because the definition of what constitutes a pharmacokinetic "occasion" is unclear.

Specifying a pharmacokinetic occasion is usually dependent on the available data, and on the pharmacokinetic parameter that is considered to be changing between the occasions.

For dispositions parameters (clearance and volume of distribution), which generally do not change quickly, one would consider including between-occasion between visits that are days/weeks/months apart. For parameters characterizing the absorption of orally administered drugs, however, one should consider every dose as a separate occasion, because oral absorption is a very irregular process. These considerations are particularly important when modelling data from regimens with repeated dosing, such as HIV ART. The drug concentrations are generally observed around a dose that is part of a series, so it is customary to collect a "pre-dose" sample just before the administration of the "main" study dose, followed by the collection of a complete pharmacokinetic profile aiming to characterize appearance and disappearance of the drug after the "main" dose. In this case, the pre-dose concentration depends on the dosing history and the value of the pharmacokinetic parameter before the "main" dose, so it should be considered as part of the same pharmacokinetic occasion as the preceding dose from the day before. While the "main" dose and ensuing samples should be lumped into their own pharmacokinetic occasion with its own values of absorption parameters. On the other hand, it is not feasible to include a separate occasion for each dose administered in a long regimen, as these can be a very large number. So, for all doses where no observed data is available, the BOV terms are excluded, which is consistent with their average value of 0 within each patient.

Implementation of BOV in the NONMEM dataset

In the software NONMEM, the coding of pharmacokinetic occasions consecutive to one another (e.g., repeated dosing) needs care. Depending on which subroutine is used for the model, the value of the variable used to denote a separate occasion may be carried forward or backwards. This is best explained by looking at an example dataset in **Figure 3.1**. For two consecutive occasions 1 and 2, if there is a gap in time between the last record of occasion 1 and the first record of occasion 2, the value from occasion 1 is carried forward if models with a closed form solution are used (ADVAN 1, 2, 3, 4, 5, 7, 10, 11, and 12), otherwise, it already assumes the values from occasion 2 for user-defined differential equations models (ADVAN 6, 8, 9, 13, or 14). Therefore, for these latter user-defined differential equations models, a "dummy" record should be included to protect the change of occasion. A dummy record is an EVID=2 record with the same time as the "new" occasion, but the "old" value of occasion, thus effectively reducing to 0 the gap in time between the records in which there is a change in the value of the occasion. Therefore, when preparing NONMEM-specific datasets, one should keep this in mind.

Dataset including BOV in NONMEM (ADVAN 1, 2, 3, 4, 5, 7, 10, 11, 12)

ID	TIME	AMT	OCC	WT	WHAT	COMMENT
1	0	50	0	70	Start_Rx_morning	
1	12	50	0	70	Day1_Night dose	
1	24	50	0	70	Day2_Morning dose	
1	36	50	1	70	Day2_Night dose	change1
1	47.83	.	**1**	70	Pre-dose_sample	
1	48	50	2	70	Day3_Morning dose	change2
1	50	.	2	70	2hr_sample	
1	52	.	2	70	4hr_sample	

*In models with a closed form solution, NONMEM applies "**Last observation carried forward (LOCF)**". Therefore, between times **47.83** and **48** hours, the pharmacokinetic parameter applied will be taken from OCC = 1 (occasion 1) until the 48th hour when the parameter will be taken from OCC= 2 (occasion 2)*

Dataset including BOV in NONMEM (ADVAN 6, 8, 9, 13, or 14)

ID	TIME	AMT	OCC	WT	WHAT	COMMENT
1	0	50	0	70	Start_Rx_morning	
1	12	50	0	70	Day1_Night dose	
1	24	50	0	70	Day2_Morning dose	
1	36	50	**1**	70	Day2_Night dose	Occasion change 1
1	47.83	.	1	70	Pre-dose_sample	
1	48	50	**2**	70	Day3_Morning dose	Occasion change 2
1	50	.	2	70	2hr_sample	
1	52	.	2	70	4hr_sample	

*With general models using customised differential equations, NONMEM applies **"Next observation carried Backward (NOCB)**". Therefore, between times **47.83** and **48** hours, the pharmacokinetic parameter applied will be taken from OCC = 2 (occasion 2) until the 48th hour when the parameter will also be taken from OCC= 2 (occasion 2)*

Dataset with dummy records to protect switching occasion (Trick NONMEM to use LOCF instead of NOCB)

ID	TIME	AMT	OCC	WT	WHAT	COMMENT
1	0	50	0	70	Start_Rx_morning	
1	12	50	0	70	Day1_Night dose	
1	24	50	0	70	Day2_Morning dose	
1	**36**	**.**	**0**	**70**	**DUMMY_1**	**Switch happens here**
1	36	50	1	70	Day2_Night dose	Occasion change1
1	47.83	.	1	70	Pre-dose_sample	
1	**48**	**.**	**1**	**70**	**DUMMY_2**	**Switch happens here**
1	48	50	2	70	Day3_Morning dose	Occasion change2
1	50	.	2	70	2hr_sample	
1	52	.	2	70	4hr_sample	

*Dummy records inserted at the point just before the occasion is changed are used to protect the change of occasion. These are EVID=2 records with TIME and DATE of "**new**" occasion (**proceeding/next**) row but **"old"** value of occasion (from preceding /before row)*

Figure 3.1 Implementing BOV in NONMEM

Residual unexplained variability

Residual unexplained variability (RUV) explains the deviations between the observed data and the "individual" model prediction, i.e., the prediction obtained after using the subject- and occasion-specific value of the L1 random effects.

It is therefore a measure of different sources of variability including model misspecification, measurement error of the analytical assay and inaccuracy in the reporting data (inaccurate dosing and/or sampling times). RUV can be expressed within the model with an additive, proportional or joint (additive and proportional) function of the model prediction.

With an additive (constant) error model, each prediction carries the same error regardless of its magnitude and therefore compared to higher predictions, this error more heavily affects lower predictions. On the other hand, with a proportional error model, the error is proportional to the magnitude of the prediction and therefore compared to lower predictions this error more heavily affects higher ones.

3.3.3 Covariate submodel

Between-subject and -occasion random effects allow pharmacokinetic parameters to assume different values in different individuals or visits, but they do so in a stochastic way, with random variability. This means that one cannot predict which patients will have a smaller or larger value of a specific parameter, but only how much a certain parameter will vary within a population. Sometimes the variability between individuals and/or occasions can be predicted using additional available information on the individuals or the study. These are known as "covariates" and their effect on model parameters can be estimated as an additional fixed effect. Identifying covariates is one of the key objectives of a pharmacometrics analysis because it makes the model more predictive and allows insight into what is driving the variability observed in the data. The choice of a covariate to test in the model is either decided *a priori* (and it may be the main purpose of the study) or it is based on trends identified during the data

analysis and model development. Covariates may either be classified as continuous e.g., creatinine clearance, age or categorical e.g., sex or study arm. Depending on the number of categories available, categorical covariates may be dichotomized e.g. (pregnant, not pregnant) or multiple categories can be ordered for example (first trimester, second trimester, third trimester of pregnancy). Different methods can be used to implement covariate-parameter relationships as shown in the equations below.

Categorical covariates

Categorical covariates can be added to the model by estimating a fractional change or separate parameters for each category.

For the fractional change, take two potential categories (SEX=1, 2). In **equation 3.4** below θ_1 represents the fixed-effect parameter (absorption rate constant in this example) estimate for category SEX=1 which should ideally represent the category with most observations in the dataset. θ_2 describes the fractional change of θ_1 for covariate category (SEX=2)

$$if\ SEX = 1\ then\ TVKA = \theta_1$$

$$if\ SEX = 2\ then\ TVKA = \theta_1 \cdot (1 + \theta_2)$$

Equation 3.4

If one chooses to use separate parameters for each category, the equations would be as follows.

$$if\ SEX = 1\ then\ TVKA = \theta_1$$

$$if\ SEX = 2\ then\ TVKA = \theta_2$$

Equation 3.5

Continuous covariates

For continuous parameter-covariate relationships, the modeller can define the relationship between the value of the covariate and that of the parameter using a mathematical function. The optimal value of the parameters of the function are then estimated in the model. These

functions can assume a variety of forms, but the most common are listed below. Of note, when adding the influence of continuous covariates to a model, it is good practice to centre these around a set value. Centring can be done around the mean or median value of the covariate in the observed population or around an accepted standard value. For example, when centring weight, the 70 Kg value is often used (Mould & Upton, 2013). Centring can be achieved by subtracting the individual covariate value from the centre value or by dividing the covariate by the centre value. By centring, the raw value of a covariate is transformed/ shifted by the value of interest (centre). Compared to models including uncentered covariates, centring of covariates in a model improves the precision of parameter estimates and prevents parameter estimates that would be described by data outside the range of what we observe (Goulooze et al., 2019).

Linear relationship

With a linear covariate-parameter relationship, the structural model parameter increases or decreases linearly over the observed spectrum of values for the continuous covariate. An example is provided in **equation 3.6** and **3.7** below.

Equation 3.6 $$TVCL = \theta_1 + \theta_2 \cdot (CLCR)$$

Equation 3.7 $$TVCL = \theta_1 + \theta_2 \cdot (CLCR - CLCR_{median})$$

Where θ_1 represents the typical value of clearance when the covariate *CLCR* is 0 and θ_2 is the absolute change in clearance per mL/min different from 0. Alternatively, it can be written as shown in **equation 3.7** which θ_1 represents clearance for an individual with *CLCR* at the median value of $CLCR_{median}$ in mL/min and θ_2 represents the absolute change in clearance per mL/min different from the median value.

Hockey stick or piecewise relationship

A piecewise linear relationship, known also as a hockey stick relationship is described by two different slopes (one for each piece), implying that there are two different linear covariate-parameter relationships. An example of this relationship is provided by **equation 3.8**. In this example, the covariate (COV) is centred around the covariate value of 10 (the changepoint) for the model to remain continuous and assumes different slopes for the upper and lower range of the covariates joined at the changepoint/breakpoint. θ_1 represents the typical value for an individual whose covariate value is median_COV.

$$\text{IF}(\text{COV} \leq \text{median\_COV}) \text{ then } CLCOV = \theta_2 \cdot (\text{COV} - \text{median\_COV})$$

$$\text{IF}(\text{COV} > \text{median\_COV}) \text{ then } CLCOV = \theta_3 \cdot (\text{COV} - \text{median\_COV})$$

$$\text{TVCL} = \theta_1 \cdot (1 + CLCOV)$$

Equation 3.8

The power relationship

The power parameter-covariate relationship is non-linear and allows for the description of a variety of relationships because of its flexibility that is availed by the estimated coefficient (power) parameter (θ_2). θ_1 represents the typical value of an individual with the covariate value of median_COV.

$$CLCOV = (\text{COV}/\text{median\_COV})^{\theta_2}$$

$$\text{TVCL} = \theta_1 \cdot (CLCOV)$$

Equation 3.9

3.3.4 Absorption delay for oral drugs

To model the onset of absorption, two approaches have been considered in this thesis: the lag time model and the transit compartment model. Incorporating a delay in drug absorption often helps improvement in the fit of pharmacokinetic profiles for drugs that are administered extra vascularly. Failure to account for this, may lead to erroneous parameter estimates as highlighted by Nerella *et al* (Nerella, Block & Noonan, 1993). The lag time model implies that there is a

lag between the time the drug is administered and when it is appears in the absorption compartment, from which it is absorbed. Therefore, once this lag time elapses there is sudden drug absorption. The key limitation of this model is that it is not a good representation of the processes underpinning the ingestion of the tablet/syrup/pill, its navigation through the gastro-intestinal tract and the release of the drug molecule from the formulation. From a mathematical standpoint, the lag time is associated with numerical difficulties because of the sharp change (discontinuity) in the derivative of drug concentration. The transit compartment model describes the appearance of the drug into the absorption compartment as the result of its passage through a series of compartments, whose number can be estimated. This produces a smoother transition which has no sudden change point. While not 100% "physiological" since our gastrointestinal tract is much more complex, the resulting profile is more plausible and consistent with physiology (Savic et al., 2007).The transit compartment model has a few limitations compared to the lag time. First, it requires the estimation of the additional parameter of the number of transit compartment, if not pre-specified/hard coded. Second, its implementation in NONMEM and other software requires either the use of additional compartments/differential equations - when the number of transit compartments is pre-specified – or custom-written differential equations that need to be solved with a general solver, thus significantly increasing the computational time. For complex models or large datasets, it might not be feasible to use the transit compartment model.

In conclusion, one needs to be cognizant of the fact that the absorption model most suited for a specific dataset is heavily dependent on the amount of information available regarding the absorption phase of the drug. While the transit compartment model may be more flexible, plausible, and provide better fit to the data, it may be that the benefits of its use may be outweighed by the disadvantages of much longer run times.

3.3.5 Parameter estimation

In NLME modelling, parameter estimation is usually achieved using a maximum likelihood approach, which consists in identifying a set of parameter values that maximizes the likelihood of observing the data given the model. In the software NONMEM®, a maximum likelihood approach is used to estimate the parameters, where a joint function (objective function) of all model parameters and observed data is evaluated. This 'objective function value' (OFV) is defined as minus twice the natural logarithm of the likelihood, so instead of maximizing a likelihood function, the OFV is minimised (best fit = maximum likelihood = minimum OFV) (Upton & Mould, 2014).

For nonlinear mixed-effects modelling, the exact analytical solution of the likelihood function is not derived but approximated numerically because the random effects enter the model nonlinearly. In NONMEM®, this is handled by linearization of the marginal likelihood along the random effects. Linearization methods include the first order (FO) method, first-order conditional expectation (FOCE), FOCE with interaction (FOCE-I), and Laplacian. In this work, we used the FOCE with interaction method in NONMEM®. FOCE is an iterative process in which population mean estimates together with individual-specific parameters are estimated in a single step. In the first iteration, the likelihood for an initial set of parameters is evaluated. Next, these parameters are updated towards the direction of increasing likelihood (decreasing OFV). This process is repeated until set criteria for convergence are met. Adding the interaction option to FOCE allows for eta-epsilon interaction i.e., preserves the dependence of the model for intra-individual random error (epsilons) on etas during computation of the objective function.

Another approach for parameter estimation that does not involve linearization of the likelihood is the SAEM (Stochastic Approximation expectation-maximization) algorithm. SAEM (Lavielle & Aarons, 2016) is a stochastic, iterative algorithm for calculating the maximum

likelihood estimator. Considering that the SAEM algorithm was not used in this thesis, it is not discussed in further detail.

3.3.6 Advantages of population modelling

Population pharmacokinetics modelling has several advantages over classical analysis methods such as non-compartmental (NCA) analysis. Compared to NCA, it allows for the analysis of sparse data and therefore does not suffer from the same strict requirement on data, therefore reducing the burden of frequent blood sampling and thus increasing the feasibility of studies in populations where this would be difficult for example in neonates, pediatric, geriatric, pregnant or severely ill populations (Collart et al., 1992; Ette & Williams, 2013).

Population pharmacokinetics also allows for the integration and pooling of data from different study designs including from non-traditional, unbalanced designs, which do not lend themselves to the usual forms of pharmacokinetic analysis (FDA, 1999). With population pharmacokinetic modelling one can analyse data which is a mixture of both intense and sparse sampling, and no strict adherence to protocol sampling times in all patients is required.

Population pharmacokinetics provides a semi-mechanistic platform that enables the identification of relationships between parameters and physiological processes. For example, a population-pharmacokinetic model can be used to assess the overlapping effect of weight and age on the same or different pharmacokinetic parameters instead of the overall exposure.

Lastly, pharmacokinetic models can be reliably used for prediction and extrapolation, by employing simulations of validated models (Vo et al., 2017). Simulations can be used to explore alternative regimens to facilitate treatment optimisation or to assess drug response in other sub-populations. It can also be used to optimise study design, and inform sample size requirements (Gobburu & Marroum, 2001).

3.3.7 Software

The various software tools used throughout the PhD are summarized in the table below. Briefly, pharmacokinetic analyses were performed in NONMEM®, followed by sampling important resampling and/or bootstrap to determine the parameter precision (Boeckmann, Beal & Sheiner, 2011). Perl-speaks-NONMEM, Pirana and R were used to facilitate model development, tracking and documentation, data manipulation, and generation of model diagnostics (Keizer, Karlsson & Hooker, 2013a).

Table 3.1 Software

Software	Version	Reference	Key Functionalities/packages
NONMEM®	7.5	Icon Development Solutions, Ellicot City, MD, USA (www.iconplc.com/innovation/nonmem)	FOCE-I
PsN[a]	4.6	Uppsala University, Uppsala, Sweden (uupharmacometrics.github.io/PsN)	[b]VPC functionality Bootstrap functionality [c]SSE functionality [d]SIR
Pirana	2.8.1 to 2.9.6	Pirana Software and Consulting BV (www.pirana-software.com)	
R	3.6.0 to 4.2.0	The project for statistical computing. Vienna, Austria (www.CRAN.R-project.org)	*xpose* package *xpose4* package *ggplot2* package *tidyverse* package
R Studio	1.2.5033 to 1.4.1717-3	Integrated development environment for R, Boston, MA (www.rstudio.org)	
Notepad++	6.9 to 8.4.2		

[a]PsN, Perl speaks NONMEM; [b]VPC, visual predictive check; [c]SSE, stochastic simulation, and estimation; [d]sampling importance resampling

Computationally intensive modelling and simulations were performed using the University of Cape Town's ICTS High-Performance Computing: https://ucthpc.uct.ac.za/

3.3.8 Model development approach

The general steps followed during the development of a typical population pharmacokinetic using the nonlinear mixed-effects are illustrated in **Figure 3.2** and further elucidated below.

The first step involves data cleaning, dataset generation and exploratory data analysis (graphical and/or statistical) using R.

For this thesis, the NONMEM® software was used throughout the analysis and therefore, all data to be used was formatted with numerical data records that follow NONMEM® rules. For instance, this included dose and dosing time points, pharmacokinetic sample time points, and patient-specific demographic information.

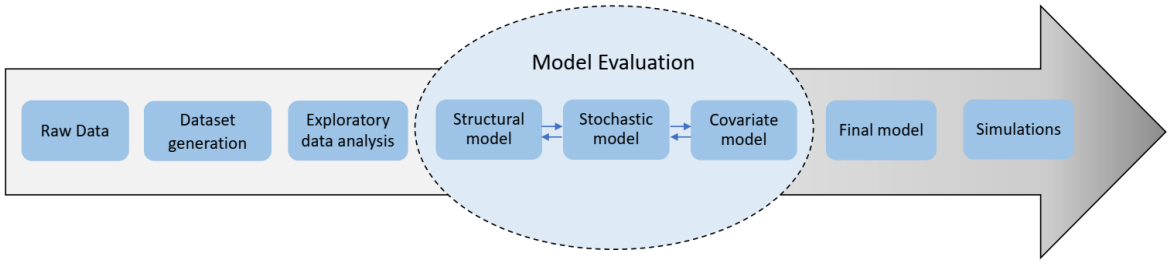

Figure 3.2 Model development procedure

The model development procedure generally started with evaluating alternative structural models, usually beginning with a simple one-compartment structural model with first-order absorption and elimination, then making things gradually more complex based on the data, scientific plausibility, and physiological rationale. This involved testing more complex disposition kinetics (such as two- or three-compartment disposition), a more flexible absorption framework (a lag time or transit compartments), saturable clearance, or more semi-mechanistic models such as the elimination from a liver compartment and first-pass extraction.

The statistical model included between-subject and -occasion variability and residual unexplained variability which comprised additive and proportional components. Allometric scaling was applied in the early phases of model development using either total body weight or fat-free mass as a size descriptor (Janmahasatian et al., 2005). The inclusion of patient covariates was then tested, following a stepwise approach, and was guided by biological plausibility and statistical significance based on a 5% level of significance in the forward step of covariate selection and a 1% in backward elimination.

The modelling process was guided by evaluating the change in objective function value (ΔOFV) between two nested models. The OFV is assumed to follow a χ^2-distribution, with a 3.84 drop in OFV significant at $p<0.05$ for one additional parameter (i.e., 1 degree of freedom). Secondly, the inspection of standard goodness of fit plots and visual predictive checks (VPC), consideration of biological plausibility, coherence with historical findings and clinical relevance were all considered in the model building process. In cases where modelling involved the pooling of different datasets, a model was developed first with one dataset (ideally the one with a richer sampling schedule) after which a new dataset was added and then the model was re-evaluated. For key interim models and the final model, parameter uncertainty was assessed via the nonparametric bootstrap method and/or sampling importance resampling (Dosne et al., 2016). To stabilise models utilising sparse data, the use of priors was explored (Chan Kwong et al., 2020).

Once we described the final model, we used this to perform Monte Carlo simulations, which is a mathematical technique involving repeated simulations that evolve stochastically. The term Monte Carlo refers to the stochastic nature of the simulations and derives its name from the gambling town in Monaco. In this research, we used Monte Carlo simulations to determine the probability of attaining dolutegravir trough concentrations above the target when different dosing regimens are used in the presence of rifampicin and rifabutin.

Chapter 4 Dolutegravir pharmacokinetics during co-administration with either artemether/lumefantrine or artesunate/amodiaquine

4.1 Abstract

Background: In sub-Saharan Africa, artemisinin-containing therapies for malaria treatment are regularly co-administered with ART. Currently, dolutegravir-based regimens are recommended as first-line therapy for HIV across most of Africa.

Objectives: To investigate the population pharmacokinetics of dolutegravir during co-administration with artemether/lumefantrine or artesunate/amodiaquine, two commonly used antimalarial therapies.

Methods: We developed a population pharmacokinetic model of dolutegravir with data from 26 healthy volunteers in two Phase I studies with a total of 403 dolutegravir plasma concentrations at steady state. Volunteers received 50 mg of dolutegravir once daily alone or in combination with standard treatment doses of artemether/lumefantrine (80/480 mg) or artesunate/amodiaquine (200/540 mg).

Results: A two-compartment model with first-order elimination and transit compartment absorption best described the concentration-time data of dolutegravir. Typical population estimates for clearance, absorption rate constant, central volume, peripheral volume and mean absorption transit time were 0.713 L/h, 1.68 h^{-1}, 13.2 L, 5.73 L and 1.18 h, respectively. Co-administration of artemether/lumefantrine or artesunate/amodiaquine increased dolutegravir clearance by 10.6% (95% CI 4.09% – 34.5%) and 26.4% (95% CI 14.3% – 51.4%), respectively. Simulations showed that simulated trough concentrations of dolutegravir alone or in combination with artemether/lumefantrine or artesunate/amodiaquine are maintained above the dolutegravir protein adjusted IC_{90} of 0.064 mg/L for more than 99% of the individuals.

Conclusions: Dolutegravir dose adjustments are not necessary for patients who are taking standard 3-day treatment doses of artemether/lumefantrine or artesunate/amodiaquine.

4.2 Introduction

HIV and malaria infections have overlapping geographical distributions, particularly in sub-Saharan Africa (Tshikuka Mulumba et al., 2012). Consequently, artemisinin-containing therapies recommended for malaria treatment are frequently administered to people living with HIV and receiving ART. In most of Africa, dolutegravir-containing antiretroviral regimens are recommended as first-line therapy for HIV (WHO, 2019). Dolutegravir is an integrase strand inhibitor that is mainly metabolized by uridine diphosphate glucuronosyltransferase 1A1 (UGT1A1) and to a lesser extent by cytochrome P450 (CYP) 3A4; (Reese et al., 2013a; Mercadel et al., 2014) both enzymes are prone to induction and inhibition (Chen et al., 2014; Guttman, Nudel & Kerem, 2019). Dolutegravir is administered at 50 mg once daily, which is sufficient to maintain trough concentrations (C_{24}) above 0.064 mg/L, the protein-adjusted 90% inhibitory concentration (PA-IC90) for HIV-1 (Cottrell, Hadzic & Kashuba, 2013).

Artesunate is a prodrug that is hydrolysed to dihydroartesunate by CYP2A6, while amodiaquine is extensively metabolized by CYP2C8 to *N*-desethylamodiaquine (Aweeka & German, 2008). Artemether and lumefantrine are metabolized to dihydroartemisinin and desbutyl-lumefantrine, respectively, mainly by CYP3A4, CYP2B6 and CYP2C9 (Aweeka & German, 2008).

Walimbwa *et al*. investigated the DDI between dolutegravir and artemether/lumefantrine or artesunate/amodiaquine using non-compartmental analysis (NCA) and showed that (i) co-administration of dolutegravir with artemether/lumefantrine resulted in a 37% and 6% decrease in dolutegravir C_{24} and $AUC_{0–24}$, respectively, and (ii) co-administration of dolutegravir with artesunate/amodiaquine resulted in a 42% and 24% decrease in dolutegravir C_{24} and $AUC_{0–24}$, respectively, compared with dolutegravir alone (Walimbwa et al., 2019).

With an adequate sampling schedule, NCA is a suitable tool to investigate the effects of a DDI on the overall exposure of the victim drug. However, quantification of the effect of a DDI on trough concentrations, which are based on single observations affected by measurement errors and possible discrepancies/uncertainty in sampling times, may be much less precise than on metrics such as AUC, which rely on concentrations measured from multiple samples, and are therefore more robust. A model-based approach uses an entire dataset to estimate the effect of a DDI on primary pharmacokinetic parameters, which can then be used to predict changes in exposure metrics like AUC and trough concentrations or to run simulations to assess the probability of attaining concentrations above the target PA-IC90 when co-administered with artemether/lumefantrine or artesunate/amodiaquine. Therefore, we have undertaken a model-based approach to further investigate the population pharmacokinetics of dolutegravir when co-administered with artemether/lumefantrine or artesunate/amodiaquine.

4.3 Methods

Two open-label clinical studies enrolling healthy volunteers were conducted by the Infectious Diseases Institute, Uganda to investigate the interaction between 50 mg of dolutegravir once daily plus standard 3-day treatment doses of artemether/lumefantrine (80/480 mg) or artesunate/amodiaquine (200/540 mg). Drugs were given with a standardized moderately fat meal. Rich sampling was performed after repeated dolutegravir dosing at steady state on two visits: (i) when the volunteers were on dolutegravir alone; and (ii) on the last day of co-administered artemether/lumefantrine or artesunate/amodiaquine. Samples were taken at 0, 1, 2, 3, 4, 8, 12 and 24 h post-dose. Dolutegravir concentrations were quantified using validated reversed-phase LC–tandem MS with a lower limit of quantification of 0.01 mg/L, as reported previously (Walimbwa et al., 2019).

Data were analysed by non-linear mixed-effects modelling with NONMEM® v7.4.3, Pearl-speaks-NONMEM v4.7.0 and Pirana v2.9.7. R v3.6.1 for computation and visualization of

graphical output. First-order conditional estimation with interaction was used for model runs. Various structural models were tested to describe the pharmacokinetics of dolutegravir, including one- and two-compartment disposition models, first-order elimination, and absorption, with or without absorption lag time and transit compartments. Log-normal distributions for between-subject and -occasion random effects were assumed, and we tested error models with additive and/or proportional components to describe the residual variability. Implausible concentrations were identified based on graphical exploration of individual concentration-time profiles and the absolute value of conditional weighted residual (CWRES) being larger than 4. CWRES follows a normal distribution with mean 0 and variance 1; hence, for a model that fits adequately, less than 0.01% of data are expected to have |CWRES| >4. These samples were excluded during the model development process and their exclusion was confirmed within the final model.

To adjust for body-size effect on disposition parameters, different descriptors, including weight and fat-free mass (FFM) as per Janmahasatian *et al*. (Janmahasatian et al., 2005), were tested with allometric exponents fixed to 0.75 and 1 for clearances and volumes, respectively. We investigated the effect of artemether/lumefantrine or artesunate/amodiaquine co-administration on dolutegravir pharmacokinetic parameters and a decrease in the objective function value (OFV) >3.84 (P<0.05) for forward addition and an increase in OFV >6.63 (P<0.01) for backward elimination were considered statistically significant.

Model development was guided by inspection of goodness-of-fit plots **(Figure S.4.1**), visual predictive checks (VPCs) and a drop in OFV. A non-parametric bootstrap (500 replicates) was run on the final model to generate the 95% CI for the parameter estimates.

The final model was used to simulate dolutegravir steady-state C_{24} concentrations for 3000 individuals on 50 mg of dolutegravir once daily alone and after 3 days of co-administration with artemether/lumefantrine or artesunate/amodiaquine. Simulations were performed for three typical males with body weights of 50, 70 and 90 kg and a height of 1.7 m. We used these

weights to derive three FFM values to investigate the interaction for different body compositions with 11%, 22% and 31% body fat. Simulated dolutegravir concentrations at C_{24} were then compared with the dolutegravir PA-IC90 of 0.064 mg/L.

4.4 Results

Twenty-six volunteers (62% male) were enrolled: 14 volunteers received dolutegravir followed by dolutegravir with artemether/lumefantrine, while 12 received dolutegravir then dolutegravir with artesunate/amodiaquine. The median (IQR) weight and age were 59.0 (54.4–63.5) kg and 28.5 (23.0–31.8) years, respectively. Volunteer demographics are summarized in **Table S 4.1** and have been reported previously (Walimbwa et al., 2019).

Four hundred and thirteen dolutegravir concentrations were available; 10 samples were identified as outliers, since they had |CWRES| >4, and were removed from the analysis. Eight of the samples were at C_{24}, with drug concentrations much higher than expected compared with the rest of the pharmacokinetic profile. No samples were below the limit of quantification.

The pharmacokinetics of dolutegravir following oral administration were adequately described by a two-compartment disposition model (ΔOFV=−47, $P<0.001$ compared with one-compartment) with transit compartment absorption. Compared to allometric scaling with weight, allometric scaling with FFM fit the data better and this was applied to all clearance and volume parameters. For a typical volunteer of (49 kg FFM), the model estimated clearance was 0.71 (95% CI 0.61–0.79) L/h, central volume of 13.2 (95% CI 11.9–14.7) L and peripheral volume of 5.73 (95% CI 4.05–28.8) L. Final parameter estimates and precision are presented in **Table S.4.2**.

Artemether/lumefantrine or artesunate/amodiaquine co-administration increased dolutegravir clearance by 10.6% (4.09–34.5) with ΔOFV=−9 ($P=0.0027$) and 26.4% (14.3–51.4) with ΔOFV=−35 ($P<0.001$), respectively. The VPC shows that the model adequately described the observed data (**Figure 4.1**). Simulated C_{24} for dolutegravir alone or co-administered with

artemether/lumefantrine or artesunate/amodiaquine showed that, in all three scenarios, more than 99% of individuals attained concentrations above the PA-IC_{90} of 0.064 mg/L (**Figure 4.2**). Our model-based simulations predicted a decrease in C_{24} of 13.2% and 27.1% during artemether/lumefantrine or artesunate/amodiaquine co-administration, respectively.

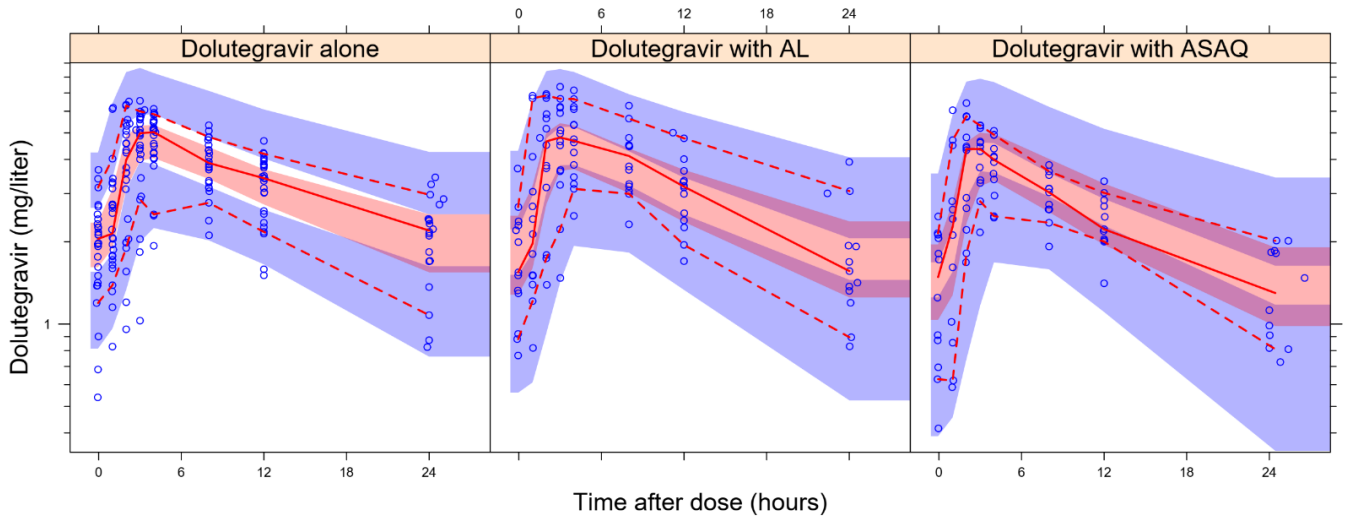

Figure 4.1 Visual predictive check of the final model

Blue circles represent observed plasma concentrations. The continuous line in the middle represents the median observed concentration, while the broken lines below and above it represents the 10^{th} and 90^{th} percentiles of the observed concentrations, respectively. The shaded areas around each line represent the 95% confidence boundary of the simulated prediction for the same percentiles. AL, artemether/lumefantrine; ASAQ, artesunate/amodiaquine.

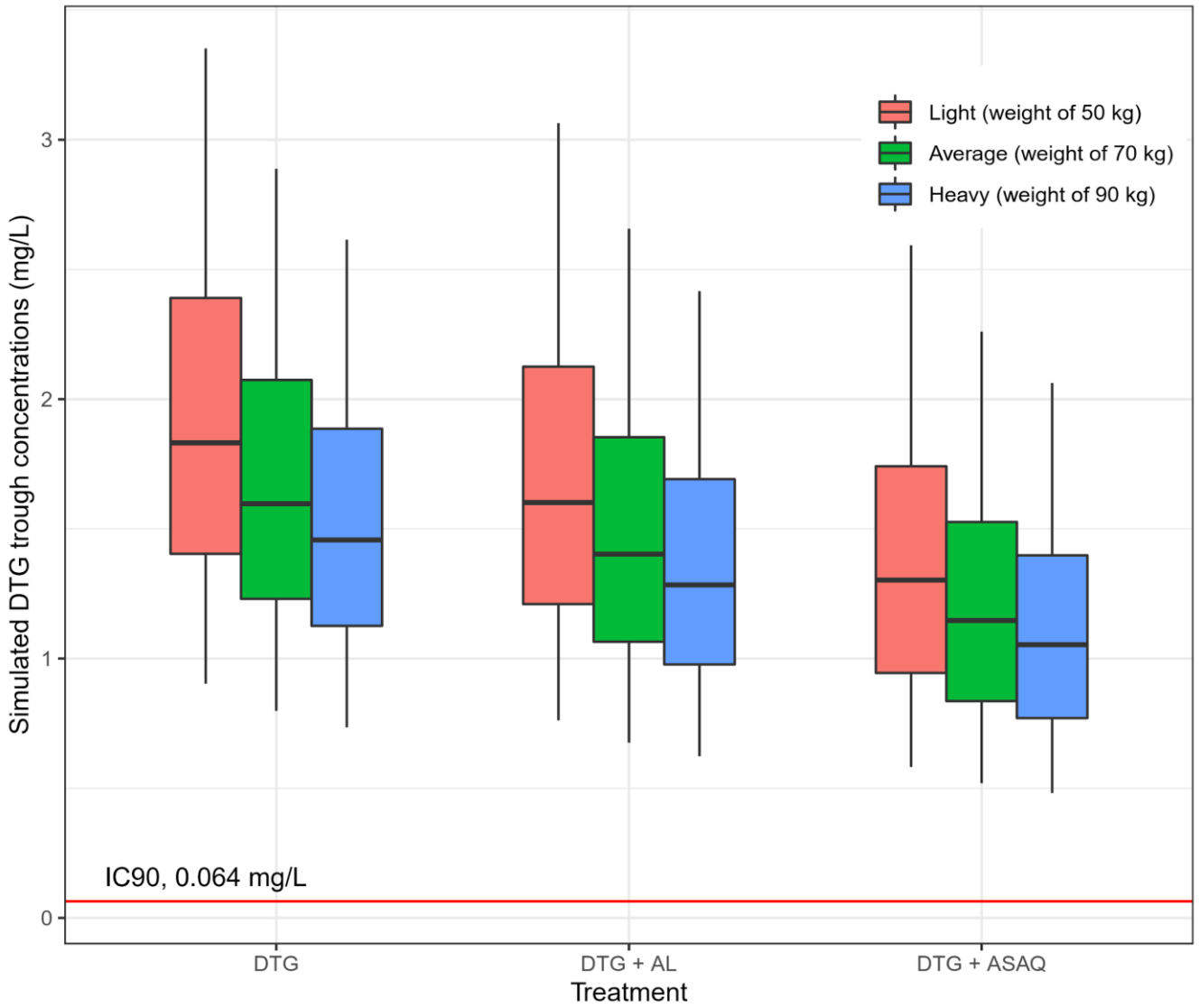

Figure 4.2 Simulated plasma trough concentrations of dolutegravir

Simulated plasma trough concentrations of 50 mg of dolutegravir once daily when administered alone (left), with artemether/lumefantrine (middle) or with artesunate/amodiaquine (right) based on 3000 simulated individuals categorized by weight. Whiskers show the 5th and 95th percentiles. The red line represents the dolutegravir PA-IC_{90} of 0.064 mg/L. DTG, dolutegravir; AL, artemether/lumefantrine; ASAQ, artesunate/amodiaquine.

4.5 Discussion

We observe that co-administration with artemether/lumefantrine led to a 10.6% increase in dolutegravir clearance, similar to the 6% decrease in AUC_{0-24} in Walimbwa *et al* (Walimbwa et al., 2019). However, we predict only a 13.2% decrease in C_{24}, which is much smaller than the 37% decrease in dolutegravir C_{24} previously reported (Walimbwa et al., 2019). The larger decrease in C_{24} observed in the NCA may have been driven by unexplainably high C_{24} in some

individuals in the dolutegravir-alone arm (Banda, Barnes & Maartens, 2019). The artemether/lumefantrine effect is consistent with the fact that artemether has been shown to induce its metabolism possibly via CYP3A4, (Lefèvre & Thomsen, 1999) which also plays a minor role in dolutegravir clearance.

Co-administration of artesunate/amodiaquine significantly increases dolutegravir clearance by 26% and decreases C_{24} by 27.1%. Both of these findings are comparable to the 24% decrease in dolutegravir AUC_{0-24}, but less than the 42% decrease in C_{24} that was observed in the NCA (Walimbwa et al., 2019). However, the mechanism for this interaction is unclear since both drugs are believed to be metabolized by different enzymes.

The artemether/lumefantrine and artesunate/amodiaquine interactions might be clinically relevant if co-administration is longer than 3 days. However, our analysis cannot determine this, because we do not know if the full induction effect is maximal after 3 days, at which we observed C_{24}. This is a limitation of our study.

We developed a model describing the pharmacokinetics of dolutegravir in healthy Ugandan volunteers and characterizing the DDI with artemether/lumefantrine or artesunate/amodiaquine. The population pharmacokinetic estimates described by our model are similar to previous reports (Zhang et al., 2015). However, we propose a two-compartment model, unlike the one-compartment model reported by Zhang *et al*. (Zhang et al., 2015). Study design differences may contribute to the different findings. The Zhang *et al*. (Zhang et al., 2015) study targeted patients rather than healthy volunteers, analysed pooled data from at least two trials and also utilized sparsely sampled data.

In conclusion, artemether/lumefantrine or artesunate/amodiaquine co-administration increases dolutegravir clearance and lowers its exposure. However, due to these malaria treatment regimens' episodic and short-term nature, coupled with their relatively small induction effect on dolutegravir clearance, trough concentrations remain above the target PA-IC90. Therefore, standard doses of dolutegravir can be maintained while on antimalarial therapy with

artemether/lumefantrine or artesunate/amodiaquine. However, should artesunate/amodiaquine be used for longer periods, e.g., for malaria prophylaxis, this interaction may become of clinical relevance and deserve further investigation. Also, clinicians would need to exercise caution if, in addition to this antimalarial therapy, dolutegravir is used with other drugs that can further reduce its concentrations, such as rifampicin or polyvalent cations.

4.6 Supplementary Materials

Table S.4.1 Participant demographics

Characteristic	Median (interquartile range) or no. (%) of volunteers		
	DTG with AL study (*n*=14)	DTG with ASAQ study (*n*=12)	Both (*n*=26)
Age (years)	25.5 (22.5-29.0)	30.5 (23.5-34.0)	28.5 (23.0-31.8)
Weight (kg)	58.5 (54.0-61.8)	60.3 (58.3-68.3)	59.0 (54.4-63.5)
Height (cm)	170 (163-171)	170 (159-174)	170 (160-173)
Fat-free mass (kg)[a]	48.5 (36.9-50.7)	49.5 (39.6-50.4)	48.6 (38.2-50.7)
Sex, n (%)			
Male	9 (64)	7 (58)	16 (62)
Female	5 (36)	5 (42)	10 (38)

DTG, dolutegravir; AL, artemether/lumefantrine; ASAQ, artesunate/amodiaquine.

[a] *Fat-free mass calculated by Janmahasatian et al.*

Table S.4.2 Final population parameter estimates for dolutegravir

Parameter description	**Typical Value (95% CI)[a]**	**Parameter Variability (% CV) [b](95%CI)**
CL_{49kg} * $(FFM/49)^{0.75}$(L/h)	0.713 (0.611 - 0.790)	BSV: 26.6 (19.5 - 32.1)
$V_{c;\ 49kg}$ * (FFM/49) (L)	13.2 (11.9 - 14.7)	
Q_{49kg} * $(FFM/49)^{0.75}$ (L/h)	0.844 (0.494 - 1.29)	
$V_{P;\ 49kg}$ * (FFM/49) (L)	5.73 (4.05 - 28.8)	
Relative bioavailability	1 Fixed	BOV: 22.0 (15.9 - 30.3)
Absorption mean transit time (h)	1.18 (0.956 - 1.55)	BOV: 60.8 (41.2 - 82.3)
Number of Transit compartments	31.6 (11.8 - 63.4)	
First-order absorption rate constant (/h)	1.68 (1.23 - 4.75)	BOV: 94.4 (63.8 - 175)
Covariates		
ASAQ co-administration on CL (%)	+26.4 (14.3 - 51.4)	
AL co-administration on CL (%)	+10.6 (4.09 - 34.5)	
Residual unexplained variability		
Proportional error (%)	4.99 (0.80 - 7.11)	
Additive error (mg/L)	0.197 (0.120 - 0.257)	

[a]95 % confidence intervals were obtained by non-parametric bootstrap (n = 500 replicates). FFM, fat-free mass (calculated by Janmahasatian et al); AL, artemether-lumefantrine; ASAQ, artesunate-amodiaquine; BSV, between-subject variability; BOV, between-occasion variability; %CV, coefficient of variation.

[b] Calculated by $\%CV = \sqrt{\omega} \cdot 100\%$

Eta and epsilon shrinkage of between-subject variability for clearance, between-occasion variability and residual error are below 25%.

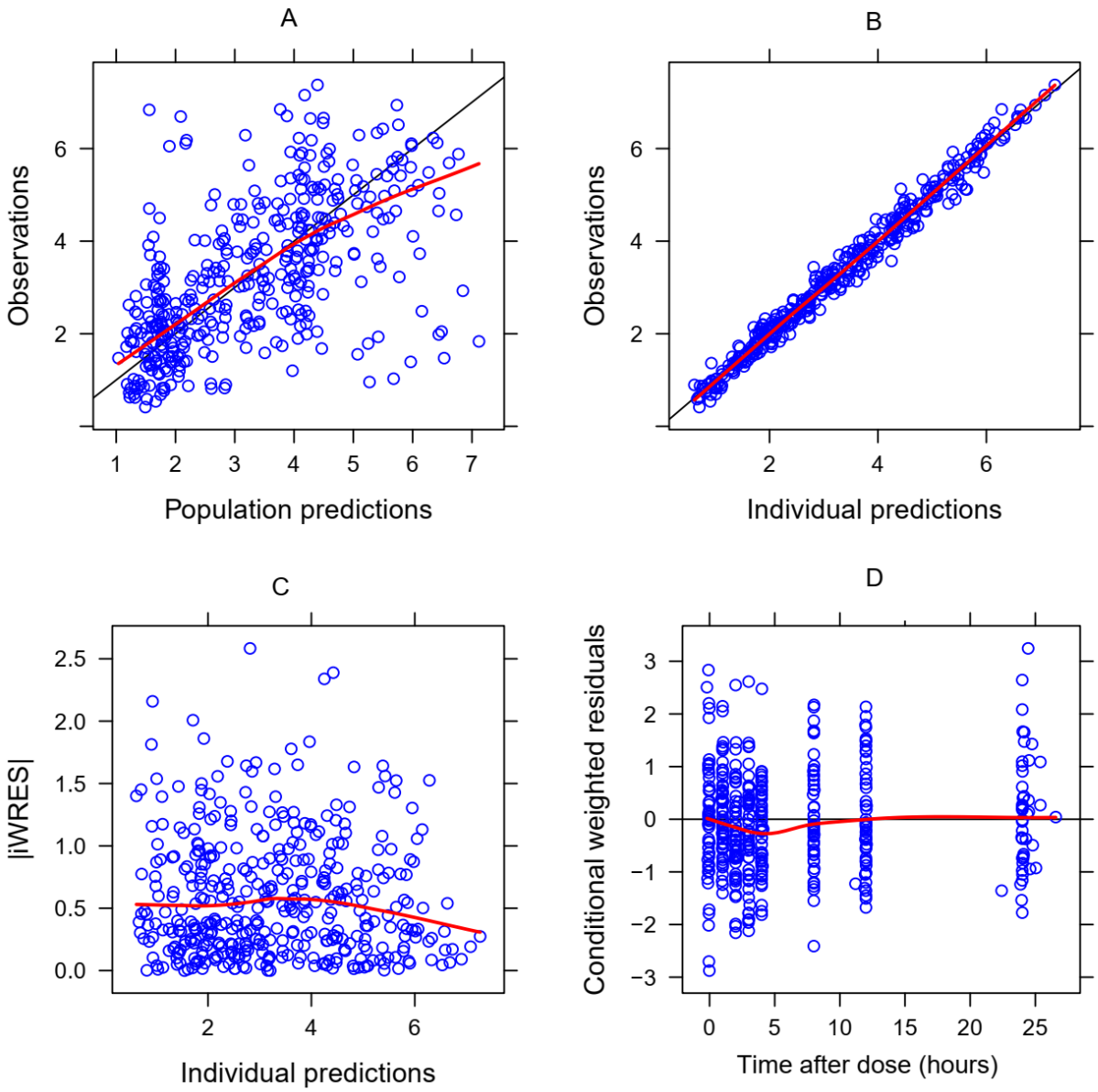

Figure S.4.1 Goodness-of-fit plots of dolutegravir final population pharmacokinetic model

Goodness-of-fit plots of dolutegravir final population pharmacokinetic model. Loess smooth curves of the ordinate values are printed in red. a) Observed concentrations vs. population predictions; line of identity is printed in black. b) Observations vs. individual predictions; the identity line is printed in black. c) Absolute individual weighted residuals (|IWRES|) vs. individual predictions. d) Conditional weighted residuals (CWRES) vs. time post-dose; ordinate value zero is printed in black.

Chapter 5 Population pharmacokinetic model and alternative dosing regimens for dolutegravir co-administered with rifampicin

5.1 Abstract

Dolutegravir-based regimens are recommended as first-line therapy for HIV in low- and middle-income countries where tuberculosis is the most common opportunistic infection. Concurrent HIV/tuberculosis treatment is challenging because of drug-drug interactions. Our analysis aimed to characterise dolutegravir's population pharmacokinetics when co-administered with rifampicin and assess alternative dolutegravir dosing regimens. We developed a population pharmacokinetic model of dolutegravir in NONMEM with data from two healthy-volunteer studies (RADIO and ClinicalTrials.gov identifier NCT01231542) and validated it with data from the INSPIRING study, which consisted of participants living with HIV. The model was developed with 817 dolutegravir plasma concentrations from 41 participants. A 2-compartment model with first-order elimination and lagged absorption best-described dolutegravir's pharmacokinetics. For a typical 70-kg individual, we estimated a clearance, absorption rate constant, central volume, and peripheral volume of 1.03 L/h, 1.61 h^{-1}, 12.7 L, and 3.85 L, respectively. Rifampicin co-administration increased dolutegravir clearance by 144% (95% confidence interval [CI], 126 to 161%). Simulations showed that when 50 or 100 mg once-daily dolutegravir is co-administered with rifampicin in 70-kg individuals, 71.7% and 91.5% attain trough concentrations above 0.064 mg/L, the protein adjusted 90% inhibitory concentration (PA-IC90), respectively. The model developed from healthy-volunteer data describes patient data reasonably well but underpredicts trough concentrations. Although 50 mg of dolutegravir given twice daily achieves target concentrations in more than 99% of individuals cotreated with rifampicin, 100 mg of dolutegravir, once daily, in the same population is predicted to achieve satisfactory

pharmacokinetic target attainment. The efficacy of this regimen should be investigated since it presents an opportunity for treatment simplification.

5.2 Background

Dolutegravir is now recommended by WHO for both first-line and second-line antiretroviral therapy (ART) regimens in low- and middle-income countries (LMIC) (WHO, 2019). Dolutegravir is mainly metabolized by uridine diphosphate glucuronosyltransferase 1A1 (UGT1A1) with cytochrome P450 (CYP) 3A4 playing a minor role. It is also a substrate of the efflux drug transporters P-glycoprotein and Breast Cancer Resistance Protein (BCRP) (Reese et al., 2013a; Mercadel et al., 2014). A once-daily dose of 50 mg is sufficient to maintain trough concentrations (C_{24}) well above 0.064 mg/L, the in-vitro protein-adjusted 90% inhibitory concentration (PA-IC_{90}) for HIV-1 (Cottrell, Hadzic & Kashuba, 2013). An alternative target of C_{24} > 0.3 mg/L has been proposed as the dolutegravir effective concentration (EC_{90}). 0.3 mg/L was the geometric mean trough concentration observed among patients in a phase IIb dose-ranging study who were dosed at 10 mg dolutegravir OD (Van Lunzen et al., 2012). 10 mg of dolutegravir once daily achieved a similar virological response as 50 mg once daily. Incidentally, all dose levels (10, 25, and 50 mg) displayed a similar profile of viral suppression and there was no signal that the lower dose achieved lower efficacy.

Tuberculosis is the most common opportunistic infection associated with HIV in resource-limited settings, causing over 25% of deaths among people living with HIV (Tshikuka Mulumba et al., 2012). Rifampicin is the cornerstone of anti- tuberculosis treatment and is a potent inducer of both UGT1A1 and CYP3A4, as well as P-glycoprotein and BCRP. The DDI between dolutegravir and rifampicin has been reported previously. In one study, twice-daily 50 mg dolutegravir plus 600 mg rifampicin achieved mean pharmacokinetic parameters (area under the concentration-time curve from 0 to 24 h(AUC_{0-24}), C_{24}) that were adequate i.e., 20% to 33% higher than once-daily 50 mg dolutegravir in the absence of rifampicin. Therefore, to

mitigate the risk of suboptimal dolutegravir concentrations, the recommended dosing for HIV/tuberculosis co-infected individuals on rifampicin-based tuberculosis treatment is 50 mg dolutegravir twice daily (Dooley et al., 2013).

However, BD dosing presents challenges, especially in LMIC where dolutegravir is dispensed as a fixed-dose combination (FDC) pill with tenofovir and lamivudine or emtricitabine, and stock-outs of the 50 mg single tablet are likely. Furthermore, once-daily (OD) dosing is associated with better adherence than twice-daily dosing (Nachega et al., 2014). A study in Botswana among HIV/ tuberculosis co-infected participants highlighted the challenge associated with the administration of an extra 50 mg dolutegravir single pill; 43.6% of the participants received only the once-daily FDC and did not receive the extra dose of 50 mg dolutegravir as recommended by the Botswana National and WHO anti-retroviral treatment (ART) guidelines for co-administration with rifampicin (Modongo et al., 2019).

In this analysis, we characterise the population pharmacokinetics of dolutegravir and identify relevant covariates, assess the interaction between dolutegravir and rifampicin, and identify and explore alternative dolutegravir dosing regimens. We pool data from two healthy volunteer studies to develop the model and validate it with data from patients with HIV-associated tuberculosis. Unlike non-compartmental analysis in a single study, the modelling approach allows us to simultaneously combine different studies and evaluate alternative dosing scenarios.

5.3 Methods

Study design and procedures

This analysis comprises data from two healthy volunteer studies: RADIO and NCT01231542, and one study conducted in persons living with HIV (INSPIRING). Study designs are visualized in **Figure 5.1**.

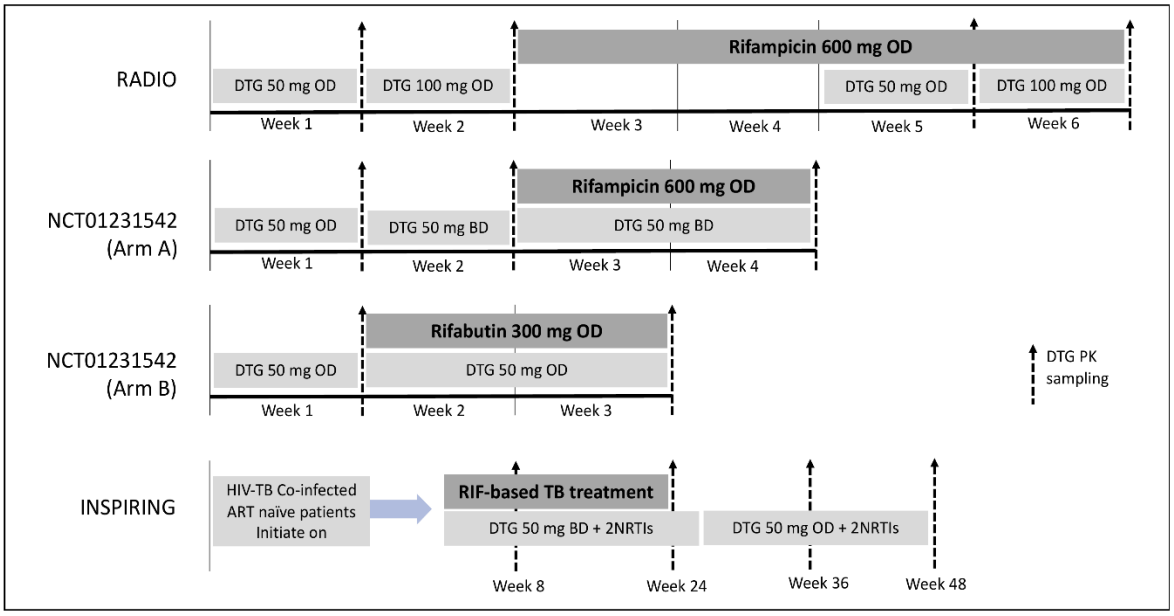

Figure 5.1 Schematic of the dosing regimen and pharmacokinetic sampling
Schematic of the dosing regimen and dolutegravir (DTG) pharmacokinetic (PK) sample collection for the different studies. This analysis excludes concentrations in arm B of the NCT01231542 study during weeks 2 and 3 (when participants received rifabutin). Once-daily (OD), twice-daily (BD), rifampicin (RIF), tuberculosis (TB), human immunodeficiency virus (HIV), nucleotide reverse transcriptase inhibitor (NRTI).

The RADIO study was a phase II, open-label, sequential pharmacokinetic study conducted at the St Stephen's Centre in London, UK (Wang et al., 2019). Healthy HIV-negative adults between 18 and 60 years with a body mass index between 18 and 35 kg/m^2 were included. Pregnant and lactating females were excluded**.** Volunteers received 50 mg dolutegravir OD for seven days, then 100 mg dolutegravir OD for seven days, then 600 mg rifampicin OD only for 14 days, followed by 50 mg dolutegravir OD plus 600 mg rifampicin OD for seven days, and lastly 100 mg dolutegravir OD plus 600 mg rifampicin OD for seven days. On the 7th day of each dolutegravir regimen, plasma samples were drawn pre-dose and 2, 4, 8, 12, and 24 hours post-dose. Dolutegravir doses were taken after a standard breakfast (Wang et al., 2019).

The NCT01231542 study was a phase I, open-label, two-arm, fixed-sequence crossover study in healthy adults between 18 and 65 years run in Baltimore, Maryland, United States (Dooley

et al., 2013). INSPIRING was carried out across 7 countries: Argentina, Peru, Brazil, Mexico, Russia, South Africa, and Thailand. South Africa alone had 8 recruiting sites and accounted for the largest number of participants.

Arm-A volunteers received 50 mg dolutegravir OD for seven days, then 50 mg dolutegravir twice daily (BD) for seven days, and lastly 50 mg dolutegravir BD with 600 mg rifampicin OD for 14 days. Arm-B volunteers received 50 mg dolutegravir OD for seven days, followed by 50 mg dolutegravir OD with 300 mg rifabutin OD for 14 days. Steady-state plasma samples were collected pre-dose and 1, 2, 3, 4, 5, 6, 8, and 12 hours post-dose on the last day of each dolutegravir regimen. For the OD regimens, a 24-hour sample was also collected. Dolutegravir doses were taken after an overnight fast (Dooley et al., 2013). Dolutegravir concentrations in the presence of rifabutin (part data from Arm-B of NCT01231542) were not included in the current analysis.

INSPIRING was a non-comparative, active control, randomized, open-label study conducted among treatment-naive adults living with HIV and with drug-sensitive tuberculosis (Dooley et al., 2020). Participants on rifampicin-based tuberculosis therapy (also containing isoniazid) were randomized to receive either dolutegravir- or efavirenz-based antiretroviral therapy during and after tuberculosis treatment. For this analysis, we utilized data from those randomized to receive the dolutegravir-based regimen. Participants were dosed at 50 mg BD during and 2 weeks after rifampicin-based tuberculosis treatment (according to local tuberculosis program protocols), followed by 50 mg OD for 52 weeks without rifampicin. Sparse pharmacokinetic samples were drawn at week 8 (on rifampicin) and week 36 (off rifampicin) pre-dose, 1–3, and 4–12 hours post-dose. A pre-dose sample was also drawn at weeks 24 and 48, on and off rifampicin respectively. 68% of the participants in the dolutegravir arm were of African heritage.

Analytical assay

For RADIO, dolutegravir plasma concentrations were measured by a validated reverse-phase ultra-high-performance liquid chromatography method as reported previously (Wang et al., 2019). Dolutegravir was measured at a wavelength of 258 nm and the assay was validated over a calibration range of 0.05–10 mg/L. In NCT01231542, dolutegravir was quantified using a liquid chromatographic method with tandem mass spectrometric detection, as previously described (Dooley et al., 2013). The calibration range for dolutegravir was 0.02–20 mg/L. For INSPIRING, plasma pharmacokinetic analysis was performed by PPD Laboratories Middleton, Wisconsin, USA. Concentrations were quantified via ultra-performance liquid chromatography, with tandem mass spectrometry detection using positive ion electrospray. The assay was validated over a concentration range of 0.02 to 20 mg/L. Quality controls for run acceptance were prepared and analysed with each batch of samples against separately prepared calibration standards to assess the day-to-day performance of the assay. For this analysis, no more than one-third of the quality control results deviated from the nominal concentration by more than 15% with at least 50% of the quality control results acceptable at each concentration.

Pharmacokinetic analysis

Concentration-time data were analysed using nonlinear mixed-effects modelling in NONMEM version 7.5.0 with first-order conditional estimation with eta-epsilon interaction. Perl-speaks-NONMEM (PsN) version 5.0.0, Piraña, and R v3.6.1 were used to aid the modelling process and to prepare model diagnostics. For RADIO, we used protocol sampling times because actual sample times were unavailable, while for NCT01231542 actual sampling times were used. We tested several structural models to describe the pharmacokinetics of dolutegravir including one- and two-compartment disposition models and first-order elimination and absorption, with or without absorption lag time, or transit compartments (Savic et al., 2007). In addition, we explored a model with elimination via hepatic extraction characterising the first-pass effect (Gordi et al., 2005). We included between-subject (BSV) and between-occasion (BOV)

random effects on the model parameters assuming a log-normal distribution. An occasion was defined as a dosing event leading to at least one observation. In this instance, each pharmacokinetic sampling visit had two occasions: the pre-dose occasion, and the post-dose occasion. BOV was incorporated on absorption parameters, while BSV was tested on disposition parameters. A combined error model with both additive and proportional components was used to describe the residual variability. The additive error was constrained to be at least 20% of the lower limit of quantification of the assay used in each study.

Model development and the inclusion of covariates were based on physiological plausibility, the inspection of goodness-of-fit plots, visual predictive checks (VPC), and a drop in the objective function value (OFV). The OFV was assumed to follow a chi-square distribution where, for every additional degree of freedom, a drop in OFV of at least 3.84 points was assumed as statistically significant at $P<0.05$. To adjust for the effect of body size on the disposition parameters, we included allometric scaling in the model and tested total body weight and fat-free mass (FFM) as body size descriptors (Janmahasatian et al., 2005). The allometric exponents for clearance and volume parameters were fixed to 0.75 and 1 respectively (Anderson & Holford, 2008). After the inclusion of allometric scaling, we investigated the following covariate effects on the pharmacokinetic parameters: sex, age, rifampicin co-administration, race, and study effect (RADIO vs. NCT01231542).

We added covariates in a stepwise manner in order of importance determined by the largest significant drop in the OFV. We also performed a backward elimination step where an increase in OFV> 6.63 ($P<0.01$) was considered statistically significant. A non-parametric bootstrap with 500 replicates stratified by the study was performed on the final model to generate the 95% confidence interval (CI) for the parameter estimates.

External validation

Pharmacokinetic data from the INSPIRING study was used to externally validate the final model (Dooley et al., 2020). A VPC was used to evaluate the predictive performance of the final model on the concentrations observed in INSPIRING. After external validation, we also aimed to fit a model to jointly describe patient data from the INSPIRING study together with the healthy volunteer data from RADIO and NCT01231542.

Simulations of target achievement with alternative regimens

The final model was used to simulate dolutegravir steady-state plasma C_{24} and C_{12} (for twice-daily dosing) for 3000 individuals with representative body weights of 50, 70, and 90 kg dosed with 50 mg OD dolutegravir alone, 50 mg OD dolutegravir with 600 mg OD rifampicin, 50 mg BD dolutegravir with 600 mg OD rifampicin, and 100 mg OD dolutegravir with 600 mg OD rifampicin. We then compared the individual simulated dolutegravir trough concentrations (C_{24} and C_{12}) across the different regimes and determined the percentage of the population achieving concentrations above 0.064 mg/L, the dolutegravir in vitro PA-IC_{90}.

5.4 Results

Study data.

A total of 41 participants (68% male) were enrolled in both healthy-volunteer studies. RADIO enrolled 16 participants: 14 completed the study, and 2 withdrew after the second week. All pharmacokinetic data from the 16 participants are included in the analysis. In the study under ClinicalTrials.gov identifier NCT01231542, 25 participants provided concentrations, 12 in arm A and 13 in arm B. The model was developed from a total of 817 samples, with a median (interquartile range) weight and age of 81.5 (69.5 to 88.6) kg and 43 (31 to 50) years, respectively. Participant demographics are summarized in **Table 5.1**. None of the samples had a concentration below the lower limit of quantification.

Table 5.1 Participant demographics

Characteristic	Median (interquartile range) or no. (%) of volunteer				
		NCT01231542 Study			
	RADIO Study (*n*=16)	Arm A (*n*=12)	Arm B (*n*=13)	INSPIRING (*n*=63)	All studies (*n*=104)
Male, n (%)	10 (62.5)	10 (83.3)	8 (61.5)	36 (57.1)	64 (61.5)
Weight (kg)	79.1 (67.1 – 88.2)	78.8 (68.6 – 93.3)	82.3 (80 – 87.5)	55.5 (49.5 – 65.3)	65.4 (52.8– 79.4)
Age (years)	31.5 (27.8 – 46.5)	48.0 (44.0 – 54.5)	43.0 (37.0 – 41.8)	34.0 (27.0 – 38.0)	35.0 (29.0 – 46.0)
Height (cm)	172 (168 – 177)	169 (166 – 182)	174.5 (170.2 – 179)	162 (157 – 168)	167 (160 – 172)
Fat-free mass (kg)	52.5 (47.04 – 62.6)	57.4 (51.3 – 62.6)	60.4 (48.5 – 63.5)	43.8 (36.5 – 47.1)	45.7 (40.4 – 54.9)

Dolutegravir pharmacokinetics.

The pharmacokinetics of dolutegravir were adequately described by a two-compartment disposition model (ΔOFV [change in the objective function value] = 247; P, 0.001 compared to the one-compartment model) with lagged absorption. The model with hepatic extraction characterising a first-pass effect did not describe the data better than the simpler first-order elimination from the central compartment. Allometric scaling with total body weight applied to all clearance and volume parameters improved the model (ΔOFV = 214.7). Scaling with fat-free mass (FFM) did not describe the data any better than scaling with total body weight. The model estimated a clearance of 1.03 L/h, a central volume of 12.7 L, and a peripheral volume of 3.85 L for a typical 70-kg individual. Final parameter estimates and their precision are presented in **Table 5.2**.

Table 5.2 Final population parameter estimates for dolutegravir.

Parameter description	**Typical value (95% CI)**[a]	**Parameter variability (% CV)** [c] **(95%CI)**
CL (L/h) [b]	1.03 (0.922, 1.15)	25.2 (14.5, 36.0)*
V_c(L) [b]	12.7 (10.6, 14.4)	
Q (L/h) [b]	0.883 (0.467, 1.64)	
V_P (L) [b]	3.85 (2.89, 5.72)	
Relative Bioavailability	1 Fixed	43.2 (35.9, 51.0)[#]
Absorption lag time NCT01231542 (h)	0.185 (0.00185, 0.406)	45.8 (14.4, 83.7)[#]
Absorption lag time RADIO (h)	0.984 (0.579, 1.44)	
K_a (/h)	1.61 (1.04, 2.87)	55.1 (33.4, 71.7)[#]
Covariates		
Rifampicin co-administration on CL (%)	+144 (+126, +161)	
Male sex on K_a (%)	-43.0 (-23.5, -60.1)	
Residual unexplained variability		
Proportional error (%)	8.83 (7.43, 9.91)	
Additive error (mg/L)	0.0318 (0.000318, 0.0742) + 20% LLOQ[d]	

[a]*95% confidence intervals were obtained by non-parametric bootstrap (n = 500 replicates).*

[b] Allometric scaling with weight (for a reference individual of 70 kg) was used for the clearance (CL), inter-compartmental clearance (Q), central volume of distribution (V_c), and peripheral volume of distribution (V_p). Coefficient of variation (%CV), bioavailability (F), absorption rate constant (K_a).
[c] Between-subject variability (BSV) and between-occasion variability (BOV) were assumed to be log-normally distributed and calculated by $CV\% = \sqrt{\omega^2} \cdot 100$
[d] lower limit of quantification (LLOQ) was study specific. 0.02 mg/L for NCT01231542 and 0.05 mg/L for RADIO. Eta and epsilon shrinkage of between-subject variability for clearance, between-occasion variability for all absorption parameters and residual error are below 20%.
** Between-subject variability. [#] Between-occasion variability*

Rifampicin co-administration increased dolutegravir clearance by 144% (95% confidence interval [CI], 126 to 161%) (ΔOFV = 2200; P, 0.001), while we did not observe any effect of rifampicin co-administration on dolutegravir bioavailability. Males had a 43% lower absorption rate constant (K_a) (ΔOFV = 210.1; P, 0.05), but no differences in clearance and bioavailability between sexes were identified.

We observed that the absorption lag time of dolutegravir for RADIO (in which participants received the drug with food) was about 5 times longer than that for NCT01231542 (where the drug was given under fasted conditions), 59 versus 11 min (ΔOFV = 239.1; P, 0.01). No statistically significant difference was observed in bioavailability between the two studies. The visual predictive check (VPC) in **Figure 5.2** shows that the final model described the observed data adequately, with the median, 10th, and 90th percentiles of the observed data falling within their respective 95% confidence intervals of prediction. The NONMEM code for the final model is provided in the supplemental material.

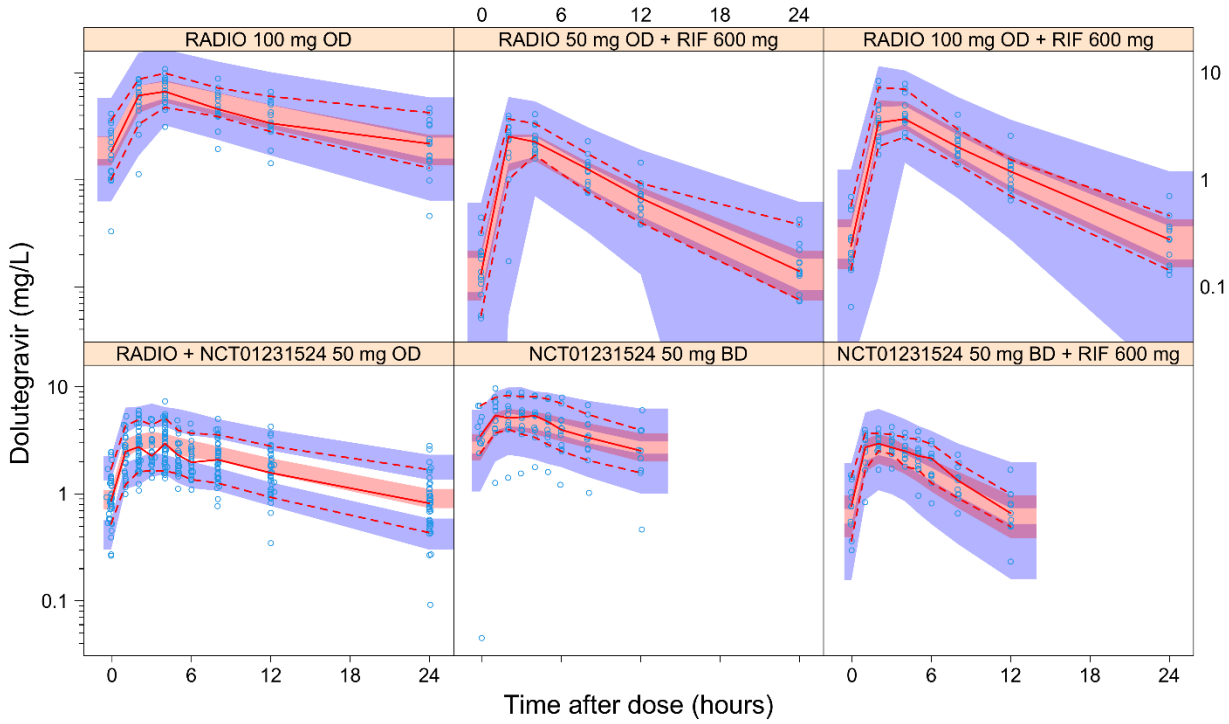

Figure 5.2 Visual predictive check of the final model

Blue circles represent observed plasma concentrations. The solid line in the middle represents the median observed concentration, the broken lines below and above it represent the 10th and 90th percentiles of the observed concentrations, respectively. The shaded areas around each line represent the 95% confidence boundary of the simulated prediction for the same percentiles. Once-daily (OD), twice-daily (BD), rifampicin (RIF).

External validation.

The external validation of the model with the INSPIRING data is provided in **Figure 5.3**. The VPC shows reasonable consistency, with the median, 10th, and 90th percentiles of the observed data falling within or close to their respective 95% confidence intervals. However, the model tends to underpredict pre-dose $C_{24/12}$ for both scenarios, whether patients are on or off tuberculosis treatment containing rifampicin. On the other hand, when participants are off rifampicin, the model overpredicts concentrations at the peak and after the peak. However, this is not expected to have any bearing on our predictions of different dolutegravir dosing scenarios when it is administered with rifampicin.

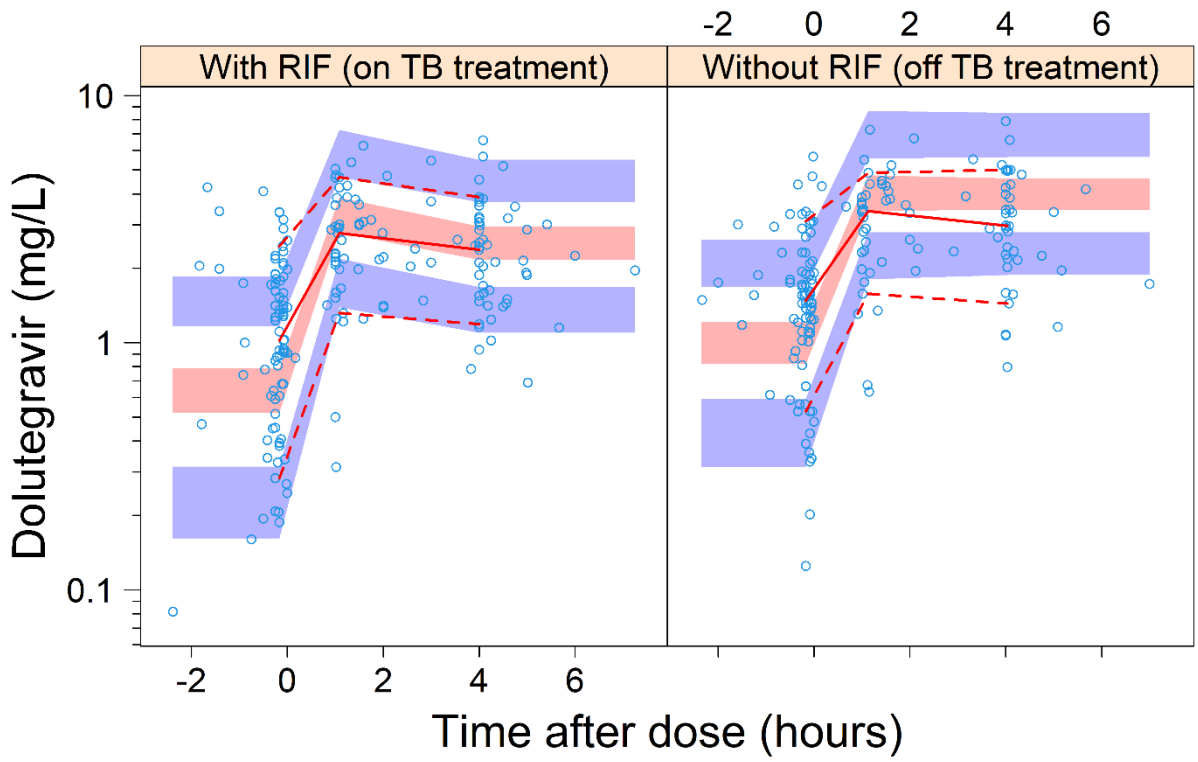

Figure 5.3 Visual predictive check of the final model in healthy volunteers fitted to patient pharmacokinetic data from the INSPIRING study

Visual predictive check of the final model in healthy volunteers fitted to patient pharmacokinetic data from the INSPIRING study. Blue circles represent observed plasma concentrations. The solid line in the middle represents the median observed concentration, the broken lines below and above it represent the 10th and 90th percentiles of the observed concentrations, respectively. The shaded areas around each line represent the 95% confidence boundary of the simulated prediction for the same percentiles. Rifampicin (RIF), tuberculosis (TB).

When we attempted to jointly describe the INSPIRING, RADIO, and NCT01231542 concentrations in a single model, we could not reliably identify a single explanation for the difference observed between healthy-volunteer (RADIO and NCT01231542) and patient (INSPIRING) data. Different values for ka, bioavailability, clearance, or the central volume of distribution, either singly or simultaneously, provided similar levels of goodness of fit. The most parsimonious model estimated a doubling of the central volume in patients compared to healthy volunteers. However, since the data could not reliably discriminate between the options, and this choice is crucial when performing simulations of $C_{24/12}$

(the parameter of interest for dolutegravir dosing), we decided not to proceed with co-modelling the three data sets. We preferred to perform simulations with the healthy-volunteer model while keeping in mind that it may slightly underpredict the trough concentrations.

Simulations.

Table 5.3 and **Figure 5.4** highlight the findings of the alternative dolutegravir regimens that we explored. When we simulate a regimen in which dolutegravir is co-administered with 600 mg rifampicin and dosed at 50 mg BD and 100 mg OD in 70-kg individuals, 99% and 91.5% attain trough concentrations above 0.064 mg/L (the PA-IC90), respectively. However, If the more conservative target of 0.3 mg/L is used, only 37.5% of 70-kg individuals attain concentrations above this target when dosed at 100 mg of dolutegravir OD with rifampicin. Of note, although there are suggestions of non-linearity at doses above 50 mg once daily, for this analysis, we did not observe any non—linearity for the 100 mg dose compared to the 50 mg dose and our model/ simulations did not incorporate this.

Table 5.3 Simulation results for alternative dosing regimens.

Regimen[a]	% attaining C_{24} [b] above 0.064 mg/L (IC_{90}) for population			Geometric mean individual predicted C_{24} (mg/L) for population[c]		
	90 Kg	70 Kg	50 Kg	90 Kg	70 Kg	50 Kg
50 mg OD	>99.0	>99.0	>99.0	0.765	0.878	1.05
50 mg OD with rifampicin	69.6	71.7	73.6	0.098	0.104	0.113
50 mg BD with rifampicin	>99.0	>99.0	>99.0	0.532	0.608	0.723
100 mg OD with rifampicin	91.0	91.5	92.2	0.205	0.220	0.239

[b]For the 50 mg BD with rifampicin regimen, values refer to the percentage above C_{12}
[a]OD; Once daily, BD; twice daily
*[c]Simulations were run under fasted conditions, with the final model described in **Table 5.2** including between-subject and between-occasion variability*

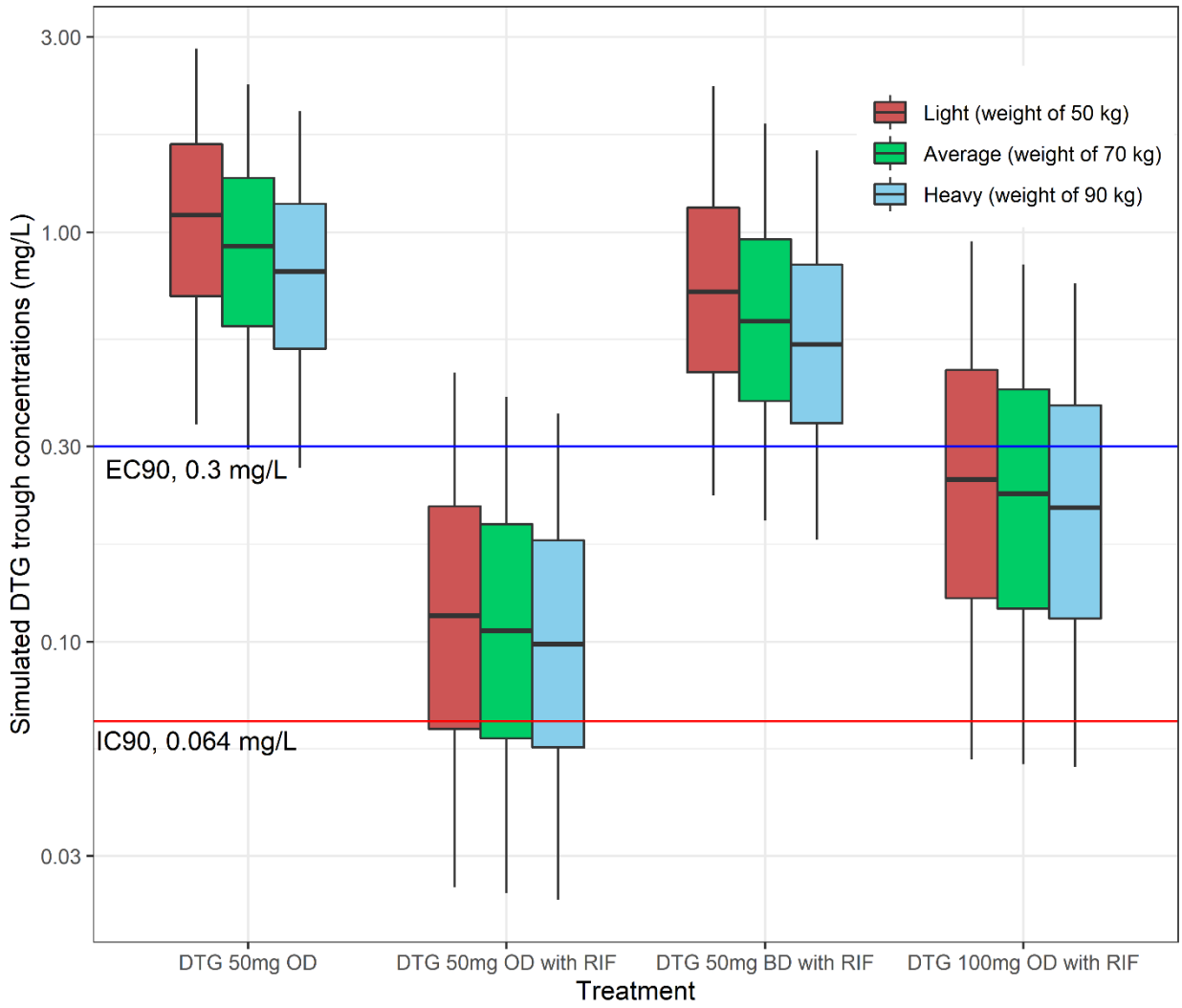

Figure 5.4 Simulated dolutegravir trough concentrations.

Simulated trough concentrations (C_{24} and C_{12} for the twice-daily regimen) of dolutegravir (DTG) when administered (from left to right) at 50 mg once-daily (OD), 50 mg OD with rifampicin (RIF), 50 mg twice-daily (BD) with rifampicin, and 100 mg OD with rifampicin respectively under fasted conditions with the final model described in ***Table 5.2*** *including between-subject and between-occasion variability. For the absorption lag time, we used the value estimated for the NCT01231542 study since this was done under fasted conditions. Simulations are based on 1000 individuals categorized by weight. The boxes represent the 25^{th,} 50^{th,} and 75th percentiles while the whiskers show the 5th and 95th percentiles. Protein-adjusted 90% inhibitory concentration (IC90), effective concentration (EC90)*

5.5 Discussion

We developed a model characterising the pharmacokinetics of dolutegravir at 50 mg OD and BD and 100 mg OD with or without co-administration of rifampicin 600 mg OD in healthy volunteers. We quantified the effect of rifampicin induction, which more than doubled dolutegravir clearance and dramatically reduced overall exposure. The increase in dolutegravir clearance we observed is in line with earlier studies (Barcelo et al., 2019; Parant et al., 2019) and consistent with the fact that rifampicin is a potent inducer of UGT1A1 and CYP3A4, the main enzymes involved in dolutegravir metabolism, as well as of the efflux drug transporters P-glycoprotein and BCRP.

Simulations from our model predict that dolutegravir 100 mg OD achieves trough concentrations above 0.064 mg/L in 91% of subjects receiving rifampicin. This pharmacokinetic result is encouraging, as it suggests that an effective dosing strategy to counteract rifampicin induction may be achieved without resorting to BD dosing. While this regimen may help improve adherence in the sense that medication (one FDC plus one 50 mg pill of dolutegravir) is taken in one go, this would still not mitigate the issue of possible dolutegravir stockouts of the single pill. A further encouraging finding is represented by the fact that, when our model predictions were compared with data from tuberculosis/HIV patients collected in INSPIRING, it was found to slightly under-predict trough concentrations observed in patients. This suggests that target achievement in tuberculosis/HIV patients maybe even better than our prediction.

The reasons for the difference in dolutegravir concentrations we observed between the data from healthy volunteers and that from patients are unclear, as many factors could offer a plausible explanation. First, it cannot be excluded that this finding may simply be due to imbalances between the specific studies in this analysis and may not reflect a genuine (and therefore consequential) difference between healthy volunteers and tuberculosis/HIV patients.

RADIO and NCT01231542 were both early phase, healthy volunteer, tightly controlled studies with intense pharmacokinetic sampling and therefore yielded reliable concentration-time data. Instead, INSPIRING was a multi-centre, outpatient study with only sparse pharmacokinetic sampling and as such characterised by more uncertainty about adherence and other details about pre-clinic doses, including their timing and whether they were taken after a meal or not. On the other hand, several key differences between healthy volunteers and patients and the treatment they received may offer a valid explanation. First, there are small but potentially significant differences in the drugs tuberculosis/HIV patients received during treatment compared to the healthy volunteers. In RADIO and NCT01231542, participants received only dolutegravir and rifampicin, as single-drug formulations, whereas in INSPIRING dolutegravir was given with a nucleoside reverse transcriptase inhibitor backbone that included lamivudine or emtricitabine and either tenofovir disoproxil, abacavir, or zidovudine. In INSPIRING, rifampicin was also combined with isoniazid, pyrazinamide and ethambutol during the intensive phase. It has been suggested that isoniazid may inhibit CYP3A4 (Desta, Soukhova & Flockhart, 2001; X et al., 2002), which plays a minor role in dolutegravir metabolism. Therefore, it is possible that the additional use of isoniazid in INSPIRING as compared to RADIO and NCT01231542 may have mitigated the inducing effect of rifampicin and caused a relative increase in dolutegravir exposure. This is in line with findings by Ignatius *et al.* (Ignatius et al., 2021), who found a similar discrepancy between healthy volunteers and patients when investigating the effect of rifampicin on the anti-tuberculosis drug pretomanid, a CYP3A4 substrate. They report the rifampicin induction to be stronger in healthy volunteers receiving rifampicin alone vs. what they observed in patients receiving full tuberculosis treatment, which included both rifampicin and isoniazid. On the other hand, it cannot be excluded that formulation differences or even DDI with the other drugs could be the reason for the difference we observed. Second, we expect tuberculosis-co-infected individuals to have relatively lower weights compared to their non-tuberculosis, co-infected HIV counterparts

(Kennedy et al., 1996; Zachariah et al., 2002) and our model (and the theory of allometry) predicts a decrease in clearance with a lower weight. Third, tuberculosis may cause physiological changes to the body such as reduced albumin levels, which may lead to a decrease in protein binding for a drug like dolutegravir, which is more than 99% protein bound. However, this would cause larger unbound fraction and larger volume of distribution and clearance, thus leading to a decrease in total dolutegravir concentrations, and not an increase.

When we attempted to fit a single model to all three datasets, we found that many potential combinations of parameter values could describe the differences between the healthy volunteer studies and the patient study. In terms of goodness of fit to the data, a different value of clearance, central volume of distribution, speed of absorption, or a combination thereof all gave similar satisfactory improvements. However, given the limited data available, especially in terms of the short sampling schedule in INSPIRING (0-6 hours), the model could not reliably discriminate which of the scenarios was the most convincing explanation, thus leaving this choice largely in the domain of speculation. This is a crucial decision that has a major bearing on how the model predicts trough concentrations, so we were unable to produce a reliable model that could jointly describe both healthy volunteers and patient data.

Our model describes a 2-compartment disposition similar to recently reported studies (Dickinson et al., 2020; Kawuma et al., 2021), but unlike the 1-compartment model reported in a large analysis by Zhang *et al.* (Zhang et al., 2015). While this may be attributed to a difference in the sampling schedules of the available data, it is interesting to mention that it was only after the inclusion of between-occasion variability (random effects within an individual on different dosing occasions) on all absorption parameters (and after considering the pre-dose sample as belonging to a different dosing occasion), that our model was able to identify the 2-compartment disposition kinetics. The model from Zhang *et al.* did not include any between-occasion difference in absorption, despite including data from multiple visits, and this may have precluded the correct identification of the structural model.

Song *et al.* (Song et al., 2012) showed that food increases dolutegravir exposure ($AUC_{0\text{-}24}$, C_{max}) and reduces its rate of absorption (later T_{max}) with increasing fat content. In this analysis, we observed a similar effect, in that the absorption of dolutegravir was slower in RADIO, where drugs were given with food, than in NCT01231542, which dosed under fasted conditions. Interestingly, we found no effect of food on bioavailability. We speculate that this may be because of a low-fat content in the breakfast provided in RADIO. Although we tested age and sex as covariates on different dolutegravir pharmacokinetic parameters, we did not observe an increased clearance of dolutegravir with older age or increased bioavailability for females, as reported previously. (Zhang et al., 2015). However, we did observe a significantly slower absorption rate constant for males. Although previous reports have alluded to the possibility of sex differences in the speed of drug absorption (Schwartz, 2003; Marazziti et al., 2013), we are uncertain about the mechanism that could account for this difference.

In this analysis, we choose to target a trough concentration of 0.064 mg/L because this target was established to inhibit the HIV-1 virus; but we do recognize that since it was derived in vitro, there might be some drawbacks to an in vivo translation. While we acknowledge that the 0.3 mg/L trough concentration is widely referenced, we consider this target to be conservative. It was derived from a phase IIb study investigating dolutegravir doses of 10, 25, and 50 mg in ART-naïve adults with HIV (Van Lunzen et al., 2012). All dose levels displayed a very similar profile of viral suppression and there was no signal that the lowest dose achieved lower efficacy, as such no dose-response relationship could be established. The geometric mean trough concentration in the 10 mg dose group was reported to be 0.3 mg/L, and hence this concentration is now used as a target. However, one needs to recognize that half of the patients in this group had a concentration below this geometric mean, while not compromising viral suppression.

A limitation to this analysis is that we used protocol sampling times for RADIO since actual sampling times were unavailable. However, considering this was a well-controlled study and

only minimal deviations from the stipulated sampling schedule are expected, we trust this to have no bearing on our outcome. A more significant limitation is represented by the fact that our final model was developed from healthy volunteer data only, yet we would like our recommendations to apply to patients. As has been extensively discussed above, we identified that our model slightly under-predicts the trough concentrations in patients, which makes our target attainment estimates conservative. On the other hand, we could not identify a reason for the difference we observed and further data would be useful to shed some light on this important detail.

Our work highlights the discrepancy that may arise from studies conducted in healthy volunteers vis-à-vis those in a patient population. Currently, drug-drug interaction studies are commonly performed in healthy volunteers, as was the case for two of the studies included in our analysis and as we show here, this might yield different results than what is observed in patients. Therefore, healthy volunteer studies should be designed to be as good of a reflection as possible of patients and subsequently drug-drug interaction studies should ideally be confirmed in a patient population. In the case of drug-drug interactions between ART and tuberculosis therapy, studies should be conducted in the context of the whole regimen to be utilized as opposed to only single, inclusive drugs.

In conclusion, 100 mg of dolutegravir OD is predicted to attain acceptable levels of exposure in patients co-treated with rifampicin. This regimen presents an attractive opportunity for treatment simplification while reducing the risk of suboptimal concentrations and its efficacy should be investigated.

Chapter 6 Drug-drug interaction between rifabutin and dolutegravir: a population pharmacokinetic model

6.1 Abstract

Background

Dolutegravir-based regimens are recommended as first-line therapy for HIV, and first-line tuberculosis treatment contains rifampicin, which is a potent inducer, thus causing a marked reduction of dolutegravir exposure. Rifabutin, a less potent inducer than rifampicin, may offer an alternative to rifampicin. The objective of this analysis was to characterise the population pharmacokinetics of dolutegravir co-administered with rifabutin.

Methods

We extended an existing population pharmacokinetic model of dolutegravir to include data in which volunteers were co-administered dolutegravir 50 mg with rifabutin 300 mg once daily. We used the updated model to run simulations when dolutegravir is administered alone versus with rifabutin and compare dolutegravir trough concentrations with efficacy targets of 0.064 mg/L and 0.3 mg/L.

Results

A 2-compartment model with first-order elimination and lagged absorption best described dolutegravir pharmacokinetics. Rifabutin co-administration decreased dolutegravir's central volume of distribution (V_c) and C_{min} by 33.1 % (95% confidence interval (CI): 25.1 to 42.3) and 30.1% (95% CI: 24.7 to 51.5) respectively; increased dolutegravir's C_{max} by 15.1% (95% CI: -49.8 to 268) and had no effect on the area under the concentration-time curve. Simulations showed that when 50 mg dolutegravir is co-administered with rifabutin once daily, the probability to attain trough concentrations above the IC_{90} of 0.064 mg/L is more than 99%.

Conclusion

Although rifabutin decreases dolutegravir's trough concentrations, these still achieve acceptable levels and there is no need for dose adjustment when dolutegravir is dosed with rifabutin. Therefore, rifabutin may offer an alternative to rifampicin for the treatment of HIV-tuberculosis co-infected individuals.

6.2 Background

Dolutegravir is a second-generation integrase strand inhibitor that has now been adopted widely as first-line therapy for HIV in combination with two nucleoside reverse transcriptase inhibitors. It is mainly metabolized by uridine diphosphate glucuronosyltransferase 1A1 (UGT1A1) with cytochrome P450 (CYP) 3A4 playing a minor role. Dolutegravir is also a substrate of the efflux drug transporters P-glycoprotein and breast cancer resistance protein (BRCP) (Reese et al., 2013b).

Tuberculosis causes more than 25% of deaths among people living with HIV (PLWH) in resource-limited settings (Tshikuka Mulumba et al., 2012). The treatment of tuberculosis amongst PLWH is often challenging because of the risk of drug-drug interactions. Rifampicin, the preferred rifamycin for the treatment of tuberculosis, is a potent inducer of many phase-1 and -2 metabolizing enzymes including CYP3A4, and UGT1A1 (Reinach et al., 1999), as well as of the efflux transporters P-glycoprotein and BRCP (Niemi et al., 2003). When co-administered, rifampicin causes a greater than 100% increase in dolutegravir clearance and markedly reduces exposure. Therefore, to mitigate the risk of sub-optimal dolutegravir concentrations, the recommended dosing for PLWH and infected with tuberculosis on rifampicin-based tuberculosis treatment is 50 mg dolutegravir twice daily, but this might be challenging to implement in high-burden countries (Dooley et al., 2013). A study in Botswana on PLWH and tuberculosis reported that despite the twice-daily recommended treatment,

guidelines for dolutegravir while on rifampicin, 43.6% of study participants did not receive the second dose of dolutegravir (Modongo et al., 2019).

Rifabutin, a rifamycin with potent bactericidal activity against drug-susceptible tuberculosis, is a less potent inducer of liver enzymes compared to rifampicin and therefore it has been used to substitute rifampicin in scenarios where rifampicin profoundly reduces the exposure of co-administered drugs such as in HIV/tuberculosis co-infected individuals who are on protease inhibitors (Horne, Spitters & Narita, 2011). Rifabutin has also been used widely for preventing and treating the *Mycobacterium avium* complex in PLWH.

Considering that rifabutin came off patent in 2014 and was listed on the WHO essential drugs list for the treatment of tuberculosis in HIV co-infected individuals, we may begin to see a decline in cost and an increase in its availability with more generic versions. The objective of this analysis was to characterise the drug-drug interaction between rifabutin and dolutegravir and investigate the feasibility of using rifabutin as an alternative for rifampicin when co-administered with dolutegravir.

6.3 Methods

Study design

This analysis consists of participants from two healthy volunteer studies: RADIO and NCT01231542. Study designs are visualized in **Figure S.6.1.** RADIO was a phase II, open-label, healthy volunteer, sequential pharmacokinetic study (Wang et al., 2019). Volunteers were dosed sequentially as follows, once daily (OD) with 50 mg dolutegravir for seven days, 100 mg dolutegravir for seven days, 600 mg rifampicin only for 14 days, 50 mg dolutegravir plus 600 mg rifampicin for 7 days, and finally 100 mg dolutegravir plus 600 mg rifampicin for 7 days. Intense pharmacokinetic sampling was done on the seventh day of each sequence. NCT01231542 was a phase I, open-label, two-arm, (arm-A and arm-B) study. Arm-A

volunteers received 50 mg dolutegravir OD for seven days, then 50 mg dolutegravir twice daily (BD) for seven days, and finally 50 mg dolutegravir BD with 600 mg rifampicin OD for 14 days. Arm-B volunteers received 50 mg dolutegravir OD for seven days, followed by 50 mg dolutegravir OD with 300 mg rifabutin OD for 14 days. Intense pharmacokinetic sampling was done on the last day of each regimen.

Pharmacokinetic analysis

A previously published model describing the population pharmacokinetics of dolutegravir and characterising the drug-drug interaction with rifampicin was used as the starting point (Kawuma et al., 2022). Concentration-time data were analysed using nonlinear mixed-effects modeling in NONMEM version 7.5.0, Pearl-speaks-NONMEM v4.7.0, and Pirana v2.9.7. R v3.6.1 was used for graphical output (Keizer, Karlsson & Hooker, 2013a). First-order conditional estimation with interaction was used for all model runs. The inclusion of rifabutin as a covariate was based on the inspection of visual predictive checks (VPC), and a drop in the objective function value (OFV). The OFV was assumed to follow a chi-square distribution where, for one additional degree of freedom (df), the statistically significant cut-off was a drop in OFV of at least 3.84 points, corresponding to P <0.05. The final model was used to simulate dolutegravir steady-state plasma concentrations for 1000 individuals with a weight of 70 kg dosed with 50 mg dolutegravir once-daily with and without rifabutin and twice-daily with rifampicin (WHO, 2019). Simulated dolutegravir trough concentrations were compared with the dolutegravir in vitro protein-adjusted IC_{90} target of 0.064 mg/L (Cottrell, Hadzic & Kashuba, 2013) and with the median target of 0.3 mg/L (Van Lunzen et al., 2012), the proposed dolutegravir minimal effective concentration.

6.4 Results

A total of 41 volunteers (68% male) were enrolled in both studies: 16 in the RADIO study and 25 in the NCT01231542 study with 12 in arm-A and 13 in arm-B. The model parameters were estimated with a total of 907 samples and of these 90 were taken from volunteers in arm-B during rifabutin co-administration. Participants had a median (interquartile range) weight and age of 81.5 (69.5 to 88.6) kg and 43 (31 to 50) years, respectively. Further details on participant demographics have been reported previously (Kawuma et al., 2022). None of the samples had a concentration below the lower limit of quantification. The model consists of 2-compartments with first-order elimination and lagged first-order absorption. Final parameter estimates and their precision are presented in **Table 6.1.**

Table 6.1 Final population parameter estimates for dolutegravir

Parameter description	**Typical value (95% CI)**[a]
CL/ *F* (L/h) [b]	1.03 (0.945, 1.15)
V_c/F (L) [b]	13.3 (11.7, 14.5)
Q/F (L/h) [b]	0.675 (0.439, 1.02)
V_P/F (L) [b]	3.52 (2.69, 4.24)
Relative bioavailability	1 Fixed
Absorption lag time NCT01231542 study [d](h)	0.205 (0.00205, 0.381)
Absorption lag time RADIO study [e](h)	0.986 (0.602, 1.43)
Absorption rate constant (K_a) (/h)	1.63 (1.16, 2.73)
Covariates	
Rifampicin co-administration on CL (%)	+143 (+126, +155)
Male sex on K_a (%)	- 38.1 (-15.1, -56.1)
Rifabutin co-administration on V_c (%)	- 33.1 (-25.1, -42.3)
Parameter variability (% CV) [c] **(95%CI)**	
BSV Clearance	25.1 (15.7, 34.4)
BOV bioavailability	43.0 (37.0, 49.6)
BOV lag time	46.9 (16.5, 79.8)

BOV Absorption rate constant	60.7 (41.9, 79.2)
Residual unexplained variability	
Proportional error (%)	8.85 (7.32, 9.79)
Additive error NCT01231542 study (mg/L)	0.036 (0.00435, 0.0801)
Additive error RADIO study (mg/L)	0.0485 (0.0103, 0.0861)

[a] 95 % confidence intervals were obtained by non-parametric bootstrap (n = 500 replicates). [b] Allometric scaling with weight (median of 70 kg) was used for the clearance (CL), inter-compartmental clearance (Q), central volume of distribution (V_c), and peripheral volume of distribution (V_p). %CV, coefficient of variation, between-subject variability (BSV), and between-occasion variability (BOV). [c] Calculated by $CV\% = \sqrt{\omega^2} \cdot 100$
[d] Dolutegravir taken under fasted conditions, [e] under fed condition

The VPC in **Figure 6.1** shows that the final model described the observed data adequately. The median, 10th, and 90th percentiles of the observed data fall within their 95% confidence interval (CI).

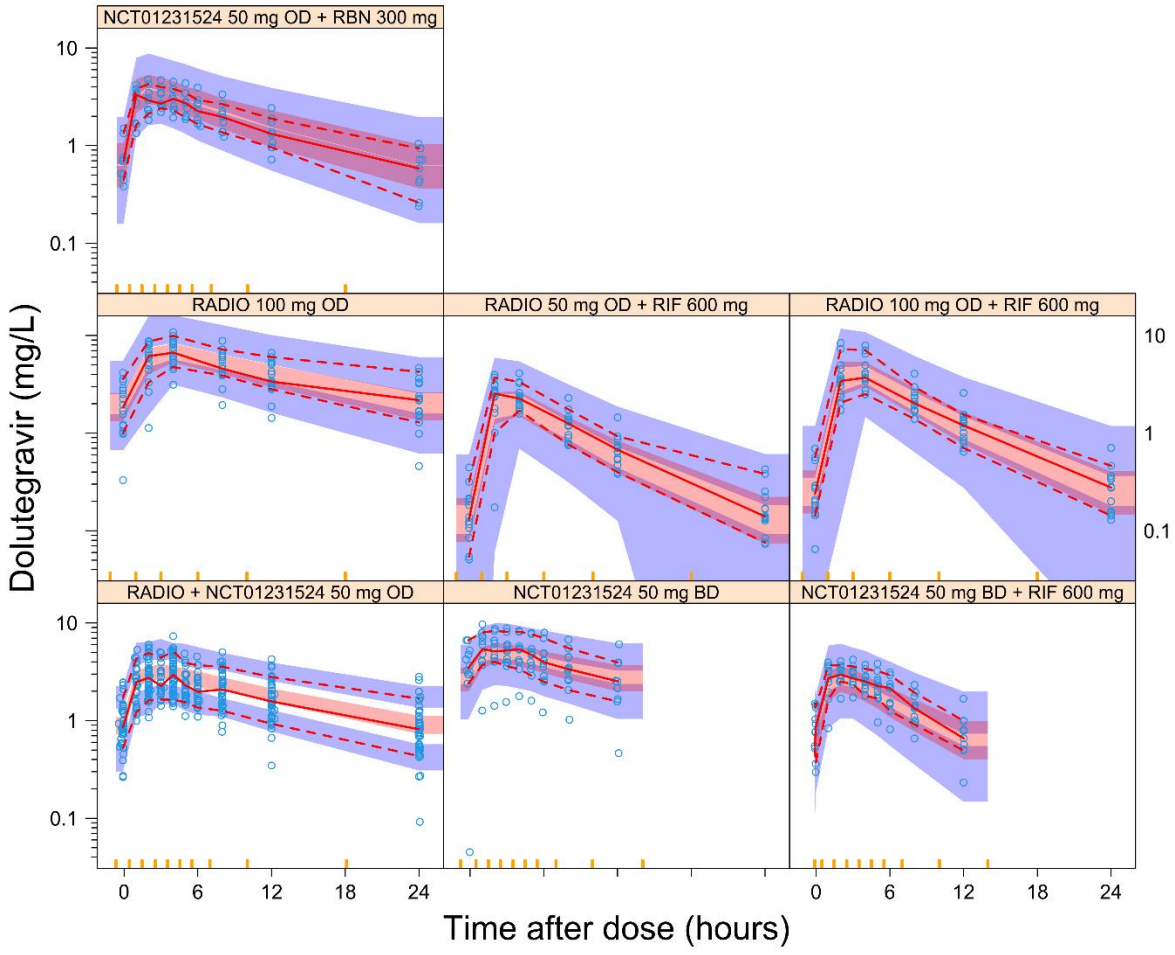

Figure 6.1 Visual predictive check of the final model.
Blue circles represent observed plasma concentrations. The solid line in the middle represents the median observed concentration, and the broken lines below and above it represent the 10th and 90th percentiles of the observed concentrations, respectively. The shaded areas around each line represent the 95% confidence boundary of the simulated prediction for the same percentiles. OD, once-daily; BD, twice-daily; RIF, rifampicin; RBN, rifabutin

We tested the effect of rifabutin co-administration on different pharmacokinetic parameters of dolutegravir. The most convincing model, both in terms of goodness of fit and plausibility of the results, found a 33.1% decrease (95% CI 25.1 to 42.3) in dolutegravir's central volume of distribution (ΔOFV = -56, df =1, p<0.001). When the effect was tested on clearance, the model estimated a 36% increase, but the improvement in the goodness of fit was not as significant (ΔOFV = -52 points, df =1) and the diagnostic plots were not as convincing (results not shown). An effect of rifabutin on dolutegravir bioavailability alone was not significant. Finally, a model that simultaneously included rifabutin as a covariate on both dolutegravir's clearance and bioavailability estimated a 41% increase in clearance and a 32% increase in bioavailability (ΔOFV = -59, df =2). Using the Bayesian Information Criterion (BIC) to compare these two non-nested models, the effect on the volume of distribution had a lower BIC of -870.7 compared to the BIC of -866.1 for the model with both clearance and bioavailability.

As a consequence of this effect on volume, the model predicts that rifabutin co-administration increases dolutegravir's C_{max} by 15.1% (95% CI: -49.8 to 268), reduces C_{min} by 30.1% (95% CI: 24.7 to 51.5) and has no effect on the area under the concentration-time curve (AUC). **Figure 6.2** shows the median simulated concentration-time profile of dolutegravir when administered alone vis-à-vis co-administered with rifabutin. Importantly, we show that in both dosing scenarios, there is a greater than 99% probability that dolutegravir trough concentrations are higher than the IC_{90} of 0.064 mg/L in a 70-kg individual and the probability that they are greater than the target of 0.3 mg/L is more than 85.9%.

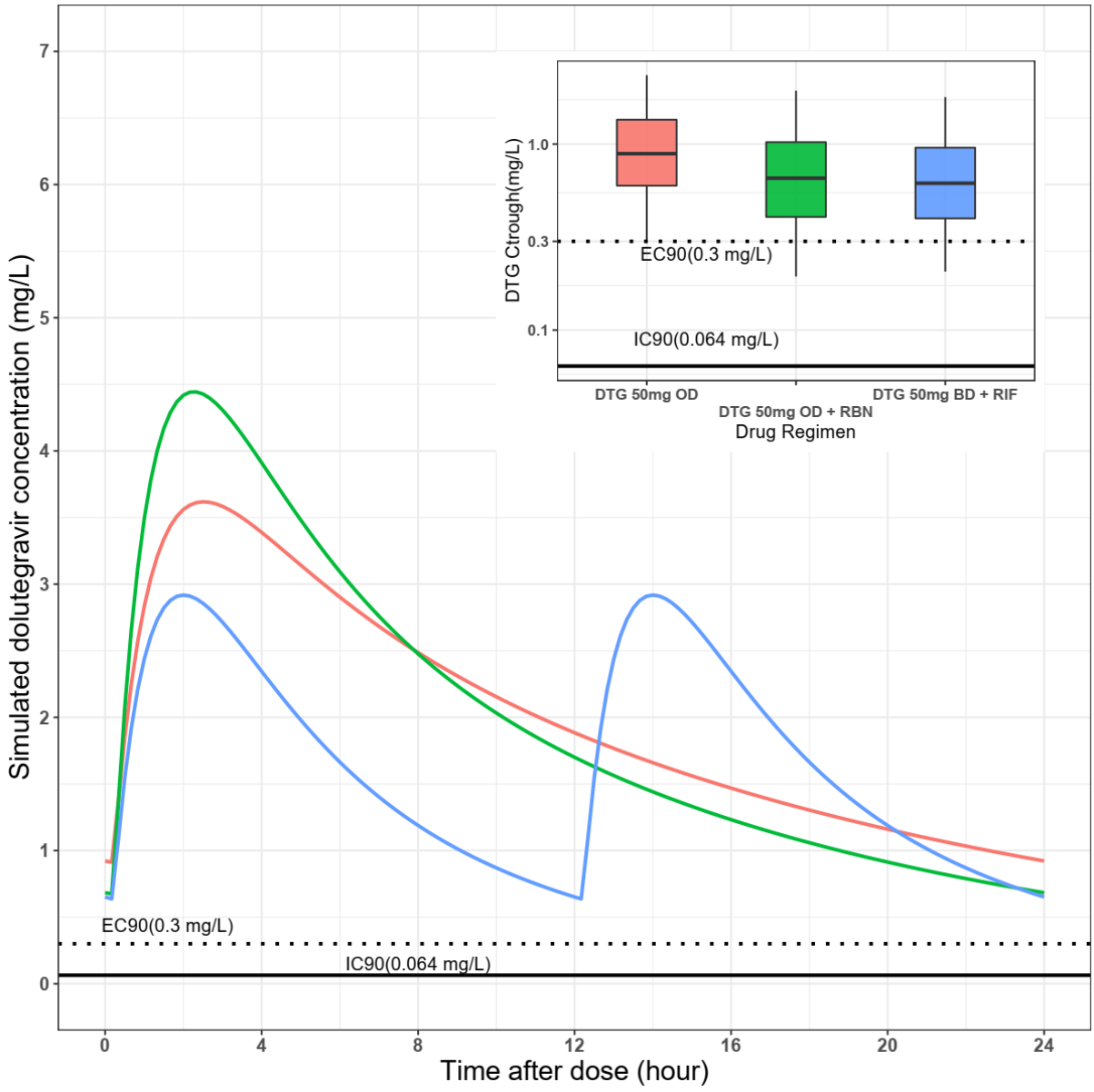

Figure 6.2 Concentration-time profile of dolutegravir (DTG) in steady-state for a typical 70 kg individual.

When administered alone at 50 mg once-daily (OD), with 300 mg rifabutin (RBN) OD, and with 600 mg rifampicin (RIF) twice-daily. Inset, simulated trough concentrations of dolutegravir in the three dosing scenarios highlighted, based on 1000 simulations with a representative weight of 70 kg. The boxes represent the 25^{th,} 50^{th,} and 75th percentiles while the whiskers show the 5th and 95th percentiles. 90% inhibitory concentration (IC90), effective concentration (EC90)

6.5 Discussion

We explored the effect of rifabutin on dolutegravir pharmacokinetics and found that rifabutin changes the half-life of dolutegravir by reducing its volume of distribution. Rifabutin increased dolutegravir C_{max} while reducing the C_{min} and overall, there was no change in dolutegravir's AUC_{0-24}. Our simulations showed that when administered with rifabutin, the probability that dolutegravir trough concentrations are higher than the IC_{90} of 0.064 mg/L in a 70kg individual is more than 99%, similar to concentrations attained when dolutegravir is dosed at 50 mg twice daily with rifampicin. Even when the more conservative target of 0.3 mg/L is used, the probability to attain trough concentrations above this is 85.9%.

We conclude that the lack of a significant change in AUC_{0-24} that was observed by Dooley *et al*., when dolutegravir was co-administered with rifabutin can be explained by its effect on dolutegravir's central volume (Dooley et al., 2013). Our findings offer a good explanation for the decrease in trough and increase in peak concentrations that they observed. These findings are similar to those observed when rifabutin is co-administered with raltegravir, a first-generation integrase strand inhibitor. Brainard *et al.* reported that on average, co-administration of rifabutin 300 mg with raltegravir 400 mg led to a 20% decrease in C_{12}, and a 39% increase in C_{max} (Brainard et al., 2011).

The mechanism by which rifabutin alters dolutegravir's volume of distribution is unclear. However, we speculate that it is through rifabutin's induction effect on drug transporters like P-glycoprotein. Dolutegravir is a P-glycoprotein substrate and both rifampicin and rifabutin have been shown to induce it (Lutz et al., 2018; Elmeliegy et al., 2020). We hypothesize that induction of this efflux pump by rifabutin would reduce the distribution of dolutegravir, especially to sensitive areas, where efflux transporters serve a protective role to limit drug distribution to these tissues. This effect could result in a reduced volume of distribution for dolutegravir. Although not documented specifically for rifabutin, various studies have reported

how drug transporters can influence a drug's volume of distribution (Grover & Benet, 2009). For example, Ding *et al*. showed that ritonavir, a potent inhibitor of P-glycoprotein, increased digoxin volume of distribution by 77% (Ding et al., 2004). Also, studies have shown that the absence of P-glycoprotein in knockout mice substantially facilitates the distribution of drugs in the brain (Huisman et al., 2001). We postulate that inducing P-glycoprotein would have the opposite effect.

The alternative model we tested, which included rifabutin as a covariate on both clearance and bioavailability, did not fit the data as well and the results were less plausible. Dolutegravir already has good oral bioavailability, so such an increase is not easy to explain. Moreover, it seems odd that the same induction mechanism increasing clearance would have the opposite effect on exposure by also increasing bioavailability. It is not impossible that two separate mechanisms elicited by rifabutin could be responsible for these two changes, but it seems less plausible than a single effect on P-glycoprotein decreasing volume.

We have demonstrated that rifabutin co-administration would not require dose adjustments for dolutegravir and could therefore be considered as a substitute for rifampicin. It has been shown that rifabutin has similar potency to rifampicin for the treatment of tuberculosis (Schwander et al., 1995). However, there is still limited evidence comparing the use of rifampicin versus rifabutin in HIV co-infected individuals taking newer and current standard antiretroviral regimens (Davies, Cerri & Richeldi, 2007). Earlier studies have demonstrated the efficacy of rifabutin in PLWH, albeit when HIV regimens were different (Gonzalez-Montaner et al., 1994; Grassi & Peona, 1996). A non-inferiority randomized controlled trial in tuberculosis/HIV co-infected individuals would go a long way in further encouraging the use of rifabutin and its possible integration into a fixed-dose combination for the treatment of tuberculosis.

6.6 Supplementary material

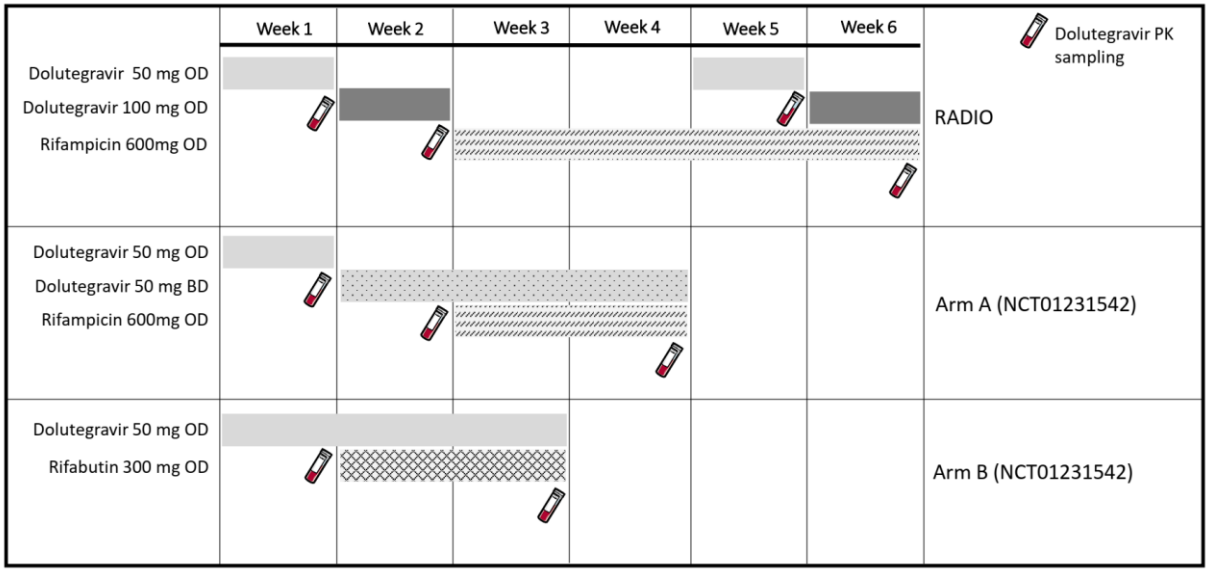

Figure S.6.1*: Schematic of the dosing regimen and dolutegravir pharmacokinetic (PK) sample collection for the different studies. Once-daily (OD), twice-daily (BD).*

Chapter 7 Population pharmacokinetics of dolutegravir in Africans living with HIV

7.1 Abstract

Africans living with HIV may exhibit different dolutegravir pharmacokinetics compared with non-African populations due to genetic differences in transporters and metabolizing enzymes. We characterised the population pharmacokinetics of dolutegravir in South Africans living with HIV. Compared with previous reports in HIV-positive patients, which included few people of African ancestry, we observed higher trough and peak concentrations. In addition, because Africa has the world's greatest genetic diversity (Papathanasopoulos, Hunt & Tiemessen, 2003), and limited data regarding dolutegravir pharmacogenetics in Africa, we evaluated the genetic association between select *UGT1A1* polymorphisms and dolutegravir clearance. In the population pharmacokinetic model, we found that individuals who were homozygous (T/T) and heterozygous (C/T) for *UGT1A1* rs887829 had 25.9% and 10.8% decreases in dolutegravir clearance, respectively, compared to C/C.

7.2 Background

Dolutegravir is recommended as first-line antiretroviral therapy (ART) in low and middle-income countries for the management of HIV (WHO, 2019). Millions of people living with HIV (PLWH) in sub-Saharan Africa have initiated dolutegravir-based ART regimens (UNITAID, 2017). Dolutegravir is mainly metabolized by UGT1A1 (Reese et al., 2013a). Genetic diversity is highest in people of African ancestry (Rajman et al., 2017). Therefore, polymorphism within the UGT1A1 gene might result in differences in dolutegravir exposure compared to other populations. We aimed to develop the first model to characterise the population pharmacokinetics of dolutegravir in a patient population of African descent and to

investigate the effect of *UGTIAI* polymorphism on dolutegravir pharmacokinetics in the ADVANCE study (Venter et al., 2019).

7.3 Methods

Study population and procedures

Concentration-time data was available from a pharmacokinetic sub-study nested within the ADVANCE trial (NCT03122262), an open-label, phase 3, randomized non-inferiority trial comparing three first-line antiretroviral regimens in treatment-naïve patients initiating ART in South Africa. Full study procedures have been reported previously (Venter et al., 2019). Briefly, the efficacy and safety of two prodrugs of tenofovir, tenofovir disoproxil fumarate (TDF) and tenofovir alafenamide (TAF), both combined with emtricitabine (FTC), were evaluated with dolutegravir versus a TDF/FTC/efavirenz regimen (the standard of care at the time). Rich pharmacokinetic sampling at steady state was performed in a subset of participants in the dolutegravir arms after at least 48 weeks of treatment. Samples were taken pre-dose and at 1, 2, 4, 6, 8, and 24 hours post-dose. Sparse pharmacokinetic sampling (one sample per individual) was performed for all other individuals at either week 48 or 96.

Analytical assay

Dolutegravir plasma concentrations were determined with validated liquid chromatography with tandem mass spectrometry as reported previously (Griesel et al., 2022). The calibration range was 0.030 to 10 mg/L. The combined accuracy and precision of the quality control samples were between 103.5% – 106.0%, and 4.6% – 6.1%, respectively.

Population pharmacokinetic modelling (Intensively sampled individuals)

Data were analysed by non-linear mixed-effects modelling with NONMEM (v7.4.3), and Pearl-speaks-NONMEM (PsN) v4.7.0, using the first-order conditional estimation with

interaction method. We explored one- and two-compartment disposition models with first-order elimination and absorption, with or without absorption lag time and transit compartments (Savic et al., 2007). Between-subject (BSV) and -occasion (BOV) variability were assumed to be log-normal distributed. A combined additive and proportional error model was used to describe residual errors, with the additive component of the error constrained to be at least 20% of the lower limit of quantification (LLOQ).

To discriminate between nested models, a decrease in the objective function value (OFV) of 3.84 was equivalent to model improvement at a significance level of $p<0.05$. Allometry with either total body weight or fat-free mass (FFM) (Janmahasatian et al., 2005) was tested in the model and allometric exponents for clearance and volume were fixed to 0.75 and 1 respectively (Anderson & Holford, 2008). We investigated the following covariate effects on dolutegravir's pharmacokinetic parameters; sex, age, and TAF- vs. TDF-based antiretroviral treatment. Covariates were assessed by stepwise inclusion (ΔOFV >3.84, $p<0.05$) followed by backward elimination (ΔOFV >6.63, $p<0.01$). Model performance was evaluated with a visual predictive check (VPC) and a non-parametric bootstrap (n=500) was used to generate the 95% confidence interval (95%CI) for parameter estimates.

Generating secondary pharmacokinetic parameters

We used the final model to generate individual steady-state estimates of peak (C_{max}), trough (C_{24}) plasma concentrations, area under the concentration-time curve ($AUC_{0\text{-}24h}$), and unexplained variability in $AUC_{0\text{-}24h}$ (AUC_{VAR}) and clearance (BSVCL) for individuals with at least one pharmacokinetic sample (intensively and sparsely sampled). Individual estimates of all model parameters were obtained from the final model by a post-hoc Bayes estimation method, considering an individual's pharmacokinetic data and characteristics. Individual estimates of $AUC_{0\text{-}24h}$ were obtained using the formula $AUC_{0\text{-}24h} = F_i \times Dose_i/CL_i$, where Dose

represents the actual dose given to each individual and CL_i and F_i represent individual estimates of clearance and bioavailability, respectively.

We used $AUC_{0\text{-}24h}$ values in a regression analysis to test for a concentration-response relationship of dolutegravir (combined with tenofovir disoproxil fumarate and emtricitabine) with changes in weight and fat distribution, derived from dual-energy x-ray absorptiometry scans. Findings from that regression have been published (Griesel et al., 2022).

UGT1A1 Phenotypes from genotyping data

A subset of individuals in ADVANCE consented to genotyping. Details regarding genotyping have been described elsewhere. Briefly, genetic information was used to derive *UGT1A1* phenotypes of interest and patients were stratified into normal CC, heterozygous T/T and homozygous C/T with regards to *UGT1A1* rs887829 (Cindi et al., 2022). This information was used to test associations between *UGT1A1* rs887829 polymorphism and dolutegravir exposure using values of (AUC_{VAR}) and BSVCL in a regression analysis. Complete details of this regression have been published elsewhere (Cindi et al., 2022).

Population pharmacokinetic modelling with genetic information.

Based on the results of genotyping, we assessed the effects of *UGT1A1* rs887829 polymorphisms on dolutegravir clearance on all available pharmacokinetic data (intensive and sparse samples). For individuals who did not have genotype information, we assigned a phenotype using mixture modelling as described by Keizer et al (Keizer et al., 2012).

7.4 Results

Dolutegravir population pharmacokinetics without genetics (intense individuals only)

Forty-one individuals provided 276 dolutegravir concentrations. Median (interquartile range) weight and age were 73.1 (67.2 – 85.2) kg and 31 (29 – 36) years, respectively. The

concentration of one pre-dose sample was below the LLOQ and was retained in the model as LLOQ/2, with an additional additive error of 20% LLOQ.

A two-compartment disposition model (ΔOFV=-47, p<0.001 compared to one-compartment) with first-order elimination and transit compartments absorption (ΔOFV=-4.8, p=0.028 compared to absorption lag) best described the pharmacokinetics of dolutegravir (**Figure 7.1)**.

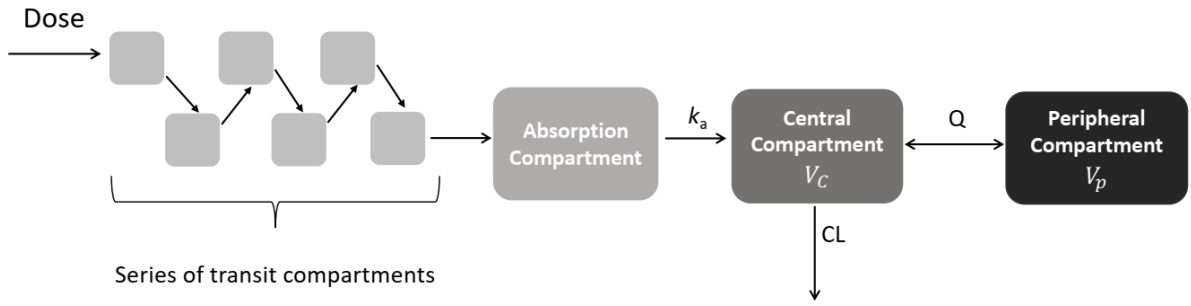

Figure 7.1 Schematic of the dolutegravir structural model
Once administered, the dose of dolutegravir goes through a series of transit compartments (characterised by a mean transit time and several compartments) before being absorbed into the central compartment. It then distributes to a peripheral compartment and is eliminated from the central compartment with first-order kinetics. K_a, absorption rate constant; V_c, central volume of distribution; V_p, peripheral volume of distribution; Q, intercompartmental clearance; CL, central clearance

Allometric scaling with FFM best described the effect of body size on disposition parameters and was applied to all clearance and volume parameters. We estimated clearance of 0.732 (95% CI 0.666–0.801) L/h, central volume of 12.2 (95% CI 1.12–13.4) L, and peripheral volume of 5.87 (95% CI 1.74–41.6) L for a typical individual with a 47 kg FFM and included BSV on clearance and BOV on mean transit time (MTT), absorption rate constant, and bioavailability. The effect of TAF vs. TDF on pharmacokinetic parameters was explored, but no statistically significant difference was observed. Final parameter estimates and precision are presented in **Table 7.1**. The VPC in **Figure 7.2** shows that the final model described the observed data adequately, with the median, 5th, and 95th percentiles of the observed data falling within the 95% confidence interval of the respective prediction.

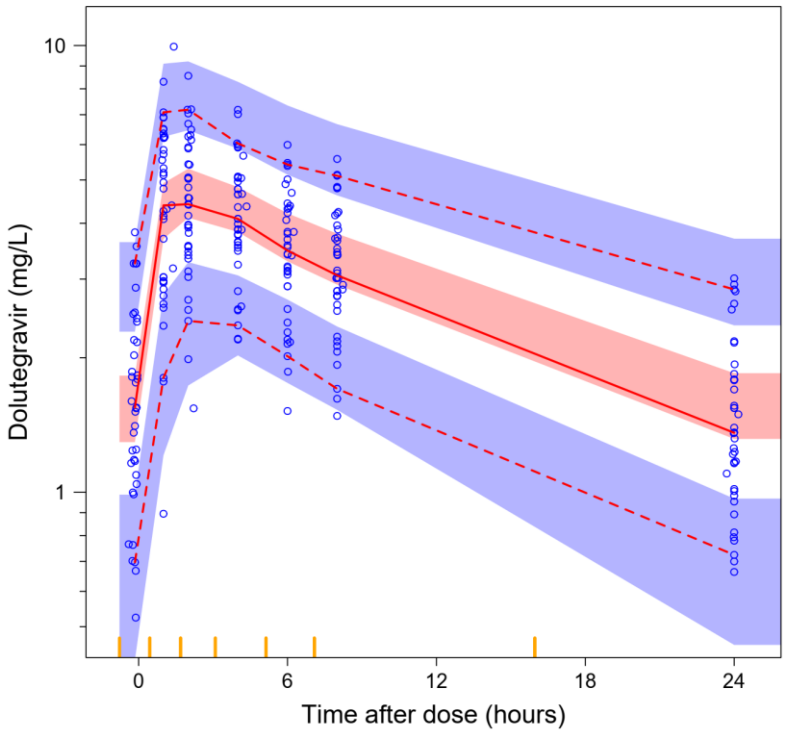

Figure 7.2 Visual predictive check of the final model fitted to intense samples only (without genetic information).
Blue circles represent observed plasma concentrations. The solid line in the middle represents the median observed concentration, and the dashed lines below and above represent the 5th and 95th percentiles of the observed concentrations, respectively. The shaded areas around each line represent the 95% confidence interval for the same percentiles based on simulations with the model.

Including genotype in the population pharmacokinetic model

Among the 41 intensively sampled individuals, 26 (8 with C/C, 10 with C/T, 8 with C/T) had *UGT1A1* rs887829 genotype information and when this was tested on dolutegravir clearance, the effect was borderline significant with reduced clearance for C/T and T/T individuals. Therefore, we proceeded to fit a mixture model to all available pharmacokinetic data (intensive and sparse samples) which consisted of 472 individuals (188 not genotyped) providing 742 concentrations. There was a significant and graded effect of *UGT1A1* rs887829 genotype on dolutegravir clearance (ΔOFV= -24.7, P < 0.00001 compared to no genotype). We estimated (95% CI) a clearance of 0.786 (0.730–0.846) L/h for C/C, with a 10.8% (2.09–18.4) and 25.9%

(16.7–33.8) decrease in clearance for C/T, and T/T, respectively. Simulations performed using the final model show that dolutegravir trough concentrations are highest with T/T genotypes.

Table 7.1 Final population parameter estimates for dolutegravir

Parameter description	Typical Value (95% CI)[a]	
	Intensive samples only *n*=41 participants	**Intensive and sparse *n*=472 participants*** (With genetic information included)
Clearance (CL) (L/h) [b]	0.732 (0.666–0.801)	0.786 (0.730–0.846)
Effect of Homozygous for *UGT1A1* rs887829 on CL (%)		-25.9% (-33.8– -16.7)
Effect of Heterozygous for *UGT1A1* rs887829 on CL (%)		-10.8% (-18.4– -2.09)
Central volume (L) [b]	12.2 (1.12–13.4)	10.5 (8.44–12.3)
Inter-compartmental clearance (L/h) [b]	0.509 (0.252–3.86)	1.29 (0.524–2.81)
Peripheral volume (L) [b]	5.87 (1.74–41.6)	3.77 (2.40–5.36)
Relative bioavailability (*F*)	1 Fixed	1 Fixed
Absorption mean transit time (MTT) (h)	0.166 (0.00625–0.396)	0.180 (0.086–0.292)
Number of Transit compartments (n)	7.85 (2.64–22.3)	5 Fixed
Absorption rate constant (K_a) (/h)	2.41 (0.242–4.28)	1.67 (1.17–2.30)
Parameter Variability (% CV) [c]		
Between-subject variability in CL	22.3% (14.1–27.8)	27.9% (24.6–31.6)
Between-occasion variability in F	31.6 % (21.4–41.7)	38.7% (31.9–45.1)
Between-occasion variability in MTT	130 % (63.5–445)	184% (130–251)
Between-occasion variability in K_a	69.9 % (30.9–97.1)	60.7% (43.8–78.6)
Residual unexplained variability		
Proportional error (%)	7.41 (4.51–10.2)	7.52 (5.89–9.35)
Additive error (mg/L)	0.191 (0.0602–0.256)	0.180 (0.127–0.232)

[a] The 95% confidence intervals were obtained by sampling importance resampling. FFM, fat-free mass calculated according to Janmahasatian et al (Janmahasatian et al., 2005). [b] Clearance and volume of distribution parameters were scaled with fat-free mass (FFM) using the exponents 0.75 and 1, respectively.

The typical values reported here refer to an individual with an FFM of 47 kg. %CV, coefficient of variation. [c] *Calculated by* $\%CV = \sqrt{\omega}.100\%$.
**Of these, 384 were genotyped and those with missing genotypes were assigned one via mixture modelling as described here (Keizer et al., 2012).*

7.5 Discussion

We developed a model that describes the population pharmacokinetics of dolutegravir in PLWH in South Africa and compared our findings with those from five previous studies (**Table 7.2**): three in PLWH (Min et al., 2011; Van Lunzen et al., 2012; Dooley et al., 2013) and two in healthy volunteers (Walimbwa et al., 2019; Wang et al., 2019). Compared to the studies in PLWH (NCT01231542, SPRING-1, and ING111521), our study found the highest $AUC_{0\text{-}24}$, C_{24}, and C_{max} and the lowest clearance. These differences in exposure could be explained by participant weight and ethnicity or whether the drugs were taken while fed or fasted. We enrolled a 100% African population while the other studies were predominantly in individuals of European ancestry. Dolutegravir $AUC_{0\text{-}24}$ and C_{max} in our participants are comparable to those from DOLACT, which enrolled healthy volunteers from Uganda. The $AUC_{0\text{-}24}$, $C_{24,}$ and C_{max} from DOLACT are higher than those from RADIO, another healthy volunteer study that enrolled 79% Caucasian participants.

This observation may be driven in part by polymorphisms in *UGT1A1*, which encodes for the major enzyme responsible for dolutegravir metabolism. The *UGT1A1*28* polymorphism is associated with reduced enzyme activity, which could cause higher dolutegravir concentrations in individuals of African ancestry (Teh et al., 2012). This could explain the lower dolutegravir clearance we observed compared with other studies in PLWH.

After comparing our findings in the 41 intensively sampled individuals, we proceeded to characterise the effect of the *UGT1A1* rs887829 polymorphism on dolutegravir clearance in the population pharmacokinetic model. the *UGT1A1* rs887829 T allele was associated with

greater exposure since the rs887829 C/T and T/T genotypes were associated with 10.8% and 25.9% decreases in dolutegravir clearance, respectively, and thus higher exposures compared to C/C individuals. The *UGT1A1* rs887829 T allele is known to be in strong linkage with the Gilbert trait decreased expression allele, *UGT1A1*28*, a promoter TA_n dinucleotide (Gammal et al., 2016). Our finding supports previous reports associating *UGT1A1*28* with dolutegravir concentrations (Chen et al., 2014; Yagura et al., 2017; Elliot et al., 2020).

In conclusion, we show that it is prudent to investigate dolutegravir pharmacokinetics in PLWH since these may be different from those in healthy volunteers and we also show that polymorphism on the *UGT1A* locus is associated with dolutegravir clearance and thus exposure in a black African population.

Table 7.2 Pharmacokinetic parameters of dolutegravir after oral dosing (50 mg once daily at steady state)

Parameter	Studies in people living with HIV[a]					Healthy volunteer studies		
	ADVANCE n=40[#]	**NCT01231542** (Dooley et al., 2013)		**SPRING-1** (Van Lunzen et al., 2012)	**ING111521** (Min et al., 2011)*	**RADIO** (Wang et al., 2019)[b]	**DOLACT** (Walimbwa et al., 2019)[,c,§]	
		Arm 1 (n=11)	**Arm 2 (n=9)**	***n*=15**	***n*=10**	***n*=14**	**Study A (*n*=14)**	**Study B (*n*=12)**
Food status	Fed	Fasted	Fasted	NR[†]	Fasted	Fed	Fed	Fed
Weight (range) kg	73.8 (49.9–118)	79 (63–99)[d]	83(66–97)[e]	NR	NR	27 (18–32)[§]	58.5 (54.0-61.8)	60.3 (58.3-68.3)
African ancestry n (%)	40 (100%)	8 (67%)[d]	10 (71%)[e]	8 (16%)[f]	3 (30%)	2 (14%)	14 (100%)	12 (100%)
$AUC_{0\text{-}24}$ (mg.h/L)	61.7 (38.7)	32.1 (44)	39.1 (38)	48·1 (40)	43.4 (20)	52.1 (40.2–67.5)	78.8 (70.6–86.9)	77.9 (67.8–88.1)
C_{24} (mg/L)	1.39 (44.5)	0.55 (91)	0.76 (43)	1·20 (62)	0.83 (26)	1.06 (0.745–1.51)	2.46 (2.06–2.85)	2.17 (1.57–2.78)
C_{max} (mg/L)	4.69 (32.7)	2.65 (32)	2.95 (38)	3·40 (27)	3.34 (16)	3.97 (3.21–4.90)	5.02 (4.51–5.53)	5.11 (4.56–5.67)
Clearance (L/h)	0.764 (26.2)	1.56 (44)	1.28 (38)	1.04[‡]	1.15[‡]	0.96[‡]	0.63 (0.53–0.74)	0.64 (0.54–0.74)

$AUC_{0\text{-}24}$, area under the curve; C_{max}, peak plasma concentration; C_{24}, trough plasma concentrations; $t_{1/2}$, half-life; NR, not reported in the original publication.

[a] *Data are geometric means (coefficient of variance, %)*

[b] *Data are geometric mean (95% confidence interval)*

[c] *Data are geometric mean (90% confidence interval)*

[d] *Value reported is for 12 participants, 11 of whom were eligible for pharmacokinetic analysis*

[e] *Value reported is for 14 participants, 9 of whom were eligible for pharmacokinetic analysis*

[f] *Value reported is for 51 participants who were randomized to 50 mg once daily.*

**Monotherapy study. Patients did not receive any other accompanying antiretroviral drugs,*

[†] *Dolutegravir was given without regard to food.*

[#] *Parameters are reported for 40 participants who had full concentration-time profiles over 24 hours*

[‡] *Clearance value not reported in original publication but derived here for purpose of comparison using the formulae AUC=Dose/Clearance*

[§] *Data are body mass index (range)*

Chapter 8 Population pharmacokinetics of Tenofovir given as TDF or TAF

8.1 Abstract

Tenofovir disoproxil fumarate (TDF) and tenofovir alafenamide (TAF) are prodrugs of the nucleotide analogue tenofovir, which acts intracellularly to inhibit HIV replication. While TDF converts to tenofovir in plasma and may cause kidney and bone toxicity, TAF mostly converts to tenofovir intracellularly, so it can be administered at lower doses. TAF leads to lower tenofovir plasma concentrations and lower toxicity, but there is limited data on its use in Africa. We used data from 41 South African adults living with HIV from the ADVANCE trial and described, with a joint model, the population pharmacokinetics of tenofovir given as TAF or TDF. TDF was modelled to appear in plasma as tenofovir with a simple first-order process. Instead, two parallel pathways were used for a TAF dose: an estimated 32.4% quickly appeared as tenofovir into the systemic circulation with first-order absorption, while the rest was sequestered intracellularly and released into the systemic circulation as tenofovir slowly. Once in plasma (from either TAF or TDF), tenofovir disposition followed two-compartment kinetics and had a clearance of 44.7 L/h (40.2 – 49.5), for a typical 70-kg individual. This semi-mechanistic model describes population pharmacokinetics of tenofovir when dosed as either TDF or TAF in an African population living with HIV and can be used as a tool for exposure prediction in patients, and to simulate alternative regimes to inform further clinical trials.

8.2 Background

Tenofovir is a nucleotide analogue that inhibits HIV replication. Because of its poor membrane permeability and low oral bioavailability, tenofovir is administered as a prodrug: either as TDF or TAF. TDF or TAF are widely used in combination with other antiretroviral agents for the treatment of HIV because of their effective antiviral activity, favourable safety profile, and

their availability within several fixed-dose co-formulated tablets (Estrella, Moosa & Nachega, 2014).

For their conversion to tenofovir, TDF and TAF undergo distinctly different processes, as portrayed in **Figure 8.1**. After oral administration, TDF is rapidly converted to tenofovir by esterase enzymes in the gut and plasma, leading to higher plasma concentrations of tenofovir relative to TAF.(Cressey et al., 2020) Tenofovir is then taken into the cells and sequentially activated to tenofovir-diphosphate (TFV-DP) (Kearney, Flaherty & Shah, 2004). On the other hand, TAF more efficiently delivers tenofovir to HIV-target cells because of its relative stability in plasma and its rapid absorption intracellularly. Consequently, in plasma, TAF has a short half-life of approximately 25 minutes and reaches undetected levels by about 4 to 6 hours post-dose (Ruane et al., 2013). Intracellularly, TAF is converted to tenofovir by cathepsin A and then activated to TFV-DP. This allows TAF to be given at a lower dose than TDF, leading to markedly lower levels of tenofovir in plasma, and as a result reduces off-target exposure. Higher tenofovir exposures when receiving TDF have been associated with an increased incidence of proximal tubular dysfunction, acute kidney injury, chronic kidney disease, and reduced bone mineral density (Cooper et al., 2010; Scherzer et al., 2012; Tourret, Deray & Isnard-Bagnis, 2013). The WHO HIV treatment guidelines recommend the use of TAF (instead of TDF) for adults with established osteoporosis and/or impaired kidney function. Tenofovir is eliminated renally by a combination of active tubular secretion and glomerular filtration. Tenofovir is not a substrate of cytochrome P450, P glycoprotein (P-gp) or multidrug resistance protein type 2 (Ray et al., 2006). Conversely, TAF is a substrate of P-gp and human breast cancer resistance protein (BCRP) and the pharmacokinetic boosters ritonavir and cobicistat, which inhibit intestinal P-gp can increase TAF plasma concentrations about twofold (Atta, De Seigneux & Lucas, 2019).

The ADVANCE study (NCT03122262), carried out in South Africa showed that a regimen of TAF, dolutegravir and emtricitabine was safe and well-tolerated in a South African population living with HIV (Venter et al., 2019). The objective of our analysis was to develop a single population pharmacokinetic model that characterises tenofovir appearance in plasma and disposition whether it is administered as TAF or TDF in South Africans living with HIV.

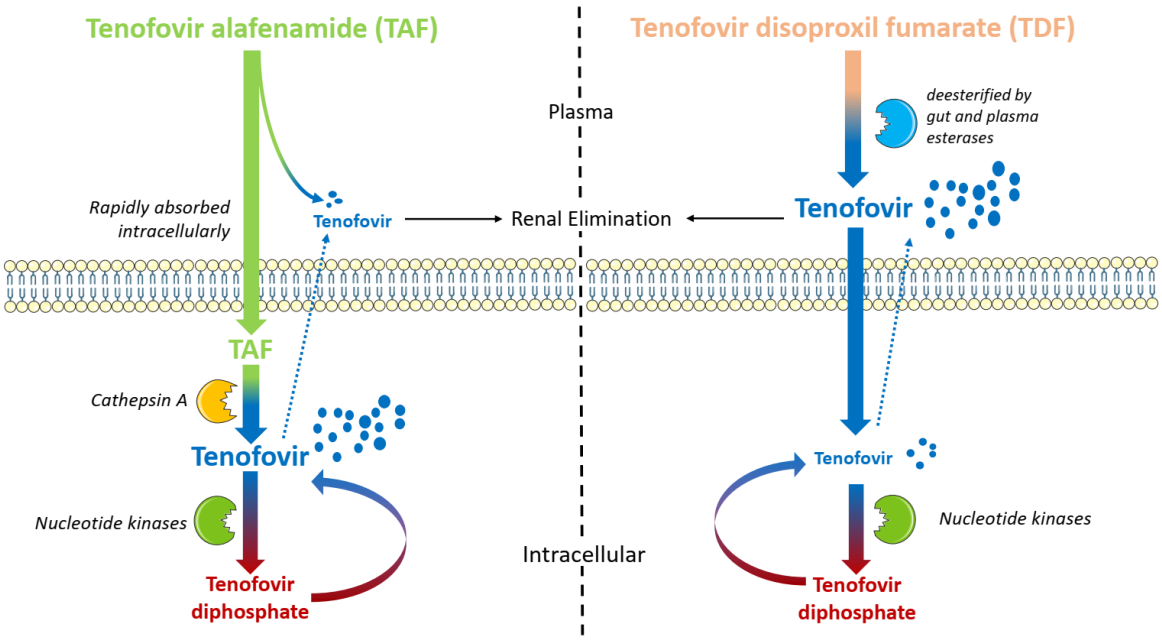

Figure 8.1 Schematic of the conversion of TDF and TAF to tenofovir
TAF is rapidly absorbed intracellularly where it is sequentially converted to TFV-DP. TFV-DP then degrades to tenofovir intracellularly which seeps back to the plasma. TDF is mostly converted to tenofovir in the plasma and then tenofovir is absorbed intracellularly where it undergoes sequential conversion to TFV-DP. Overall, when given as TDF, tenofovir in the plasma is more than 10-fold higher than when TAF is administered.

8.3 Methods

Study population and procedures

Tenofovir concentration-time data were available from a pharmacokinetic sub-study nested within the ADVANCE study, an open-label, phase 3, randomized non-inferiority trial comparing three first-line antiretroviral regimens in treatment-naïve adults with HIV initiating antiretroviral therapy in South Africa. Full study procedures have been reported previously

(Venter et al., 2019). Briefly, the efficacy and safety of two prodrugs of tenofovir, TAF and TDF both combined with emtricitabine, were evaluated with dolutegravir versus a TDF-emtricitabine-efavirenz regimen (the standard of care at the time). Drugs in the 3 arms were dosed as dolutegravir (50 mg, ViiV Healthcare) plus co-formulated TAF (25 mg)/emtricitabine (200 mg, Gilead Sciences); dolutegravir (50 mg, ViiV Healthcare) plus generic versions of co-formulated TDF (300 mg)/emtricitabine (200 mg); and co-formulated TDF (300 mg)/emtricitabine (200 mg)/efavirenz (600 mg) from generic manufacturers. Rich pharmacokinetic sampling was performed in a subset of participants in the dolutegravir arms after at least 48 weeks of treatment. Samples were taken pre-dose and 1, 2, 4, 6, 8, and 24 hours post-dose.

Analytical assay

Plasma tenofovir concentrations were determined with a validated liquid chromatography-tandem mass spectrometry assay developed at the Division of Clinical Pharmacology, University of Cape Town. The method utilized plasma protein precipitation, followed by high-performance liquid chromatography with tandem mass spectrometry detection. Chromatographic separation was achieved on a Waters Atlantis T3 column (2.1 mm x 100 mm, 3 µm) with a total runtime of 6 minutes. A Sciex 5500 Qtrap mass spectrometer at unit resolution in the multiple reaction monitoring mode was used to monitor the transition of the protonated precursor ions, 288.1 and 294.1 to the product ions 176.1 and 182.1 for tenofovir and tenofovir-d6 (internal standard), respectively. Electrospray ionization was used for ion production. The calibration curve fitted a quadratic (weighted by 1/concentration) regression based on peak area ratios over the range of 0.500 to 300 ng/mL. The combined accuracy (%Nom) of the limit of quantification, low, medium, and high-quality controls (3 validation batches, N=18) were between 93.8% and 103.8%, with precision (%CV) less than 13%.

Population pharmacokinetic modelling

Data were analysed by non-linear mixed-effects modelling with NONMEM (v7.5.0) using the first-order conditional estimation method with interaction. Pearl-speaks-NONMEM (PsN) v5.2.6, R v3.6.1 and Pirana v2.9.7. were used to assist model development (Keizer, Karlsson & Hooker, 2013b). Using their molecular weights, the dose of TDF and TAF in mg was converted to tenofovir (molecular weight = 287.2 g/mol) amounts in mg. 300 mg of TDF (molecular weight = 635.5 g/mol) provided 136 mg of tenofovir while 25 mg of TAF (molecular weight = 476.5 g/mol) provided 15 mg of tenofovir.

We first modelled the kinetics of tenofovir when given as TDF, and explored one- and two-compartment disposition models with first-order elimination and absorption, with or without absorption lag time and transit compartments (Savic et al., 2007). Afterwards, we modelled tenofovir in the TAF arm and initially fixed the disposition parameters to what was observed for TDF. This was to reflect the fact that, once tenofovir appears in plasma, its kinetics will be the same irrespective of the prodrug used to administer it. We explored different semi-mechanistic models to describe how TAF appears as tenofovir in plasma. Once the structure for TAF absorption and conversion to tenofovir was identified, both arms (TAF and TDF) were jointly fit in the same model and all parameter values were re-estimated. We included between-subject (BSV) and between-occasion (BOV) variability on disposition and absorption parameters respectively, assuming a log-normal distribution. A combined additive plus proportional error model was used to describe residual variability, with the additive component of the error constrained to be at least 20% of the LLOQ. Allometry with either total body weight or fat-free mass (FFM) (Janmahasatian et al., 2005) was tested in the model and allometric exponents for clearance and volume were fixed to 0.75 and 1, respectively (Anderson & Holford, 2008). To discriminate between nested models, a decrease in the OFV of 3.84 was equivalent to model improvement at a significance level of $p<0.05$, for one additional degree

of freedom. We investigated the effect of age and baseline creatinine clearance on tenofovir's pharmacokinetic parameters. Covariates were assessed by stepwise inclusion (ΔOFV>3.84, p<0.05) followed by backward elimination (ΔOFV>6.63, p<0.01). Model performance was evaluated with a visual predictive check (VPC), and we used sampling importance resampling to generate the 95% confidence interval (95%CI) for parameter estimates (Dosne et al., 2016).

8.4 Results

Forty-one individuals in a 1:1 ratio (21 on TDF versus 20 on TAF) provided 279 tenofovir concentrations. Median (interquartile range) of weight, age, and creatinine clearance (at screening) estimated by Cockcroft and Gault were 73.1 (67.2 – 85.2) kg, 31 (29 – 36) years and 120 (96.0 – 140) mL/min respectively. There was no significant difference in weight, age, or creatinine clearance (at screening) between the TDF and TAF arms. Participant demographics are reported in **Table 8.1.**

A schematic illustrating the structure of the pharmacokinetic model is shown in **Figure 8.2**. A two-compartment disposition model (ΔOFV= -47, p<0.001 compared to one-compartment) best described the pharmacokinetics of tenofovir in plasma. Allometric scaling with weight described the effect of body size on disposition parameters and was applied to all clearance and volume parameters (ΔOFV= -18 compared to no allometry). For a typical individual of 70 kg, clearance was estimated at 44.7 (40.2 – 49.5) L/h. Adding creatinine clearance (collected at screening) as a covariate on clearance did not improve the model significantly and neither did age. TDF was found to quickly appear as tenofovir in plasma with a first-order rate constant of 3.04 (2.11 – 3.88) h^{-1}. Instead, the release of tenofovir after TAF administration was described by two absorption pathways: a fraction available for immediate absorption into the systemic circulation ($Frac_{TAF\text{-}Fast}$) and a slow fraction ($Frac_{TAF\text{-}Slow}$) modelled as if it was first absorbed intracellularly into a reservoir and then slowly released as tenofovir to the systemic

circulation. $Frac_{TAF\text{-}Fast}$ was estimated to be 32.4% (27.0 – 37.7) and to become plasma tenofovir with a first-order rate constant of 1.45 h^{-1} (0.924 – 2.60). The remaining $Frac_{TAF\text{-}Slow}$ appeared as tenofovir in the systemic circulation with a half-life $T_{½\_TAF-Slow}$ which was fixed to 6.8 days. This value was initially estimated from the data, but the parameter estimate was poorly identifiable. A likelihood profiling exercise revealed that values in the range of 5 to 60 days provided only small changes in terms of goodness of fit. For this reason, we decided to fix the parameter value to 6.8 days, which has been previously reported as the half-life of intracellular TFV-DP decay (Jackson et al., 2013). Results of the sensitivity analysis for this $T_{½\_TAF-Slow}$ parameter are reported in **Table S.8.1 and Figure S.8.1** in the supplementary material. The relative bioavailability of tenofovir when given as TAF, was estimated to be 82.2% (95% CI, 72.3 – 93.9).

Final parameter estimates and their precision are presented in **Table 8.2**. A visual predictive check stratified by treatment arm (TDF versus TAF) in **Figure 8.3** shows that the final model described the observed data adequately, with the median, 5^{th}, and 95^{th} percentiles of the observed data falling within the 95% confidence interval of the respective prediction.

Table 8.1 Participant demographics

Characteristic	**Median (interquartile range) or no. (%) of volunteers (*n*=41)**
Sex, n (%) Male/Female	27 (65.9) / 14 (34.1)
Age (years)	31.0 (29.0, 36.0)
Weight (kg)	73.1 (67.2, 85.2)
Height (cm)	167 (161, 174)
Creatinine clearance at screening (mL/min)*	120 (96.0, 140)
Regimen TDF/TAF (plus FTC-DTG)	21 (51.2%) / 20 (48.8%)

*Tenofovir disoproxil fumarate (TDF), tenofovir alafenamide (TAF), emtricitabine (FTC), dolutegravir (DTG). *Creatinine clearance was calculated by Cockcroft and Gault.*

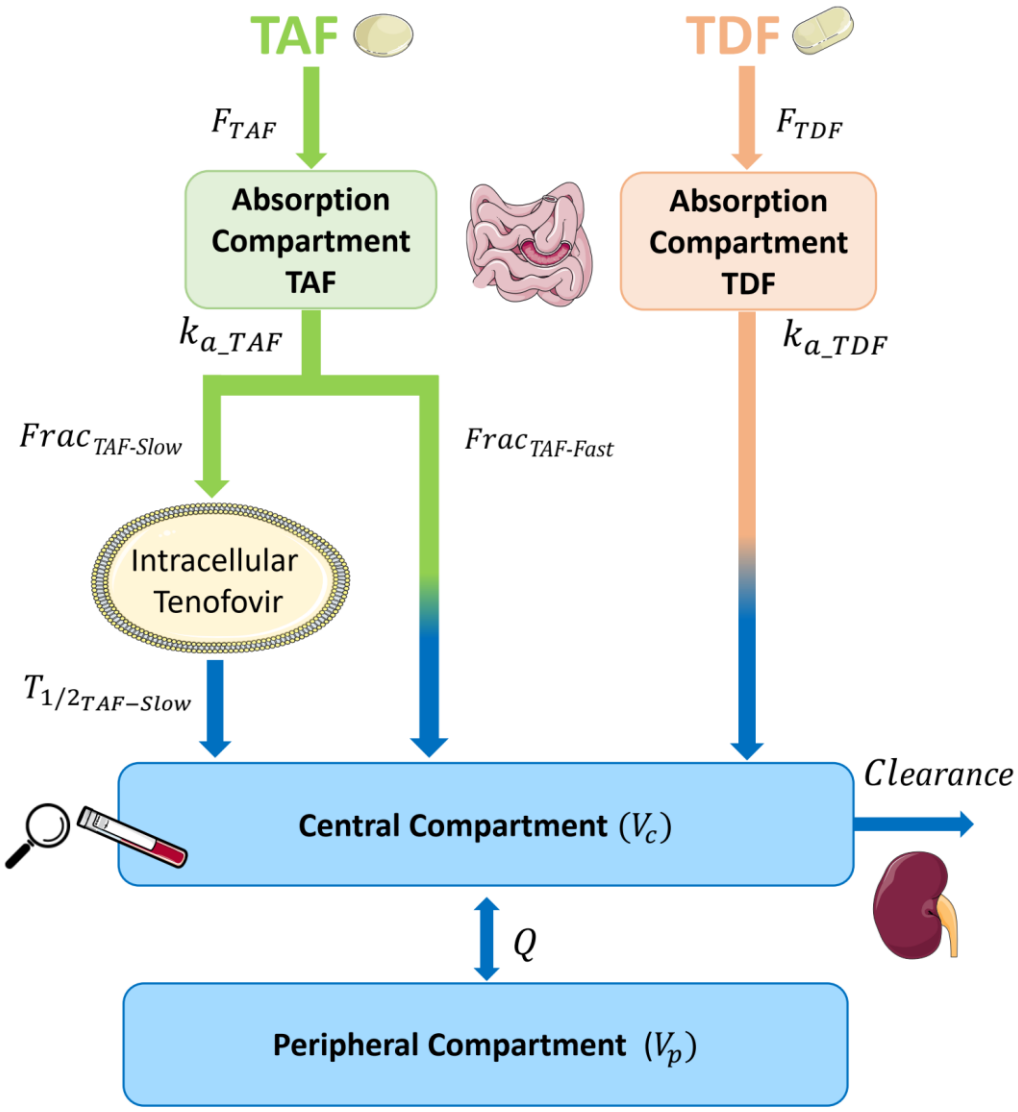

Figure 8.2 Schematic of the tenofovir structural model.

Once administered, the dose of tenofovir given as TDF is absorbed into the central compartment. It then distributes to a peripheral compartment and is eliminated from the central compartment with first-order kinetics. When given as TAF, a fast fraction ($Frac_{TAF\text{-}Fast}$) is immediately absorbed into systemic circulation while a slow fraction ($Frac_{TAF\text{-}Slow}$) = (1-F $Frac_{TAF\text{-}Fast}$) is first absorbed intracellularly and then slowly transitioned to the systemic circulation via a first-order process with a half-life in days ($T_{1/2\_TAF\text{-}Slow}$). K_a, absorption rate constant; V_c, central volume of distribution; V_p, peripheral volume of distribution; Q, intercompartmental clearance; CL, central clearance; TAD, tenofovir disoproxil fumarate; TAF, tenofovir alafenamide.

Table 8.2 Final population parameter estimates for tenofovir

Parameter description	**Typical value (95% CI)**[a]	**Parameter variability (% CV)**[b] **(95%CI)**[a]
CL (L/h) [c]	44.7 (40.2 – 49.5)	20.1 (16.1 – 24.7)*
V_c (L) [c]	378 (319 – 459)	
Q (L/h) [c]	157 (103 – 233)	
V_p (L) [c]	356 (298 – 438)	
F_{TDF} (.)	1 - Fixed	23.9 (18.2 – 30.3)[#]
F_{TAF} (.)	0.822 (0.723 – 0.939)	
K_{a_TDF} (1/h)	3.04 (2.11 – 3.88)	114.5 (68.4 – 162)[#]
K_{a_TAF} (1/h)	1.45 (0.924 – 2.60)	66.3 (31.0 – 91.6)[#]
$T_{1/2\_TAF\text{-}Slow}$ (days)	6.83 - Fixed	
$Frac_{TAF\text{-}Fast}$ (%)	32.4 (27.0 – 37.7)	
Proportional error (%)	11.9 (10.8 – 13.4)	
Additive error (mg/L)	20% of LLOQ[d] - Fixed	

[a]*95% confidence intervals were obtained by Sampling importance resampling.*

[b]*Between-subject variability (BSV) and between-occasion variability (BOV) were assumed to be log-normally distributed and calculated by* $CV\% = \sqrt{\omega^2} \cdot 100$

[c]*Allometric scaling with weight (for a reference individual of 70 kg) was used for the clearance (CL), inter-compartmental clearance (Q), central volume of distribution (V_c), and peripheral volume of distribution (V_p). Coefficient of variation (%CV), absorption rate constant (K_a). The half-life of the first-order process by which tenofovir leaves the intracellular compartment to the central compartment ($T_{1/2\_TAF\text{-}Slow}$). Percentage of tenofovir that is immediately available for absorption into the systemic circulation ($Frac_{TAF\text{-}Fast}$).*

[d] *lower limit of quantification (LLOQ) was 0.0005 mg/L.*

** Between-subject variability.*

[#] *Between-occasion variability*

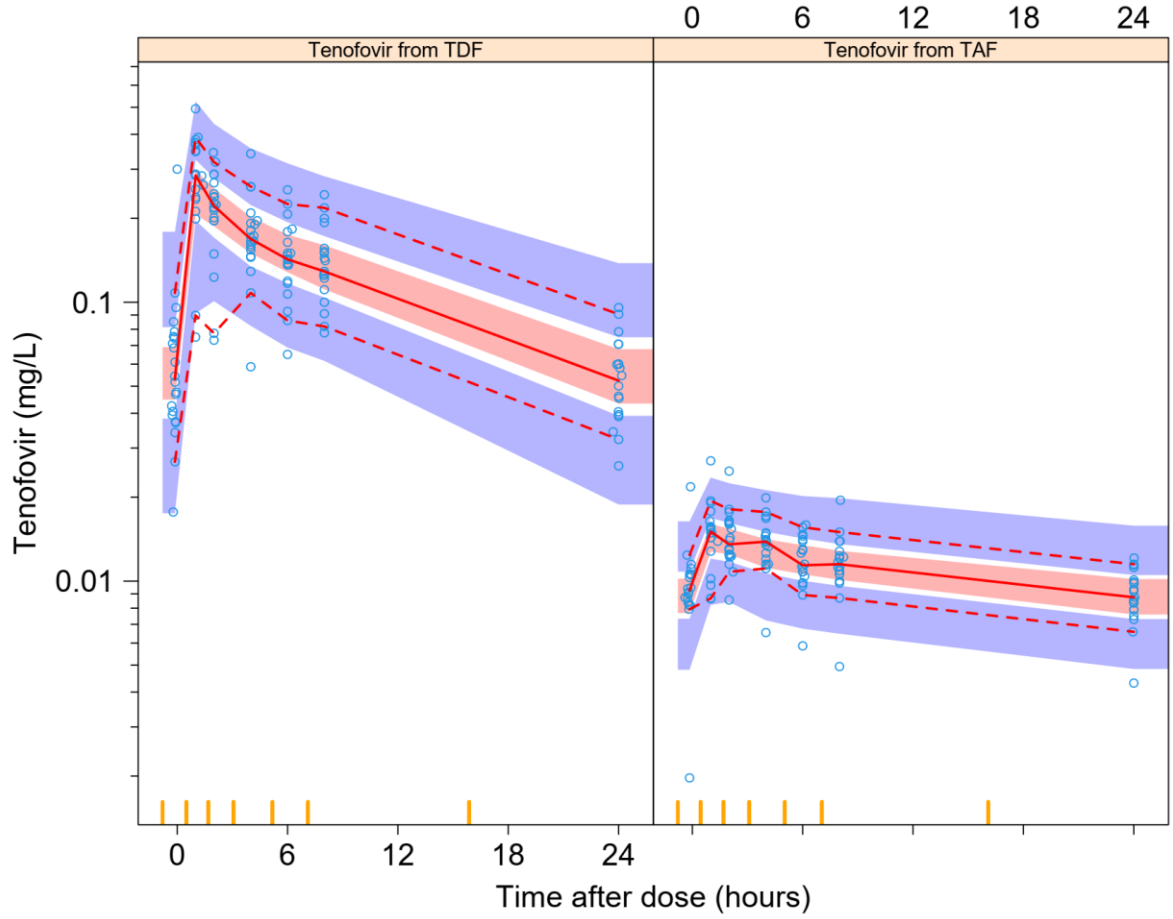

Figure 8.3 Visual predictive check of the final model

Blue circles represent observed plasma concentrations. The solid line in the middle represents the median observed concentration, the broken lines below and above it represent the 5th and 95th percentiles of the observed concentrations, respectively. The shaded areas around each line represent the 95% confidence interval for the same percentiles based on simulations with the model.

8.5 Discussion

We developed a joint semi-mechanistic model that describes the population pharmacokinetics of tenofovir after TAF and TDF administration. A key strength of our model is the fact that the model uses the same disposition parameters (and therefore clearance) for tenofovir in plasma, regardless of the prodrug used to administer it. In addition, we describe separate absorption processes for TDF and TAF. TDF quickly appears in plasma as tenofovir, while after TAF administration the absorption of tenofovir is described using two pathways as illustrated in **Figure 8.2.** With this implementation, we aim to mimic the fact that once absorbed, most TAF

is rapidly taken up intracellularly and then subsequently converted to TFV-DP. TFV-DP is then degraded intracellularly to tenofovir which then seeps back into the plasma.

Several population pharmacokinetic models for tenofovir have been reported previously, the majority when dosed as TDF (Jullien et al., 2005; Dumond et al., 2012; Lu et al., 2016a; Collins, Heyward Hull & Dumond, 2017; Valade et al., 2017; Eke et al., 2021; Tanaudommongkon et al., 2022). An exception is a model by Greene *et al.*,(Greene et al., 2019) in which the authors describe tenofovir pharmacokinetics after both TDF and TAF administration in men living with HIV in the United States. However, they use two separate models, one when TDF is administered and another when TAF is administered. As such, they reported two separate clearance values, with a ~10-fold difference). While the models sufficiently described their observed data, the use of two separate disposition models is a limitation of their approach and is difficult to justify from a mechanistic perspective. Once tenofovir has reached the plasma, it should distribute and be eliminated in the same manner, regardless of the prodrug whence it came. The lack of a mechanistic interpretation for the models may imply that, while suited to describe the data on which they were developed, they may not be reliable to extrapolate to new dosing scenarios, or when predicting the effect of drug-drug interactions.

Ruane *et al*. showed that tenofovir had a terminal half-life of 14.86 hours when given as TDF, while this value increased to 40.19 hours when given as TAF, thus demonstrating that tenofovir disappears from plasma more slowly when the TAF prodrug is administered (Ruane et al., 2013). In our approach, we postulate that the observed difference in the terminal half-life of tenofovir when dosed as TAF versus TDF must be explained by the different mechanisms with which tenofovir from the two prodrugs eventually appears in plasma, and not by the distribution and elimination of tenofovir. In the case of TAF, our model assumes that a large fraction of the prodrug is absorbed into a reservoir compartment outside of the plasma.

Although this reservoir may consist of many cell types, we believe it largely represents the peripheral blood mononuclear cells (PBMCs), into which the majority of tenofovir is sequestered when given as TAF. It is some of this intracellular tenofovir that then leaks back out into the plasma. This is in line with results by Lee *et al*., (Lee et al., 2005) who showed that compared to TDF, TAF preferentially concentrates in PBMCs as opposed to red blood cells.

Like previous reports, we describe a 2-compartment disposition model with first-order elimination for tenofovir. Our values of clearance (central and intercompartmental), and volume of distribution (central and peripheral) are all within the range of previous reports (Jullien et al., 2005; Gagnieu et al., 2008; Baheti et al., 2011; Burns, Hendrix & Chaturvedula, 2015; Lu et al., 2016b; Eke et al., 2021). Weight was a predictor of clearance and volume and its inclusion as a covariate improved the model significantly. Our sampling schedule allowed for adequate estimation of two separate first-order absorption rate constants for the TAF ($1.45 h^{-1}$) and TDF ($3.04\ h^{-1}$) arms. These values are in line with previous reports, with one publication reporting a value (median 95%CI) of 1.06 (0.62 – 1.86) h^{-1}, (Parant et al., 2019) and another as high as 4.7 (1.46 – 128.15) h^{-1} (Lu et al., 2016b).

One limitation of our model is that we were not able to quantify the effect of renal function on tenofovir clearance, which has previously been reported to be significant. This could be due to the narrow distribution of values of creatinine clearance in our cohort (with a median and interquartile range of 120 and 96.0 – 140 mL/min, respectively). In addition, the fact that creatinine measurements were not taken at the time of pharmacokinetic sampling (but at baseline and other arbitrary times) could have precluded our ability to estimate an effect of renal function. However, since the disposition of tenofovir in our model is compatible with previous reports, one can speculate that results on the effect of renal function on clearance could be carried across.

A major limitation is that we do not have plasma TAF concentrations and neither do we have tenofovir concentrations in PBMCs. We only have plasma tenofovir concentrations and therefore, we validate our predictions in terms of the way tenofovir appears in plasma. However, TAF is very short-lived in plasma and usually reaches undetectable levels in plasma 4 to 6 hours post-dose. Therefore, even though we did not observe this in our study, our model is consistent with the literature.

In conclusion, the semi-mechanistic model we developed adequately described tenofovir concentrations in a cohort of South African adults living with HIV. This model plausibly describes the differences observed between the conversion of TDF and TAF to tenofovir and the resulting different exposures in plasma. The model should foster further investigation of the use of TAF as it offers a tool for investigating drug-drug interactions, exposure predictions in patients, and for simulation of alternative dosing regimens and for further clinical trials that may increasingly involve the use of TAF in place of TDF for the treatment of HIV in resource-constrained settings. Considering that there are still limited published pharmacokinetic data on TAF in low-and middle-income countries, especially in persons co-infected with tuberculosis, children and pregnant women, more studies are needed to further elucidate the dosing of this drug in such scenarios and compare it with TDF. We believe a semi-mechanistic approach such as the one that we suggest here is going to be essential to correctly interpret the results from these studies.

8.6 Supplementary material

Table S.8.1: Sensitivity analysis for the $T_{1/2\_TAF\text{-}Slow}$ Parameter

Parameter description	**Typical value**								
$T_{1/2\_TAF\text{-}Slow}$ (days) [a] Fixed	0.083 (2 hours)	0.25 (6 hours)	0.5 12 (hours)	1.71	3.42	6.83 [d]	13.7	30	90
OFV	-2420	-2442	-2483	-2512	-2514	-2515.5	-2515.7	-2515.8	-2515.5
CL (L/h) [b]	26.2	38.6	42.0	44.7	44.7	44.7	44.7	44.7	44.7
V_c (L)[b]	377	378	396	377	377	378	377	377	377
Q (L/h) [b]	171	179	158	157	157	157	158	157	157
V_p (L)[b]	405	435	386	350	350	356	350	351	350
F_{TDF} (.) fixed	1	1	1	1	1	1	1	1	1
F_{TAF} (.)	0.292	0.616	0.768	0.836	0.812	0.822	0.821	0.820	0.819
K_{a_TDF} (1/h)	3.22	2.94	3.08	3.05	3.04	3.04	3.05	3.05	3.04
K_{a_TAF} (1/h)	2.14	3.66	1.46	1.45	1.45	1.45	1.36	1.28	1.45
$Frac_{TAF\text{-}Fast}$ (%)	0.773	0.312	0.29	0.300	0.331	32.4	32.8	33.1	33.1
Proportional error (%)	12.3	13.5	12.7	12.0	11.9	11.9	11.9	11.9	11.9
Additive error (mg/L) [c]	0.0001	0.0001	0.0001	0.0001	0.0001	0.0001	0.0001	0.0001	0.0001

[a] Parameter was fixed to a listed value for each of the runs.
[b]Allometric scaling with weight (for a reference individual of 70 kg) was used for the clearance (CL), inter-compartmental clearance (Q), central volume of distribution (V_c), and peripheral volume of distribution (V_p). Absorption rate constant (K_a). The half-life of the first-order process by which tenofovir leaves the intracellular compartment to the central compartment ($T_{1/2\_TAF\text{-}Slow}$). Percentage of tenofovir that is immediately available for absorption into the systemic circulation ($Frac_{TAF\text{-}Fast}$).
[c] fixed to 20% of the lower limit of quantification (LLOQ) which was 0.0005 mg/L.
[d] The final model has the value fixed to 6.83 days

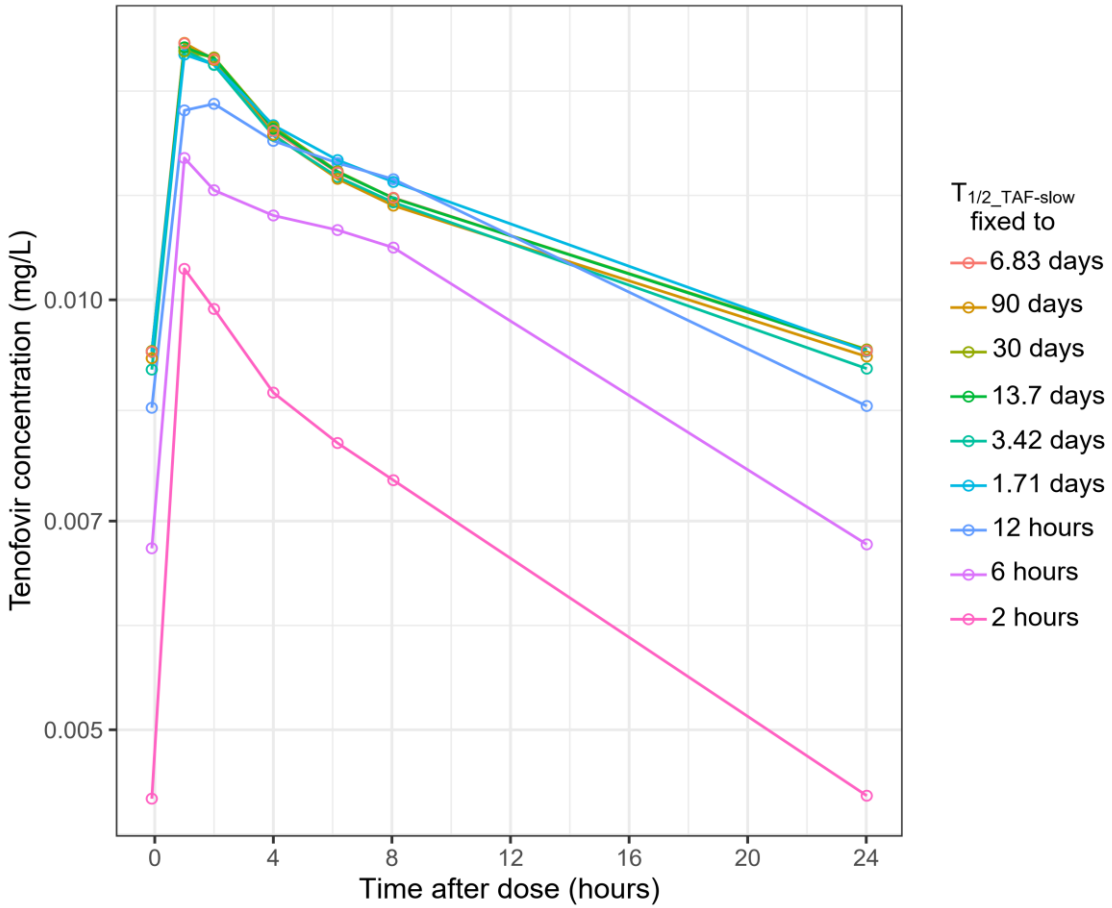

Figure S.8.1:*Predicted concentration-time profile of a single individual in the TAF (Tenofovir alafenamide) arm (weight 71.3 kg) when the* $T_{1/2\_TAF\text{-}slow}$ *parameter is fixed to different values and the model re-estimated.*

Chapter 9 Discussion and conclusions

9.1 Overall summary

The findings of this research provide insights to improve and optimise the treatment of HIV amongst persons with co-morbidities including tuberculosis and malaria. By employing NLME modelling techniques, it was possible to pool and analyse data from different studies carried out in healthy volunteers and PLWH and to incorporate both intensive and sparsely sampled datasets.

This thesis describes dolutegravir pharmacokinetics, pharmacogenetics, and DDI with the anti-tuberculosis drugs rifampicin and rifabutin, and with the anti-malarial drugs artemether-lumefantrine and artesunate-amodiaquine. It also describes the pharmacokinetics of tenofovir when dosed as either TDF or TAF in South Africans living with HIV.

One of the more significant findings to emerge from our research in **Chapter 5** is that, although rifampicin leads to reduced dolutegravir concentrations and thus warrants twice-daily dosing of dolutegravir when co-administered (50 mg BD), a simpler regimen of 100 mg OD may be sufficient to achieve desired trough target concentrations. Based on these findings, we encourage further studies involving the use of the 100 mg regimen.

In **Chapter 6**, we showed that rifabutin decreases dolutegravir volume of distribution, thus leading to a higher peak and lower trough, but without an overall change in AUC. Surprisingly, rifabutin did not impact the clearance of dolutegravir. This is encouraging, considering rifabutin has been considered a possible replacement for rifampicin in situations where its enzyme induction properties would severely reduce exposure of victim drugs, as seen with dolutegravir.

Furthermore, in **Chapter 7**, we confirm that UGT1A1 polymorphisms play a role in dolutegravir exposure within an African population. Homozygous individuals (T/T) and

heterozygous (C/T) for *UGT* rs887829 were estimated to have 25.9% and 10.8% lower dolutegravir clearance, respectively.

Our research in **Chapter 4** showed that the DDI between dolutegravir and the antimalarials artemether-lumefantrine and artesunate-amodiaquine is not clinically relevant, and no dose adjustment is required when these are co-administered. This supports the use of dolutegravir-based regimens in malaria-endemic areas.

In **Chapter 8**, we report a joint model describing tenofovir pharmacokinetics when given either as TAF or TDF. This is a step forward compared to all previously published models, which utilized separate models to describe the population pharmacokinetics of tenofovir, one when administered as TDF, and a different one when administered as TAF. Our joint model is more physiologically plausible and mechanistic, and as such it is expected to be more reliable when characterising drug-drug interactions, predicting exposures in patients, and simulating alternative regimes to inform further clinical trials that involve either TDF or TAF, especially since African countries are beginning to explore the use of TAF.

This thesis has provided a deeper insight into modelling strategies for pharmacokinetic data, dolutegravir and tenofovir pharmacokinetics, and has highlighted relevant implications for future practice, which are discussed further below.

9.2 General methodological considerations

9.2.1 Exposure metrics

The summary exposure parameters AUC, C_{min}, and C_{max} are often used to relate drug exposure to its response, both efficacy and safety. However, identifying the most predictive amongst them is often puzzling. Unless this question is explicitly looked at within specific dose-finding or dose-fractionation studies, it is very difficult to gather empirical evidence to support the use of one against the others. Within a study where the drug is dosed at the same frequency and

strength in all patients, all three parameters are very tightly correlated, so it is nearly impossible to differentiate. C_{min} is an often-attractive option, especially where the collection of multiple samples is not feasible. As such, C_{min} is a commonly used parameter in therapeutic drug monitoring (TDM). However, C_{min} alone does not offer any insight into separating the absorption, distribution, and elimination processes of a drug since it mostly depends on the terminal half-life and, importantly, on the time of intake of the previous dose, which is generally not observed and often not accurately reported by patients.

On the other hand, C_{max} is a parameter that mostly reflects the rate and extent of absorption of a drug and is an important measure in bioequivalence studies (Japan Agency, 1997). Also, C_{max} is affected by the distribution and elimination of a drug. Since the absorption of orally administered drugs is very variable and for some drugs erratic, several blood draws may be necessary to reliably determine C_{max}.

Finally, AUC is informed by the bioavailability and clearance of a drug and is the key metric in bioequivalence studies (FDA, 2001). Others suggested include the ratio of C_{max}/AUC and time to C_{max} (T_{max}) (Chen, Lesko & Williams, 2001). However, outside of bioequivalence studies, a fundamental limitation of AUC measurements is the necessity to collect many samples; except if a modelling approach is to be utilized, but even then, more than one sample is generally necessary for a reliable estimate. For pharmacokinetic-pharmacodynamic studies, investigators should probe which metric of exposure is more informative or important, taking into consideration the drug's mechanism of action. The AUC metric is a more robust target since it is less variable compared to C_{min} and C_{max} which are dependent on the time of dose and an absorption process that is largely variable. Nevertheless, for some drugs, C_{min} might be the more important parameter. Therefore, unless there is strong evidence to support one exposure metric over another for a particular drug, scientists should avoid adhering to one as the gold standard. In **Chapter 6**, where we characterised the interaction between dolutegravir

and rifabutin, we also showed that a perpetrator drug may affect these exposure metrics differently. While the C_{min} of dolutegravir was decreased and its C_{max} increased by rifabutin, there was no overall change in the AUC. Therefore, when investigating DDIs, it is prudent to test the effect on different physiological/primary parameters (Cl, V, and bioavailability) as opposed to secondary pharmacokinetic parameters such as C_{min} and C_{max}.

9.2.2 Assign variability where it is due

Throughout these analyses, it has become apparent that when analysing data with NLME modelling, it is important to assign variability correctly, i.e., to its most probable and plausible source. For model parameters that are expected to vary between individuals but to remain mostly constant within an individual, one should allocate a BSV random effect. On the other hand, for parameters whose variability is expected to be significant within an individual, one should include a BOV random effect. This would be, for example, due to separate dosing/sampling occasions which should also be assigned as such. Similar to BSV, which is constant within an individual and averages out to zero at a population level, BOV changes between different occasions but is expected to average out to zero over time within an individual. Often, the available data may not be informative enough for the model to support both BSV and BOV on the same parameter, in which case it may be necessary to simplify the stochastic model and only retain the term that is plausibly more relevant for that parameter. In general, this will also result in better goodness of fit, but in the early stages of model development, when the structure and other important effects may not have been identified yet, proper minimization of the OFV may be difficult, so it is a good strategy to use knowledge and physiological plausibility when guiding the model development.

Within pharmacokinetics, absorption of orally administered drugs tends to be the most variable process and can fluctuate significantly from dose to dose. Different physiological factors

including diurnal variation, alterations in gastric emptying times, differences in food intake and co-medication administered with a drug support the assumption that the rate and extent of absorption of drugs can change from day to day and even within the same day. Therefore, including BOV on absorption parameters is sound practice and should be implemented in scenarios where one has data from repeated dosing and sampling. While some individual-specific factors do exist that may affect drug absorption, their influence is generally smaller, so unless very rich data from multiple dosing occasions is available, it may not be possible to separate the individual-specific component of the variability in absorption.

Of note, when studying drugs that are dosed repeatedly within a maintenance regimen, a pre-dose sample is often collected, and its concentration depends on the dosing history and the pharmacokinetic parameters on the day(s) before (i.e., leading up to) the sampling visit. Outpatient pharmacokinetic studies often rely on self-reports for the timing of doses before the pharmacokinetic visit. These are generally inaccurate. Factors mentioned earlier, such as food intake with the drug, may cause differences in absorption between the previous and the observed dose. Therefore, it is good practice for pre-dose samples to be considered as a separate pharmacokinetic occasion, thus allowing for the estimation of differences in absorption parameters.

During the model building process in **Chapter 5**, an interesting observation was that if the data was analysed by testing and including only BSV on all parameters, the resulting final model was very different from when BOV plus BSV were tested and included, namely BOV on absorption parameters and BSV on disposition parameters. First, the inclusion of BOV markedly improved the fit of the models, evidenced by a significant drop in OFV. Second, when only BSV was included in the model, it was difficult to characterize the absorption robustly: one could not identify variability in the absorption lag time (so every patient implausibly had the same exact absorption delay) and the typical value of K_a could not be

estimated precisely and had to be fixed to a literature value. As an alternative strategy to make the absorption more stable, the model had to be simplified from two- to one-compartment disposition, despite a significant increase in OFV. Moreover, the model including BSV only had a much larger proportional error of 25% vs 7.8%. However, when BOV was included on absorption parameters and BSV on disposition parameters, it was possible to adequately characterize two-compartment disposition, estimate the K_a, a lag-time with its variability and subsequently identify an effect of sex on K_a.

In conclusion, failure to correctly include BOV in population pharmacokinetic analysis may cause spurious attribution of variability between different parameters, or inflated residual unexplained variability, as previously reported (Karlsson & Sheiner, 1993). Moreover, and more importantly, it may lead to inaccurate and unstable estimates of typical values of absorption parameters, the inability to identify the effect of a covariate, or even the identification of the wrong structural model. Therefore, I recommend the inclusion of BOV in population pharmacokinetics models and the handling of pre-dose samples as separate pharmacokinetic occasions, even with semi-intensively sampled data.

9.2.3 Nominal versus actual dosing and sampling times

The time of dosing is one of the most important inputs in a pharmacokinetic model. However, and especially for outpatients on chronic medication, getting accurate dosing information is often difficult because most doses are not taken under observation and dosing times are self-reported. While many interventions have been employed to improve the accuracy of this information, including targeted pharmacokinetic training to ensure medical staff and participants understand why this is vitally important, video-calling participants to observe them as they swallow medication, and giving participants diaries to record the time of dosing,

pharmacometricians still find themselves with dosing information that is either missing or inaccurate.

The consequence of these inaccurate dosing times on model parameters is hard to predict, and some parameter values may not be affected much, while others may vary significantly. A paper by Jin *et al.* compared the effect of two methods used to report dosing times, medication event monitoring system (MEMS) vs. patient-reported, on the pharmacokinetics of escitalopram. They found that there was no effect on the estimates of oral clearance, with values of 25.5 (relative standard error 7.0%) and 26.9 (6.6%) L/hr for MEMS versus patient-reported methods, respectively (Jin et al., 2009). However, for V and K_a, there was a significant difference in the estimates obtained between the two methods of reporting. V was 1000 (17.3%) and 767 (17.5%) L for MEMS and patient-reported methods respectively while the K_a was 0.74 (45.7%) and 0.51 (35.4%) hr^{-1} for MEMS versus patient-reported (Jin et al., 2009). Importantly, inaccurate dosing times may affect therapeutic decisions in patient management and impact safety and efficacy. A paper by Roydhouse *et al.* reported how dosing decisions for intravenously administered antimicrobial drugs were impacted by the accuracy of documented dosing times. For vancomycin, they found that the discrepancy between the actual and reported time of administration led to inappropriate TDM and consequently, wrong dosing recommendations in more than 50% of cases (Roydhouse et al., 2021).

In a population pharmacokinetic model, several approaches can be used to mitigate the impact of inaccurate dosing times before a pre-dose concentration.

A rather "drastic" approach consists in modelling pre-dose concentrations as the baseline, as suggested by Dansirikul *et al.* (Dansirikul, Silber & Karlsson, 2008). With this technique, dosing history is disregarded, and drug amounts in the central compartment of the model are initialized to the observed values. A disadvantage of this approach is that it essentially disregards any information that may have been contained in the pre-dose values, which may

limit how informative your dataset might be towards the estimation of some parameters. Another issue is that, in models with disposition characterised by more than one compartment, the correct initialization of peripheral compartments is not trivial.

A less stringent approach may be to adjust (i.e., re-estimate) the times of the previous doses by including a lag time (with random variability). This can be particularly useful for drugs with shorter half-lives that might be dosed more frequently than once a day. However, the assumptions on the size and shape of the variability for this special lag time may not be trivial to establish. For example, the patients may be taking their drugs in the morning or evening, thus resulting in a bimodal distribution for dosing times on the day before the pharmacokinetic visit.

A more general approach, which is arguably good practice even with reliable dosing history, is to test and include in the model some variability terms that can account for any discrepancy, if any, between pre-dose data and the rest of the pharmacokinetic profile after an observed dose. This should be at minimum the inclusion of BOV for all absorption parameters. Including BOV allows you to treat each dose as a separate occasion and therefore account for differences in the speed and extent of absorption between the unobserved dose, and the observed dose within the model. If indeed there is more variability in the pre-dose concentrations than expected, one can add a scaling factor allowing for the BOV on absorption parameters or the RUV (extra error) on the pre-dose concentrations to be larger than after an observed dose. This approach simply estimates more error or variation when fitting the pre-dose concentrations thus accounting for the fact that there is uncertainty about the accuracy of the dosing time that led to these concentrations.

9.3 Lessons learnt

9.3.1 Involve pharmacometricians at an early stage in studies/clinical trials

Often, pharmacokinetic studies are included as smaller sub-studies nested within larger clinical trials, as was the case with data obtained from the ADVANCE trial. In other instances, data is primarily meant to be analysed with NCA and as such less emphasis is given to obtaining exact sampling and dosing times. The result of these two positions is that pharmacometricians are usually excluded from the initial discussions of the design and implementation of these studies and are only involved towards the end when pharmacokinetic/pharmacodynamic data is available for analysis. The consequence of this is that, often, the data collected is not as informative as it could have been and information that may have better informed pertinent questions is not collected. If consulted during protocol development, a pharmacometrician, through simulations, for example, could help inform an optimal pharmacokinetic sampling schedule that would allow investigators to estimate important parameters of absorption and disposition. Therefore, going forward, one recommendation is that clinical research teams should endeavour to involve and consult pharmacometricians in the early, design stages of their studies. That way, we can fully harness the potential of pharmacometrics.

9.3.2 Pharmacokinetics sampling (intensive versus sparse sampling)

The ability to adequately estimate parameters in population models is largely dependent on the sample size, the number of samples per individual, and the location of these samples relative to the dose (Roy & Ette, 2005). Sheiner and Beal (Sheiner & Beal, 1983) found that the precision of parameter estimates is improved with larger sample sizes while Hooker *et al.*

showed that the model that best fits the data (one- versus two- compartments) can be influenced by the number of samples per individual (Hooker, Staatz & Karlsson, 2007).

One of the key strengths of NLME modelling is the ability to pool and analyse data irrespective of the dosing and sampling schedule, thus allowing inclusion in the model of data from different studies with a combination of intensive and sparse sampling. While having intensive sampling in each patient provides more information and allows robust estimation of the pharmacokinetic parameters, it may not be practical, feasible, or even ethical, for example in neonatal and pediatric populations. On the other hand, sparse sampling allows the inclusion in the study of a larger number of participants, which is better suited for linking to pharmacodynamic models and estimating covariate effects caused, for example, by genetic diversity. Likewise, sparse sampling for TDM is the norm. However, the biggest drawback to this type of sampling (especially in outpatient settings) is that, usually, the time of administering the previous doses is self-reported and therefore prone to be imprecise. Subsequently, these sparse samples are often fraught with large uncertainty. When planning studies, researchers should carefully consider what the best use of resources will be vis-à-vis their research question. Do they intensively sample a few individuals, or do you sparsely sample many individuals, and if resources are limited, at what time points do they take samples?

The decision of when to take an informative sample is an important one and is mostly driven by factors specific to the drug. For instance, for drugs like digoxin, whose absorption and distribution take time, sampling after about 6 hours post-dose might be more informative because before that, distribution is still ongoing and the concentrations may be erroneously interpreted as high (Ghiculescu, 2008). On the other hand, for antibiotics given intravenously, a sample around the peak might be important, which usually falls about 30 minutes after an infusion (Gross, 1998). While for drugs with a long half-life, sampling before they get to

steady-state might be prudent to ensure that concentrations do not get to toxic amounts (Ghiculescu, 2008).

Lastly, depending on whether you are going to use a modelling approach or not, you might be able to get away with fewer sampling time points. The traditional NCA modelling approach requires rich sampling of each individual, which is not necessary for population modelling. However, from the experience of the work on this thesis, having only sparsely sampled data may leave some questions unanswered, if there are systematic differences between arms or studies. This was the case with the INSPIRING STUDY which collected only sparse samples for all individuals. With only sparse samples, we were unable to jointly model data from INSPIRING with that from RADIO and NCT01231542 and we could not reliably identify which parameter was driving the difference between INSPIRING and the other studies. If a subset of patients had been intensively sampled, we could have tested our hypotheses on these. Therefore, a reasonable approach for pharmacokinetic studies is to include a subset of patients that are intensively sampled. These allow for the correct characterisation of the structural model or the tweaking of previous models to the current population/study. This model can then be used to interpret the sparse data, which should be included in a second step. The model on the intensive data can also be used to identify implausible results from the sparse data, which can then be excluded from the pooled analysis.

9.3.3 Consideration for drug-drug interaction studies

Before a drug is granted market approval, regulatory authorities require the applicant to provide results of the assessment of CYP450 enzyme- and transporter-mediated drug- DDI for the investigational product. The goals of DDI studies are to determine whether the investigational drug alters the pharmacokinetics of other drugs and vice versa, whether this

alteration is clinically relevant and, if so, how to manage it (European Medicines Agency, 2012; FDA, 2020).

Currently, DDI studies are carried out in healthy volunteers, except in instances where the pharmacology of a drug may preclude its investigation in healthy volunteers (such as with oncology drugs). While findings in healthy volunteers are usually applicable to patients, there are exceptions. Treatment for conditions such as HIV and tuberculosis involves the use of a cocktail of drugs rather than single agents. However, when carried out with healthy volunteers, DDI studies usually investigate only the drugs of interest (victim and perpetrator) and do not include accompanying drugs used in patients. **Chapter 5** highlights the discrepancies that may arise from findings in healthy volunteers versus patients. Therefore, one recommendation arising from this work is that as much as possible, DDI studies carried out with healthy volunteers should also be confirmed in a patient population or, as much as possible, be designed to mimic the treatment context that would apply to patients.

9.4 Future work

9.4.1 Use of TAF in high-burden countries

Although we described a model characterising the disposition of tenofovir when administered as TDF or TAF in an African population, there are still unanswered questions regarding the use of TAF, including in children or pregnant women. Moreover, considering that sub-Saharan Africa has high incidences of HIV-tuberculosis co-infection, it is imperative to investigate the use of TAF within the context of drugs used for tuberculosis treatment. A trial on the use of TAF in children is underway (ISRCTN22964075)

The semi-mechanistic model we developed in **Chapter 8** lends itself to these investigations. Because it accounts for different absorption processes for TDF and TAF leading to observed

plasma tenofovir concentrations, one can investigate the influences of a DDI not only on disposition parameters but also on absorption and distribution parameters. Rifampicin, for example, is an inducer of P-glycoprotein, of which TAF is a substrate (Begley et al., 2018). With our model, one can test rifampicin's effect not only on tenofovir clearance but also on the various parameters describing its absorption when given as TAF.

Currently, in high-burden countries, tenofovir is mostly available within an FDC pill as TDF/dolutegravir/lamivudine (World Health Organization, 2018). On the other hand, TAF is currently available within an FDC with emtricitabine and either bictegravir or elvitegravir; but is only recommended for use under the USA and European ART treatment guidelines (Panel on Antiretroviral Guidelines for Adults and Adolescents, 2016) and not under WHO guidelines (World Health Organization, 2018). Currently, WHO guidelines only recommend the use of TAF for individuals with established osteoporosis or impaired kidney function. Because of the limited information about the use of TAF in children, pregnant women and tuberculosis co-infected individuals that I have highlighted above, more research may be required before WHO recommends TAF as a substitute for TDF outside of special circumstances such as kidney insufficiency.

9.4.2 IC90 versus EC90 for dolutegravir

There is little consensus on what the optimal dolutegravir pharmacokinetic target should be. Both targets, the dolutegravir PA-IC90 of 0.064 mg/L, and EC90 of 0.3 mg /L have shortcomings. Because the PA-IC90 mg/L was established *in vitro*, there are concerns about its translation to *in vivo* values. On the other hand, the 0.3 mg/L "clinical" target was the geometric mean of the C_{min} in the 10-mg arm of a study that investigated dolutegravir doses of 10, 25, and 50 (Van Lunzen et al., 2012). All patients on all dose levels displayed very similar profiles of viral suppression and there was little evidence to suggest that the lower dose (and

concentrations) achieved lower efficacy. Therefore, some consider this 0.3 mg/L target to be quite conservative. Further work to establish a more robust target would be important and could open the door to simpler dosing strategies. A secondary analysis of the data from the study by Van Lunzen *et al.* (using a population modelling approach) would allow for the development of a pharmacokinetic-pharmacodynamic model, which could link parameters such as the AUC, $C_{min,}$ and C_{max}. to treatment outcome data (viral loads). This could be sufficient to demonstrate that the individuals with the lowest trough concentration also achieved viral suppression and therefore the target might indeed be lower. Or it could reveal that C_{min} in plasma may not be meaningfully better than, say, average daily concentration (or AUC). In addition, with joint pharmacokinetic-pharmacodynamic modelling, an analysis of the dolutegravir monotherapy study (Min et al., 2011) in which dolutegravir is dosed as a single drug in HIV-positive individuals over a range of doses is ideal for characterizing a dose-effect relationship since any decrease in viral load is attributable to dolutegravir alone. Moreover, with data from this study, one can aim to incorporate dolutegravir's prolonged binding to its target into the model in order to explain the permanence of the effect observed even after dose discontinuation.

Compared to raltegravir and elvitegravir, dolutegravir exhibits prolonged binding to its target (the integrase-DNA complex) with a dissociative half-life of about 71 hours (Hightower et al., 2011b). Therefore, one can speculate that if an individual had periods during which dolutegravir concentrations are below the IC90, the long dissociative half-life means that bound dolutegravir could still prevent viral integration. Incidentally, it has been shown that compared to older antiretroviral regimens (raltegravir-, boosted PI-, and NNRT-based regimes) dolutegravir-based regimes are more forgiving to non-adherence and interrupted treatment (Parienti et al., 2021).

A more forgiving target would be important to simplify dosing strategies for dolutegravir. Currently, dolutegravir is given twice daily when it is co-administered with drugs that are known to induce its metabolism and reduce exposure including rifampicin and carbamazepine. Twice-daily dosing is also challenging to implement, especially in high-burden, resource-limited settings where treatment is given under programmatic conditions and as FDCs.

9.5 Overall conclusion

Taken together, this body of work represents a comprehensive examination of the DDIs between dolutegravir and medications used for tuberculosis and malaria, two co-morbidities that are common in Africa. Furthermore, it contributes to our understanding of the disposition of tenofovir in an African population. The use of pharmacometric techniques allowed for pooling and analysing data from different studies and the option to run simulations to suggest alternative dosing regimens.

References

Ait Moha, D. & Van den Berk, G. 2016. Unexpectedly High Rate of Intolerance for Dolutegravir in Real Life Setting. In *CROI*. Boston. 948.

Anderson, B.J. & Holford, N.H.G. 2008. Mechanism-Based Concepts of Size and Maturity in Pharmacokinetics. *Annual Review of Pharmacology and Toxicology*. 48(1):303–332. DOI: 10.1146/annurev.pharmtox.48.113006.094708.

Atta, M.G., De Seigneux, S. & Lucas, G.M. 2019. Clinical Pharmacology in HIV Therapy. *Clinical Journal of the American Society of Nephrology : CJASN*. 14(3):435. DOI: 10.2215/CJN.02240218.

Aweeka, F.T. & German, P.I. 2008. DOI: 10.2165/00003088-200847020-00002.

Baheti, G., Kiser, J.J., Havens, P.L. & Fletcher, C. V. 2011. Plasma and Intracellular Population Pharmacokinetic Analysis of Tenofovir in HIV-1-Infected Patients †. *ANTIMICROBIAL AGENTS AND CHEMOTHERAPY*. 55(11):5294–5299. DOI: 10.1128/AAC.05317-11.

Balzarini, J., Holy, A., Jindrich, J., Naesens, L., Snoeck, R., Schols, D. & De Clercq, E. 1993. Differential antiherpesvirus and antiretrovirus effects of the (S) and (R) enantiomers of acyclic nucleoside phosphonates: potent and selective in vitro and in vivo antiretrovirus activities of (R)-9-(2-phosphonomethoxypropyl)-2,6-diaminopurine. *Antimicrobial Agents and Chemotherapy*. 37(2):332. DOI: 10.1128/AAC.37.2.332.

Banda, C.G., Barnes, K.I. & Maartens, G. 2019. DOI: 10.1128/AAC.00576-19.

Barcelo, C., Aouri, M., Courlet, P., Guidi, M., Braun, D.L., Günthard, H.F., Piso, R.J., Cavassini, M., et al. 2019. Population pharmacokinetics of dolutegravir: Influence of drug-drug interactions in a real-life setting. *Journal of Antimicrobial Chemotherapy*. 74(9):2690–2697. DOI: 10.1093/jac/dkz217.

Barrett, J.S., Fossler, M.J., David Cadieu, K. & Gastonguay, M.R. 2008. Pharmacometrics: A Multidisciplinary Field to Facilitate Critical Thinking in Drug Development and Translational Research Settings. *Journal of Clinical Pharmacology*. 48:632–649. DOI: 10.1177/0091270008315318.

Barry, M., Mulcahy, F. & Back, D.J. 1998. Antiretroviral therapy for patients with HIV disease. *British Journal of Clinical Pharmacology*. 45(3):221. DOI: 10.1046/J.1365-2125.1998.00673.X.

Begley, R., Das, M., Zhong, L., Ling, J., Kearney, B.P. & Custodio, J.M. 2018. Pharmacokinetics of Tenofovir Alafenamide When Coadministered With Other HIV Antiretrovirals. *Journal of acquired immune deficiency syndromes (1999)*. 78(4):465–472. DOI: 10.1097/QAI.0000000000001699.

Boeckmann, A.J., Beal, S.L. & Sheiner, L.B. 2011. NONMEM User's Guide, Part V. Introductory Guide. *NONMEM Project Group*. (April):48. DOI: 10.1017/CBO9781107415324.004.

Brainard, D.M., Kassahun, K., Wenning, L.A., Petry, A.S., Liu, C., Lunceford, J.,

Hariparsad, N., Eisenhandler, R., et al. 2011. Lack of a clinically meaningful pharmacokinetic effect of rifabutin on raltegravir: In vitro/in vivo correlation. *Journal of Clinical Pharmacology*. 51(6):943–950. DOI: 10.1177/0091270010375959.

Burns, R.N., Hendrix, C.W. & Chaturvedula, A. 2015. Population pharmacokinetics of tenofovir and tenofovir-diphosphate in healthy women. *Journal of Clinical Pharmacology*. 55(6):629–638. DOI: 10.1002/JCPH.461.

Campbell-Yesufu, O.T. & Gandhi, R.T. 2011. HIV/AIDS: Update on Human Immunodeficiency Virus (HIV)-2 Infection. *Clinical Infectious Diseases: An Official Publication of the Infectious Diseases Society of America*. 52(6):780. DOI: 10.1093/CID/CIQ248.

Castellino, S., Moss, L., Wagner, D., Borland, J., Song, I., Chen, S., Lou, Y., Min, S.S., et al. 2013. Metabolism, excretion, and mass balance of the HIV-1 integrase inhibitor dolutegravir in humans. *Antimicrobial agents and chemotherapy*. 57(8):3536–46. DOI: 10.1128/AAC.00292-13.

Chan Kwong, A.H.X.P., Calvier, E.A.M., Fabre, D., Gattacceca, F. & Khier, S. 2020. DOI: 10.1007/s10928-020-09695-z.

Chen, M.-L., Lesko, L. & Williams, R.L. 2001. *Measures of Exposure versus Measures of Rate and Extent of Absorption*.

Chen, S., St Jean, P., Borland, J., Song, I., Yeo, A.J., Piscitelli, S. & Rubio, J.P. 2014. Evaluation of the effect of UGT1A1 polymorphisms on dolutegravir pharmacokinetics. *Pharmacogenomics*. 15(1):9–16. DOI: 10.2217/pgs.13.190.

Cindi, Z., Kawuma, A.N., Maartens, G., Bradford, Y., Venter, F., Sokhela, S., Chandiwana, N., Wasmann, R.E., et al. 2022. Pharmacogenetics of dolutegravir plasma exposure among Southern Africans living with HIV. *The Journal of Infectious Diseases*. (May, 4). DOI: 10.1093/INFDIS/JIAC174.

Collart, L., Blaschke, T.F., Boucher, F. & Prober, C.G. 1992. Potential of population pharmacokinetics to reduce the frequency of blood sampling required for estimating kinetic parameters in neonates. *Developmental pharmacology and therapeutics*. 18(1–2):71–80.

Collins, J.W., Heyward Hull, J. & Dumond, J.B. 2017. Comparison of tenofovir plasma and tissue exposure using a population pharmacokinetic model and bootstrap: a simulation study from observed data. *Journal of Pharmacokinetics and Pharmacodynamics*. 44(6):631–640. DOI: 10.1007/S10928-017-9554-9/FIGURES/4.

Cooper, R.D., Wiebe, N., Smith, N., Keiser, P., Naicker, S. & Tonelli, M. 2010. Systematic review and meta-analysis: renal safety of tenofovir disoproxil fumarate in HIV-infected patients. *Clinical infectious diseases : an official publication of the Infectious Diseases Society of America*. 51(5):496–505. DOI: 10.1086/655681.

Cottrell, M.L., Hadzic, T. & Kashuba, A.D.M. 2013. Clinical Pharmacokinetic, Pharmacodynamic and Drug-Interaction Profile of the Integrase Inhibitor Dolutegravir. *Clinical Pharmacokinetics*. 52(11):981–994. DOI: 10.1007/s40262-013-0093-2.

Cressey, T.R., Siriprakaisil, O., Kubiak, R.W., Klinbuayaem, V., Sukrakanchana, P. ornsuda,

Quame-Amaglo, J., Okochi, H., Tawon, Y., et al. 2020. Plasma pharmacokinetics and urinary excretion of tenofovir following cessation in adults with controlled levels of adherence to tenofovir disoproxil fumarate. *International Journal of Infectious Diseases*. 97:365–370. DOI: 10.1016/J.IJID.2020.06.037.

Dansirikul, C., Silber, H.E. & Karlsson, M.O. 2008. Approaches to handling pharmacodynamic baseline responses. *Journal of pharmacokinetics and pharmacodynamics*. 35(3):269–283. DOI: 10.1007/S10928-008-9088-2.

Davies, G.R., Cerri, S. & Richeldi, L. 2007. DOI: 10.1002/14651858.CD005159.pub2.

Deeks, S.G., Lewin, S.R. & Havlir, D. V. 2013. The end of AIDS: HIV infection as a chronic disease. *The Lancet*. 382(9903):1525–1533. DOI: 10.1016/S0140-6736(13)61809-7.

Deeks, S.G., Overbaugh, J., Phillips, A. & Buchbinder, S. 2015. HIV infection. *Nature Reviews Disease Primers 2015 1:1*. 1(1):1–22. DOI: 10.1038/nrdp.2015.35.

Desai, M., Iyer, G. & Dikshit, R.K. 2012. Antiretroviral drugs: Critical issues and recent advances. *Indian Journal of Pharmacology*. 44(3):288. DOI: 10.4103/0253-7613.96296.

Desta, Z., Soukhova, N. V. & Flockhart, D.A. 2001. Inhibition of cytochrome P450 (CYP450) isoforms by isoniazid: Potent inhibition of CYP2C19 and CYP3A. *Antimicrobial Agents and Chemotherapy*. 45(2):382–392. DOI: 10.1128/AAC.45.2.382-392.2001.

Dickinson, L., Walimbwa, S., Singh, Y., Kaboggoza, J., Kintu, K., Sihlangu, M., Coombs, J.-A., Malaba, T.R., et al. 2020. Infant exposure to dolutegravir through placental and breastmilk transfer: a population pharmacokinetic analysis of DolPHIN-1. *Clinical Infectious Diseases*. (December, 21). DOI: 10.1093/cid/ciaa1861.

Ding, R., Tayrouz, Y., Riedel, K.D., Burhenne, J., Weiss, J., Mikus, G. & Haefeli, W.E. 2004. Substantial pharmacokinetic interaction between digoxin and ritonavir in healthy volunteers. *Clinical Pharmacology & Therapeutics*. 76(1):73–84. DOI: 10.1016/J.CLPT.2004.02.008.

Dooley, K.E., Sayre, P., Borland, J., Purdy, E., Chen, S., Song, I., Peppercorn, A., Everts, S., et al. 2013. Safety, Tolerability, and Pharmacokinetics of the HIV Integrase Inhibitor Dolutegravir Given Twice Daily With Rifampin or Once Daily With Rifabutin. *JAIDS Journal of Acquired Immune Deficiency Syndromes*. 62(1):21–27. DOI: 10.1097/QAI.0b013e318276cda9.

Dooley, K.E., Kaplan, R., Mwelase, N., Grinsztejn, B., Ticona, E., Lacerda, M., Sued, O., Belonosova, E., et al. 2020. Dolutegravir-based Antiretroviral Therapy for Patients Coinfected with Tuberculosis and Human Immunodeficiency Virus: A Multicenter, Noncomparative, Open-label, Randomized Trial. *Clinical Infectious Diseases*. 70(4):549–556. DOI: 10.1093/cid/ciz256.

Dosne, A.-G., Bergstrand, M., Harling, K. & Karlsson, M.O. 2016. Improving the estimation of parameter uncertainty distributions in nonlinear mixed effects models using sampling importance resampling. *Journal of Pharmacokinetics and Pharmacodynamics*. 43(6):583–596. DOI: 10.1007/s10928-016-9487-8.

Dumond, J.B., Nicol, M.R., Kendrick, R.N., Garonzik, S.M., Patterson, K.B., Cohen, M.S.,

Forrest, A. & Kashuba, A.D.M. 2012. Pharmacokinetic Modelling of Efavirenz, Atazanavir, Lamivudine and Tenofovir in the Female Genital Tract of HIV-Infected Pre-Menopausal Women. *Clinical pharmacokinetics*. 51(12):809. DOI: 10.1007/S40262-012-0012-Y.

Eke, A.C., Shoji, K., Best, B.M., Momper, J.D., Stek, A.M., Cressey, T.R., Mirochnick, M. & Capparelli, E. V. 2021. Population pharmacokinetics of tenofovir in pregnant and postpartum women using tenofovir disoproxil fumarate. *Antimicrobial Agents and Chemotherapy*. 65(3). DOI: 10.1128/AAC.02168-20.

Elassaiss-Schaap, J. & Duisters, K. 2020. Variability in the Log Domain and Limitations to Its Approximation by the Normal Distribution. *CPT: Pharmacometrics & Systems Pharmacology*. 9(5):245–257. DOI: 10.1002/PSP4.12507.

Elliot, E.R., Neary, M., Else, L., Khoo, S., Moyle, G., Carr, D.F., Wang, X., McClure, M., et al. 2020. Genetic influence of ABCG2, UGT1A1 and NR1I2 on dolutegravir plasma pharmacokinetics. *Journal of Antimicrobial Chemotherapy*. 75(5):1259–1266. DOI: 10.1093/jac/dkz558.

Elmeliegy, M., Vourvahis, M., Guo, C. & Wang, D.D. 2020. DOI: 10.1007/s40262-020-00867-1.

Esté, J.A. & Cihlar, T. 2010. Current status and challenges of antiretroviral research and therapy. *Antiviral Research*. 85(1):25–33. DOI: 10.1016/J.ANTIVIRAL.2009.10.007.

Estrella, M.M., Moosa, M.R. & Nachega, J.B. 2014. Editorial Commentary: Risks and Benefits of Tenofovir in the Context of Kidney Dysfunction in Sub-Saharan Africa. *Clinical Infectious Diseases*. 58(10):1481–1483. DOI: 10.1093/CID/CIU123.

Ette, E.I. & Williams, P.J. 2013. *Pharmacometrics: the science of quantitative pharmacology*. New Jersey, USA: John Wiley & Sons.

European Medicines Agency. 2012. Guideline on the investigation of drug interactions. Available: www.ema.europa.eu/contact [2022, July 20].

FDA. 2001. Statistical Approaches to Establishing Bioequivalence. *FDA Guidance*. (January):45. Available: https://www.fda.gov/regulatory-information/search-fda-guidance-documents/statistical-approaches-establishing-bioequivalence [2022, August 03].

FDA. 2020. Clinical Drug Interaction Studies-Cytochrome P450 Enzyme-and Transporter-Mediated Drug Interactions Guidance for Industry. Available: https://www.fda.gov/Drugs/GuidanceComplianceRegulatoryInformation/Guidances/default.htm [2022, July 20].

FDA, U. 1999. *Office of Training and Communications Division of Communications Management Drug Information Branch*. Rockville: Tel.

Figueroa, D.B., Tillotson, J., Li, M., Piwowar-Manning, E., Hendrix, C.W., Holtz, T.H., Bokoch, K., Bekker, L.-G., et al. 2018. Discovery of genetic variants of the kinases that activate tenofovir among individuals in the United States, Thailand, and South Africa: HPTN067. DOI: 10.1371/journal.pone.0195764.

Food and Drug Administration. 2013. TIVICAY(dolutegravir) Tablets for Oral Use. 1–37.

Available: www.fda.gov/medwatch. [2022, April 26].

Gabrielsson, J. & Weiner, D. 2016. *Pharmacokinetic and Pharmacodynamic Data Analysis Concepts and Applications 5 th edition*. 5th editio ed. Stockholm: Swedish Pharmaceutical Press.

Gagnieu, M.C., El Barkil, M., Livrozet, J.M., Cotte, L., Miailhes, P., Boibieux, A., Guitton, J. & Tod, M. 2008. Population Pharmacokinetics of Tenofovir in AIDS Patients. *The Journal of Clinical Pharmacology*. 48(11):1282–1288. DOI: 10.1177/0091270008322908.

Gammal, R.S., Court, M.H., Haidar, C.E., Iwuchukwu, O.F., Gaur, A.H., Alvarellos, M., Guillemette, C., Lennox, J.L., et al. 2016. DOI: 10.1002/cpt.269.

Ghiculescu, R.A. 2008. Therapeutic drug monitoring: which drugs, why, when and how to do it. *Australian Prescriber*. 31(2):42–44. DOI: 10.18773/AUSTPRESCR.2008.025.

Gobburu, J.V.S. & Marroum, P.J. 2001. Utilisation of Pharmacokinetic- Pharmacodynamic Modelling and Simulation in Regulatory Decision-Making. *Clinical Pharmacokinetics*. 40(12):883–892. DOI: 10.2165/00003088-200140120-00001.

Gonzalez-Montaner, L.J., Natal, S., Yongchaiyud, P., Olliaro, P., Abbate, E., Mosca, C., Casado, G., Di Lonardo, M., et al. 1994. Rifabutin for the treatment of newly-diagnosed pulmonary tuberculosis: a multinational, randomized, comparative study versus rifampicin. *Tubercle and Lung Disease*. 75(5):341–347. DOI: 10.1016/0962-8479(94)90079-5.

Gordi, T., Xie, R., Huong, N. V., Huong, D.X., Karlsson, M.O. & Ashton, M. 2005. A semiphysiological pharmacokinetic model for artemisinin in healthy subjects incorporating autoinduction of metabolism and saturable first-pass hepatic extraction. *British Journal of Clinical Pharmacology*. 59(2):189–198. DOI: 10.1111/j.1365-2125.2004.02321.x.

Goulooze, S.C., Völler, S., Välitalo, P.A.J., Calvier, E.A.M., Aarons, L., Krekels, E.H.J. & Knibbe, C.A.J. 2019. The Influence of Normalization Weight in Population Pharmacokinetic Covariate Models. *Clinical Pharmacokinetics*. 58(1):131. DOI: 10.1007/S40262-018-0652-7.

Grassi, C. & Peona, V. 1996. Use of rifabutin in the treatment of pulmonary tuberculosis. In *Clinical Infectious Diseases*. V. 22. Oxford University Press. DOI: 10.1093/clinids/22.supplement_1.s50.

Greene, S.A., Chen, J., Prince, H.M.A., Sykes, C., Schauer, A.P., Blake, K., Nelson, J.A.E., Gay, C.L., et al. 2019. Population Modeling Highlights Drug Disposition Differences Between Tenofovir Alafenamide and Tenofovir Disoproxil Fumarate in the Blood and Semen. *Clinical Pharmacology and Therapeutics*. 106(4):821–830. DOI: 10.1002/cpt.1464.

Griesel, R., Kawuma, A.N., Wasmann, R., Sokhela, S., Akpomiemie, G., Venter, W.D.F., Wiesner, L., Denti, P., et al. 2022. Concentration–response relationships of dolutegravir and efavirenz with weight change after starting antiretroviral therapy. *British Journal of Clinical Pharmacology*. 88(3):883–893. DOI: 10.1111/BCP.15177.

Gross, A.S. 1998. Best practice in therapeutic drug monitoring. *British Journal of Clinical Pharmacology*. 46(2):95. DOI: 10.1046/J.1365-2125.1998.00770.X.

Grover, A. & Benet, L.Z. 2009. Effects of Drug Transporters on Volume of Distribution. *The*

AAPS Journal. 11(2):250. DOI: 10.1208/S12248-009-9102-7.

Gupta, S.K., Post, F.A., Arribas, J.R., Eron, J.J., Wohl, D.A., Clarke, A.E., Sax, P.E., Stellbrink, H.J., et al. 2019. Renal safety of tenofovir alafenamide vs. tenofovir disoproxil fumarate: A pooled analysis of 26 clinical trials. *AIDS*. 33(9):1455–1465. DOI: 10.1097/QAD.0000000000002223.

Guttman, Y., Nudel, A. & Kerem, Z. 2019. Polymorphism in Cytochrome P450 3A4 Is Ethnicity Related. *Frontiers in Genetics*. 10(MAR):224. DOI: 10.3389/fgene.2019.00224.

Hailu, W., Tesfaye, T. & Tadesse, A. 2021. Hyperglycemia After Dolutegravir-Based Antiretroviral Therapy. *International medical case reports journal*. 14:503–507. DOI: 10.2147/IMCRJ.S323233.

Hawkins, T., Veikley, W., St. Claire, R.L., Guyer, B., Clark, N. & Kearney, B.P. 2005. Intracellular pharmacokinetics of tenofovir diphosphate, carbovir triphosphate, and lamivudine triphosphate in patients receiving triple-nucleoside regimens. *Journal of Acquired Immune Deficiency Syndromes*. 39(4):406–411. DOI: 10.1097/01.QAI.0000167155.44980.E8.

Hightower, K.E., Wang, R., DeAnda, F., Johns, B.A., Weaver, K., Shen, Y., Tomberlin, G.H., Carter, H.L., et al. 2011a. Dolutegravir (S/GSK1349572) exhibits significantly slower dissociation than raltegravir and elvitegravir from wild-type and integrase inhibitor-resistant HIV-1 integrase-DNA complexes. *Antimicrobial agents and chemotherapy*. 55(10):4552–4559. DOI: 10.1128/AAC.00157-11.

Hightower, K.E., Wang, R., DeAnda, F., Johns, B.A., Weaver, K., Shen, Y., Tomberlin, G.H., Carter, H.L., et al. 2011b. Dolutegravir (S/GSK1349572) exhibits significantly slower dissociation than raltegravir and elvitegravir from wild-type and integrase inhibitor-resistant HIV-1 integrase-DNA complexes. *Antimicrobial Agents and Chemotherapy*. 55(10):4552–4559. DOI: 10.1128/AAC.00157-11/ASSET/CEA7696A-2F51-4751-877E-BB9102AB894C/ASSETS/GRAPHIC/ZAC9991002510005.JPEG.

Hill, A., Hughes, S.L., Gotham, D. & Pozniak, A.L. 2018. Tenofovir alafenamide versus tenofovir disoproxil fumarate: is there a true difference in efficacy and safety? *Journal of Virus Eradication*. 4(2):72. DOI: 10.1016/s2055-6640(20)30248-x.

Hirigo, A.T., Gutema, S., Eifa, A. & Ketema, W. 2022. Experience of dolutegravir-based antiretroviral treatment and risks of diabetes mellitus. *SAGE open medical case reports*. 10:2050313X221079444. DOI: 10.1177/2050313X221079444.

Hoffmann, C., Welz, T., Sabranski, M., Kolb, M., Wolf, E., Stellbrink, H.J. & Wyen, C. 2017. Higher rates of neuropsychiatric adverse events leading to dolutegravir discontinuation in women and older patients. *HIV medicine*. 18(1):56–63. DOI: 10.1111/HIV.12468.

Hooker, A.C., Staatz, C.E. & Karlsson, M.O. 2007. Conditional weighted residuals (CWRES): a model diagnostic for the FOCE method. *Pharmaceutical research*. 24(12):2187–2197. DOI: 10.1007/S11095-007-9361-X.

Horne, D.J., Spitters, C. & Narita, M. 2011. Experience with rifabutin replacing rifampin in the treatment of tuberculosis. *International Journal of Tuberculosis and Lung Disease*. 15(11):1485–1489. DOI: 10.5588/ijtld.11.0068.

Huisman, M.T., Smit, J.W., Wiltshire, H.R., Hoetelmans, R.M.W., Beijnen, J.H. & Schinkel, A.H. 2001. P-Glycoprotein Limits Oral Availability, Brain, and Fetal Penetration of Saquinavir Even with High Doses of Ritonavir. *Molecular Pharmacology*. 59(4):806–813. DOI: 10.1124/MOL.59.4.806.

Ignatius, E.H., Abdelwahab, M.T., Hendricks, B., Gupte, N., Narunsky, K., Wiesner, L., Barnes, G., Dawson, R., et al. 2021. Pretomanid Pharmacokinetics in the Presence of Rifamycins: Interim Results from a Randomized Trial among Patients with Tuberculosis. *Antimicrobial Agents and Chemotherapy*. 65(2). DOI: 10.1128/AAC.01196-20.

Imaz, A., Martinez-Picado, J., Niubó, J., Kashuba, A.D.M., Ferrer, E., Ouchi, D., Sykes, C., Rozas, N., et al. 2016. HIV-1-RNA Decay and Dolutegravir Concentrations in Semen of Patients Starting a First Antiretroviral Regimen. *The Journal of Infectious Diseases*. 214(10):1512. DOI: 10.1093/INFDIS/JIW406.

Jackson, A., Moyle, G., Watson, V., Tjia, J., Ammara, A., Back, D., Mohabeer, M., Gazzard, B., et al. 2013. Tenofovir, emtricitabine intracellular and plasma, and efavirenz plasma concentration decay following drug intake cessation: Implications for HIV treatment and prevention. *Journal of Acquired Immune Deficiency Syndromes*. 62(3):275–281. DOI: 10.1097/QAI.0B013E3182829BD0.

Janmahasatian, S., Duffull, S.B., Ash, S., Ward, L.C., Byrne, N.M. & Green, B. 2005. Quantification of lean bodyweight. *Clinical Pharmacokinetics*. 44(10):1051–1065. DOI: 10.2165/00003088-200544100-00004.

Japan Agency. 1997. Guideline for Bioequivalence Studies of Generic Products. (10):23.

Jin, Y., Pollock, B.G., Frank, E., Florian, J., Kirshner, M., Fagiolini, A., Kupfer, D.J., Gastonguay, M.R., et al. 2009. The effect of reporting methods for dosing times on the estimation of pharmacokinetic parameters of escitalopram. *Journal of clinical pharmacology*. 49(2):176. DOI: 10.1177/0091270008327538.

Jullien, V., Tréluyer, J.M., Rey, E., Jaffray, P., Krivine, A., Moachon, L., Louet, A.L. Le, Lescoat, A., et al. 2005. Population pharmacokinetics of tenofovir in human immunodeficiency virus-infected patients taking highly active antiretroviral therapy. *Antimicrobial Agents and Chemotherapy*. 49(8):3361–3366. DOI: 10.1128/AAC.49.8.3361-3366.2005.

Kamal, P. & Sharma, S. 2019. SUN-187 Dolutegravir Causing Diabetes. *Journal of the Endocrine Society*. 3(Suppl 1). DOI: 10.1210/JS.2019-SUN-187.

Karlsson, M.O. & Sheiner, L.B. 1993. The importance of modeling interoccasion variability in population pharmacokinetic analyses. *Journal of pharmacokinetics and biopharmaceutics*. 21(6):735–750. DOI: 10.1007/BF01113502.

Kawuma, A.N., Walimbwa, S.I., Pillai, G.C., Khoo, S., Lamorde, M., Wasmann, R.E. & Denti, P. 2021. Dolutegravir pharmacokinetics during co-administration with either artemether/lumefantrine or artesunate/amodiaquine. *Journal of Antimicrobial Chemotherapy*. 76(5):1269–1272. DOI: 10.1093/JAC/DKAB022.

Kawuma, A.N., Wasmann, R.E., Dooley, K.E., Boffito, M., Maartens, G. & Denti, P. 2022. Population Pharmacokinetic Model and Alternative Dosing Regimens for Dolutegravir

Coadministered with Rifampicin. *Antimicrobial Agents and Chemotherapy*. (May, 23). DOI: 10.1128/AAC.00215-22.

Kearney, B.P., Flaherty, J.F. & Shah, J. 2004. Tenofovir disoproxil fumarate: Clinical pharmacology and pharmacokinetics. *Clinical Pharmacokinetics*. 43(9):595–612. DOI: 10.2165/00003088-200443090-00003/FIGURES/TAB4.

Keizer, R.J., Zandvliet, A.S., Beijnen, J.H., Schellens, J.H.M. & Huitema, A.D.R. 2012. Performance of methods for handling missing categorical covariate data in population pharmacokinetic analyses. *AAPS Journal*. 14(3):601–611. DOI: 10.1208/S12248-012-9373-2/TABLES/5.

Keizer, R.J., Karlsson, M.O. & Hooker, A. 2013a. Modeling and Simulation Workbench for NONMEM: Tutorial on Pirana, PsN, and Xpose. *CPT: Pharmacometrics & Systems Pharmacology*. 2(6):e50. DOI: 10.1038/psp.2013.24.

Keizer, R.J., Karlsson, M.O. & Hooker, A. 2013b. Modeling and simulation workbench for NONMEM: Tutorial on Pirana, PsN, and Xpose. *CPT: Pharmacometrics and Systems Pharmacology*. 2(6). DOI: 10.1038/psp.2013.24.

Kennedy, Ramsay, A., Uiso, L., Gutmann, J., Ngowi, F.I. & Gillespie, S.H. 1996. Nutritional status and weight gain in patients with pulmonary tuberculosis in Tanzania. *Transactions of the Royal Society of Tropical Medicine and Hygiene*. 90(2):162–166. DOI: 10.1016/S0035-9203(96)90123-6.

Krishna, R., East, L., Larson, P., Valiathan, C., Butterfield, K., Teng, Y. & Hernandez-Illas, M. 2016. Effect of metal-cation antacids on the pharmacokinetics of 1200 mg raltegravir. *Journal of Pharmacy and Pharmacology*. 68(11):1359–1365. DOI: 10.1111/JPHP.12632.

Lamorde, M., Atwiine, M., Owarwo, N.C., Ddungu, A., Laker, E.O., Mubiru, F., Kiragga, A., Lwanga, I.B., et al. 2020. Dolutegravir-associated hyperglycaemia in patients with HIV. *The Lancet HIV*. 7(7):e461–e462. DOI: 10.1016/S2352-3018(20)30042-4.

Laprise, C., Baril, J.-G., Dufresne, S. & Trottier, H. 2012. Association Between Tenofovir Exposure and Reduced Kidney Function in a Cohort of HIV-Positive Patients: Results From 10 Years of Follow-up. DOI: 10.1093/cid/cis937.

Lavielle, M. & Aarons, L. 2016. What do we mean by identifiability in mixed effects models? *Journal of Pharmacokinetics and Pharmacodynamics*. 43(1):111–122. DOI: 10.1007/s10928-015-9459-4.

Lee, W.A., He, G.X., Eisenberg, E., Cihlar, T., Swaminathan, S., Mulato, A. & Cundy, K.C. 2005. Selective intracellular activation of a novel prodrug of the human immunodeficiency virus reverse transcriptase inhibitor tenofovir leads to preferential distribution and accumulation in lymphatic tissue. *Antimicrobial agents and chemotherapy*. 49(5):1898–1906. DOI: 10.1128/AAC.49.5.1898-1906.2005.

Lefèvre, G. & Thomsen, M.S. 1999. Clinical pharmacokinetics of artemether and lumefantrine (Riamet®). *Clinical Drug Investigation*. 18(6):467–480. DOI: 10.2165/00044011-199918060-00006.

Letendre, S.L., Mills, A.M., Tashima, K.T., Thomas, D.A., Min, S.S., Chen, S., Song, I.H. &

Piscitelli, S.C. 2014. ING116070: A Study of the Pharmacokinetics and Antiviral Activity of Dolutegravir in Cerebrospinal Fluid in HIV-1–Infected, Antiretroviral Therapy–Naive Subjects. *Clinical Infectious Diseases: An Official Publication of the Infectious Diseases Society of America*. 59(7):1032. DOI: 10.1093/CID/CIU477.

Lu, Y., Goti, V., Chaturvedula, A., Haberer, J.E., Fossler, M.J., Sale, M.E., Bangsberg, D., Baeten, J.M., et al. 2016a. Population Pharmacokinetics of Tenofovir in HIV-1-Uninfected Members of Serodiscordant Couples and Effect of Dose Reporting Methods. *Antimicrobial Agents and Chemotherapy*. 60(9):5379. DOI: 10.1128/AAC.00559-16.

Lu, Y., Goti, V., Chaturvedula, A., Haberer, J.E., Fossler, M.J., Sale, M.E., Bangsberg, D., Baeten, J.M., et al. 2016b. Population Pharmacokinetics of Tenofovir in HIV-1-Uninfected Members of Serodiscordant Couples and Effect of Dose Reporting Methods. *Antimicrobial Agents and Chemotherapy*. 60(9):5379. DOI: 10.1128/AAC.00559-16.

Van Lunzen, J., Maggiolo, F., Arribas, J.R., Rakhmanova, A., Yeni, P., Young, B., Rockstroh, J.K., Almond, S., et al. 2012. Once daily dolutegravir (S/GSK1349572) in combination therapy in antiretroviral-naive adults with HIV: Planned interim 48 week results from SPRING-1, a dose-ranging, randomised, phase 2b trial. *The Lancet Infectious Diseases*. 12(2):111–118. DOI: 10.1016/S1473-3099(11)70290-0.

Lutz, J.D., Kirby, B.J., Wang, L., Song, Q., Ling, J., Massetto, B., Worth, A., Kearney, B.P., et al. 2018. Cytochrome P450 3A Induction Predicts P-glycoprotein Induction; Part 2: Prediction of Decreased Substrate Exposure After Rifabutin or Carbamazepine. *Clinical Pharmacology and Therapeutics*. 104(6):1191–1198. DOI: 10.1002/cpt.1072.

Marazziti, D., Baroni, S., Picchetti, M., Piccinni, A., Carlini, M., Vatteroni, E., Falaschi, V., Lombardi, A., et al. 2013. DOI: 10.1017/S1092852912001010.

Marcus, J.L., Leyden, W.A., Alexeeff, S.E., Anderson, A.N., Hechter, R.C., Hu, H., Lam, J.O., Towner, W.J., et al. 2020. Comparison of Overall and Comorbidity-Free Life Expectancy Between Insured Adults With and Without HIV Infection, 2000-2016. *JAMA Network Open*. 3(6):e207954. DOI: 10.1001/JAMANETWORKOPEN.2020.7954.

Mercadel, C.J., Skelley, J.W., Kyle, J.A. & Elmore, L.K. 2014. Dolutegravir: An integrase strand transfer inhibitor for the treatment of human immunodeficiency virus I in adults. *Journal of Pharmacy Technology*. 30(6):216–226. DOI: 10.1177/8755122514544126.

Min, S., Sloan, L., Dejesus, E., Hawkins, T., McCurdy, L., Song, I., Stroder, R., Chen, S., et al. 2011. Antiviral activity, safety, and pharmacokinetics/pharmacodynamics of dolutegravir as 10-day monotherapy in HIV-1-infected adults. *AIDS*. 25(14):1737–1745. DOI: 10.1097/QAD.0b013e32834a1dd9.

Modongo, C., Wang, Q., Dima, M., Matsiri, O., Kgwaadira, B., Rankgoane-Pono, G., Shin, S.S. & Zetola, N.M. 2019. Clinical and Virological Outcomes of TB/HIV Coinfected Patients Treated With Dolutegravir-Based HIV Antiretroviral Regimens. *JAIDS Journal of Acquired Immune Deficiency Syndromes*. 82(2):111–115. DOI: 10.1097/QAI.0000000000002126.

Mould, D.R. & Upton, R.N. 2012. Basic Concepts in Population Modeling, Simulation, and Model-Based Drug Development. *CPT: Pharmacometrics & Systems Pharmacology*.

1(9):e6. DOI: 10.1038/PSP.2012.4.

Mould, D.R. & Upton, R.N. 2013. Basic Concepts in Population Modeling, Simulation, and Model-Based Drug Development—Part 2: Introduction to Pharmacokinetic Modeling Methods. *CPT: Pharmacometrics & Systems Pharmacology*. 2(4):e38. DOI: 10.1038/PSP.2013.14.

Mufune, P. 2015. Poverty and HIV/AIDS in Africa: Specifying the connections. *Social Theory & Health*. 13(1):1–29. DOI: 10.1057/sth.2014.14.

Nachega, J.B., Parienti, J.-J., Uthman, O.A., Gross, R., Dowdy, D.W., Sax, P.E., Gallant, J.E., Mugavero, M.J., et al. 2014. Lower Pill Burden and Once-Daily Antiretroviral Treatment Regimens for HIV Infection: A Meta-Analysis of Randomized Controlled Trials. *Clinical Infectious Diseases*. 58(9):1297–1307. DOI: 10.1093/cid/ciu046.

Nerella, N.G., Block, L.H. & Noonan, P.K. 1993. The Impact of Lag Time on the Estimation of Pharmacokinetic Parameters. I. One-Compartment Open Model. *Pharmaceutical Research: An Official Journal of the American Association of Pharmaceutical Scientists*. 10(7):1031–1036. DOI: 10.1023/A:1018970924508.

Niemi, M., Backman, J.T., Fromm, M.F., Neuvonen, P.J. & Kivistö, K.T. 2003. DOI: 10.2165/00003088-200342090-00003.

Ntem-Mensah, A.D., Millman, N., Jakharia, N., Theppote, A., Toeque, M.-G. & Riedel, D.J. 2019. 345. Acute Onset Diabetic Ketoacidosis/Hyperosmolar Hyperglycemic State in Patients Taking Integrase Strand Transfer Inhibitors. *Open Forum Infectious Diseases*. 6(Suppl 2):S183. DOI: 10.1093/OFID/OFZ360.418.

Owen, J.S. & Fiedler-Kelly, J. 2014. *Introduction to Population Pharmacokinetic / Pharmacodynamic Analysis with Nonlinear Mixed Effects Models*. V. 9780470582. Hoboken, New Jersey: John Wiley & Sons, Inc. DOI: 10.1002/9781118784860.

Palmisano, L. & Vella, S. 2011. A brief history of antiretroviral therapy of HIV infection: success and challenges. *Annali dell'Istituto superiore di sanita*. 47(1):44–48. DOI: 10.4415/ANN_11_01_10.

Panel on Antiretroviral Guidelines for Adults and Adolescents. 2016. Guidelines for the Use of Antiretroviral Agents in Adults and Adolescents with HIV. Department of Health and Human. Available: https://clinicalinfo.hiv.gov/sites/default/files/guidelines/documents/AdultandAdolescentGL.pdf [2022, September 02].

Papathanasopoulos, M.A., Hunt, G.M. & Tiemessen, C.T. 2003. DOI: 10.1023/A:1023435429841.

Parant, F., Miailhes, P., Brunel, F. & Gagnieu, M.C. 2019. Dolutegravir Population Pharmacokinetics in a Real-Life Cohort of People Living with HIV Infection: A Covariate Analysis. *Therapeutic Drug Monitoring*. 41(4):444–451. DOI: 10.1097/FTD.0000000000000618.

Parienti, J.J., Fournier, A.L., Cotte, L., Schneider, M.P., Etienne, M., Unal, G., Perré, P., Dutheil, J.J., et al. 2021. Forgiveness of Dolutegravir-Based Triple Therapy Compared With

Older Antiretroviral Regimens: A Prospective Multicenter Cohort of Adherence Patterns and HIV-RNA Replication. *Open Forum Infectious Diseases*. 8(7). DOI: 10.1093/OFID/OFAB316.

Patel, P., Song, I., Borland, J., Patel, A., Lou, Y., Chen, S., Wajima, T., Peppercorn, A., et al. 2011. Pharmacokinetics of the HIV integrase inhibitor S/GSK1349572 co-administered with acid-reducing agents and multivitamins in healthy volunteers. *Journal of Antimicrobial Chemotherapy*. 66(7):1567–1572. DOI: 10.1093/JAC/DKR139.

Piacenti, F.J. 2006. An Update and Review of Antiretroviral Therapy. *Pharmacotherapy*. 26(8):1111–1133. DOI: 10.1592/phco.26.8.1111.

Pruvost, A., Negredo, E., Benech, H., Theodoro, F., Puig, J., Grau, E., García, E., Moltó, J., et al. 2005. Measurement of Intracellular Didanosine and Tenofovir Phosphorylated Metabolites and Possible Interaction of the Two Drugs in Human Immunodeficiency Virus-Infected Patients. *Antimicrobial Agents and Chemotherapy*. 49(5):1907. DOI: 10.1128/AAC.49.5.1907-1914.2005.

Rajman, I., Knapp, L., Morgan, T. & Masimirembwa, C. 2017. African Genetic Diversity: Implications for Cytochrome P450-mediated Drug Metabolism and Drug Development. *EBioMedicine*. 17:67–74. DOI: 10.1016/J.EBIOM.2017.02.017.

Ray, A.S., Cihlar, T., Robinson, K.L., Tong, L., Vela, J.E., Fuller, M.D., Wieman, L.M., Eisenberg, E.J., et al. 2006. Mechanism of Active Renal Tubular Efflux of Tenofovir. *Antimicrobial Agents and Chemotherapy*. 50(10):3297. DOI: 10.1128/AAC.00251-06.

Ray, A.S., Fordyce, M.W. & Hitchcock, M.J.M. 2016. Tenofovir alafenamide: A novel prodrug of tenofovir for the treatment of Human Immunodeficiency Virus. *Antiviral Research*. 125:63–70. DOI: 10.1016/J.ANTIVIRAL.2015.11.009.

Reese, M.J., Savina, P.M., Generaux, G.T., Tracey, H., Humphreys, J.E., Kanaoka, E., Webster, L.O., Harmon, K.A., et al. 2013a. In Vitro Investigations into the Roles of Drug Transporters and Metabolizing Enzymes in the Disposition and Drug Interactions of Dolutegravir, a HIV Integrase Inhibitor. *Drug Metabolism and Disposition*. 41(2):353–361. DOI: 10.1124/dmd.112.048918.

Reese, M.J., Savina, P.M., Generaux, G.T., Tracey, H., Humphreys, J.E., Kanaoka, E., Webster, L.O., Harmon, K.A., et al. 2013b. In Vitro Investigations into the Roles of Drug Transporters and Metabolizing Enzymes in the Disposition and Drug Interactions of Dolutegravir, a HIV Integrase Inhibitor. *Drug Metabolism and Disposition*. 41(2):353–361. DOI: 10.1124/DMD.112.048918.

Reinach, B., De Sousa, G., Dostert, P., Ings, R., Gugenheim, J. & Rahmani, R. 1999. *Comparative effects of rifabutin and rifampicin on cytochromes P450 and UDP-glucuronosyl-transferases expression in fresh and cryopreserved human hepatocytes*.

Roy, A. & Ette, E.I. 2005. A pragmatic approach to the design of population pharmacokinetic studies. *The AAPS Journal*. 7(2):E408. DOI: 10.1208/AAPSJ070241.

Roydhouse, S.A., Carland, J.E., Debono, D.S., Baysari, M.T., Reuter, S.E., Staciwa, A.J., Sandhu, A.P.K., Day, R.O., et al. 2021. Accuracy of documented administration times for intravenous antimicrobial drugs and impact on dosing decisions. *British Journal of Clinical*

Pharmacology. 87(11):4273–4282. DOI: 10.1111/BCP.14844.

Ruane, P.J., Dejesus, E., Berger, D., Markowitz, M., Bredeek, U.F., Callebaut, C., Zhong, L., Ramanathan, S., et al. 2013. Antiviral activity, safety, and pharmacokinetics/pharmacodynamics of tenofovir alafenamide as 10-day monotherapy in HIV-1-positive adults. *Journal of Acquired Immune Deficiency Syndromes*. 63(4):449–455. DOI: 10.1097/QAI.0B013E3182965D45.

Saag, M.S., Gandhi, R.T., Hoy, J.F., Landovitz, R.J., Thompson, M.A., Sax, P.E., Smith, D.M., Benson, C.A., et al. 2020. Antiretroviral Drugs for Treatment and Prevention of HIV Infection in Adults. *JAMA*. 324(16):1651. DOI: 10.1001/jama.2020.17025.

Savic, R.M., Jonker, D.M., Kerbusch, T. & Karlsson, M.O. 2007. Implementation of a transit compartment model for describing drug absorption in pharmacokinetic studies. *Journal of Pharmacokinetics and Pharmacodynamics*. 34(5):711–726. DOI: 10.1007/s10928-007-9066-0.

Schalkwijk, S., Greupink, R., Colbers, A.P., Wouterse, A.C., Verweij, V.G.M., van Drongelen, J., Teulen, M., van den Oetelaar, D., et al. 2016. Placental transfer of the HIV integrase inhibitor dolutegravir in an ex vivo human cotyledon perfusion model. *The Journal of antimicrobial chemotherapy*. 71(2):480–483. DOI: 10.1093/JAC/DKV358.

Scherzer, R., Estrella, M., Li, Y., Choi, A.I., Deeks, S.G., Grunfeld, C. & Shlipak, M.G. 2012. Association of Tenofovir Exposure with Kidney Disease Risk in HIV Infection. *AIDS (London, England)*. 26(7):867. DOI: 10.1097/QAD.0B013E328351F68F.

Schwander, S., Rüsch-Gerdes, S., Mateega, A., Lutalo, T., Tugume, S., Kityo, C., Rubaramira, R., Mugyenyi, P., et al. 1995. A pilot study of antituberculosis combinations comparing rifabutin with rifampicin in the treatment of HIV-1 associated tuberculosis. A single-blind randomized evaluation in Ugandan patients with HIV-1 infection and pulmonary tuberculosis. *Tubercle and lung disease : the official journal of the International Union against Tuberculosis and Lung Disease*. 76(3):210–218. DOI: 10.1016/S0962-8479(05)80007-3.

Schwartz, J.B. 2003. *The Influence of Sex on Pharmacokinetics*.

Seitz, R. 2016. Human Immunodeficiency Virus (HIV). *Transfusion Medicine and Hemotherapy*. 43(3):203–222. DOI: 10.1159/000445852.

Shah, B.M., Schafer, J.J. & Desimone, J.A. 2014. DOI: 10.1002/phar.1386.

Sheiner, L.B. & Beal, S.L. 1983. Evaluation of methods for estimating population pharmacokinetic parameters. III. Monoexponential model: routine clinical pharmacokinetic data. *Journal of pharmacokinetics and biopharmaceutics*. 11(3):303–319. DOI: 10.1007/BF01061870.

Song, I., Borland, J., Chen, S., Patel, P., Wajima, T., Peppercorn, A. & Piscitelli, S.C. 2012. Effect of food on the pharmacokinetics of the integrase inhibitor dolutegravir. *Antimicrobial Agents and Chemotherapy*. 56(3):1627–1629. DOI: 10.1128/AAC.05739-11.

Song, I.H., Zong, J., Borland, J., Jerva, F., Wynne, B., Zamek-Gliszczynski, M.J., Humphreys, J.E., Bowers, G.D., et al. 2016. The Effect of Dolutegravir on the

Pharmacokinetics of Metformin in Healthy Subjects. *Journal of acquired immune deficiency syndromes (1999)*. 72(4):400–407. DOI: 10.1097/QAI.0000000000000983.

Southwood, R.L., Fleming, V.H. & Huckaby, G. 2018. *Concepts in clinical pharmacokinetics*. Seventh Ed ed. R. Bloom, K. Eckles, J. Hershey, & D. Wade, Eds. Bethesda: American Society of Health-System Pharmacists.

Tanaudommongkon, A., Chaturvedula, A., Hendrix, C.W., Fuchs, E.J., Shieh, E., Bakshi, R.P. & Marzinke, M.A. 2022. Population pharmacokinetics of tenofovir, emtricitabine and intracellular metabolites in transgender women. *British Journal of Clinical Pharmacology*. 88(8):3674–3682. DOI: 10.1111/BCP.15310.

Teh, L.K., Hashim, H., Zakaria, Z.A. & Salleh, M.Z. 2012. Polymorphisms of UGT1A1*6 UGT1A1*7 & UGT1A1*8 in three major ethnic groups from Malaysia. *Indian Journal of Medical Research*. 136(2):249–259. Available: /pmc/articles/PMC3461737/ [2021, May 20].

The Global Fund. 2021. The Impact of Covid-19 on Hiv , Tb and Malaria Services and Systems for Health : a Snapshot From 502 Health Facilities. *The Global Fund to Fight AIDS Malaria, Tuberculosis*. Available: https://openknowledge.worldbank.org/bitstream/handle/10986/34496/9781464816024.pdf [2022, April 26].

The NAMSAL ANRS 12313 Study Group. 2019. Dolutegravir-Based or Low-Dose Efavirenz–Based Regimen for the Treatment of HIV-1. *New England Journal of Medicine*. 381(9):816–826. DOI: 10.1056/nejmoa1904340.

TIVICAY (ViiV Healthcare). 2020. *Highlights of prescribing information*. Available: www.fda.gov/medwatch. [2020, June 03].

Tourret, J., Deray, G. & Isnard-Bagnis, C. 2013. Tenofovir effect on the kidneys of HIV-infected patients: a double-edged sword? *Journal of the American Society of Nephrology : JASN*. 24(10):1519–1527. DOI: 10.1681/ASN.2012080857.

Tshikuka Mulumba, J.G., Matindii, B.A., Kilauzi, A.L., Mengema, B., Mafuta, J., Eloko Eya Matangelo, G., Mukongo Bulaïmu-Lukeba, A. & Jerry, I.L. 2012. Severity of outcomes associated to types of HIV coinfection with TB and malaria in a setting where the three pandemics overlap. *Journal of Community Health*. 37(6):1234–1238. DOI: 10.1007/s10900-012-9559-7.

Twisk, J.W.R. 2013. *Applied Longitudinal Data Analysis for Epidemiology*. Cambridge: Cambridge University Press. DOI: 10.1017/CBO9781139342834.

UNAIDS. 2021. Global HIV & AIDS statistics — Fact sheet | UNAIDS. *Unaids*. 2020–2022. Available: https://www.unaids.org/en/resources/fact-sheet [2022, April 26].

UNAIDS. 2022. *In Danger: UNAIDS Global AIDS Update 2022*. Available: https://www.unaids.org/en/resources/documents/2022/in-danger-global-aids-update.

UNITAID. 2017. New high-quality antiretroviral therapy to be launched in South Africa, Kenya and over 90 low- and middle-income countries at reduced price. Available at: https:// unitaid.eu/news-blog/new-high-quality-antiretroviral-therapylaunched-south-africa-kenya-90-. 87(1,2):149–200. Available:

http://www.unaids.org/sites/default/files/20170921_PR_TLD_en.pdf.

Upton, R.N. & Mould, D.R. 2014. Basic concepts in population modeling, simulation, and model-based drug development: Part 3-introduction to pharmacodynamic modeling methods. *CPT: Pharmacometrics and Systems Pharmacology*. 3(1). DOI: 10.1038/psp.2013.71.

Valade, E., Bouazza, N., Lui, G., Illamola, S.M., Benaboud, S., Treluyer, J.M., Cobat, A., Foissac, F., et al. 2017. Population pharmacokinetic modeling of tenofovir in the genital tract of male HIV-infected patients. *Antimicrobial Agents and Chemotherapy*. 61(3). DOI: 10.1128/AAC.02062-16/SUPPL_FILE/ZAC003175930S1.PDF.

Venter, W.D.F., Moorhouse, M., Sokhela, S., Fairlie, L., Mashabane, N., Masenya, M., Serenata, C., Akpomiemie, G., et al. 2019. Dolutegravir plus Two Different Prodrugs of Tenofovir to Treat HIV. *New England Journal of Medicine*. 381(9):803–815. DOI: 10.1056/nejmoa1902824.

Vitoria, M., Granich, R., Gilks, C.F., Gunneberg, C., Hosseini, M., Were, W., Raviglione, M. & De Cock, K.M. 2009. The global fight against HIV/AIDS, tuberculosis, and malaria: current status and future perspectives. *American journal of clinical pathology*. 131(6):844–848. DOI: 10.1309/AJCP5XHDB1PNAEYT.

Vo, H., Jung, J., Kim, T. & Shin, S. 2017. *Development of Statistical Pharmacokinetic Modeling and Analysis Methodologies*.

Walimbwa, S.I., Lamorde, M., Waitt, C., Kaboggoza, J., Else, L., Byakika-Kibwika, P., Amara, A., Gini, J., et al. 2019. Drug interactions between dolutegravir and artemether-lumefantrine or artesunate-amodiaquine. *Antimicrobial Agents and Chemotherapy*. 63(2). DOI: 10.1128/AAC.01310-18.

Wang, X., Cerrone, M., Ferretti, F., Castrillo, N., Maartens, G., McClure, M. & Boffito, M. 2019. Pharmacokinetics of dolutegravir 100 mg once daily with rifampicin. *International Journal of Antimicrobial Agents*. 54(2):202–206. DOI: 10.1016/j.ijantimicag.2019.04.009.

WHO. 2019. Updated recommendations on first-line and second-line antiretroviral regimens and post-exposure prophylaxis and recommendations on early infant diagnosis of HIV. *WHO*.

Williams, P.J. & Ette, E.I. 2000. The role of population pharmacokinetics in drug development in light of the Food and Drug Administration's "Guidance for Industry: Population Pharmacokinetics". *Clinical Pharmacokinetics*. 39(6):385–395. DOI: 10.2165/00003088-200039060-00001.

World Health Organization. 2018. Updated recommendations on first-line and second-line antiretroviral regimens and post-exposure prophylaxis and recommendations on early infant diagnosis of HIV: interim guidelines. Supplement to the 2016 consolidated guidelines on the use of antiretrovir. *World Health Organization*. (December):1–79.

World Health Organization. 2019. Consolidated guidelines on HIV prevention, testing, treatment, service delivery and monitoring : recommendations for a public health approach. *World Health Organisation Guidelines*. 548. Available: https://apps.who.int/iris/rest/bitstreams/1357089/retrieve.

World Health Organization. 2022. *WHO consolidated guidelines on tuberculosis. Module 4: treatment - drug-susceptible tuberculosis treatment*. Available: https://www.who.int/publications/i/item/9789240007048.

X, W., JS, W., PJ, N. & JT, B. 2002. Isoniazid is a mechanism-based inhibitor of cytochrome P450 1A2, 2A6, 2C19 and 3A4 isoforms in human liver microsomes. *European journal of clinical pharmacology*. 57(11):799–804. DOI: 10.1007/S00228-001-0396-3.

Yagura, H., Watanabe, D., Kushida, H., Tomishima, K., Togami, H., Hirano, A., Takahashi, M., Hirota, K., et al. 2017. Impact of UGT1A1 gene polymorphisms on plasma dolutegravir trough concentrations and neuropsychiatric adverse events in Japanese individuals infected with HIV-1. *BMC Infectious Diseases*. 17(1):622. DOI: 10.1186/s12879-017-2717-x.

Zachariah, R., Spielmann, M.P., Harries, A.D. & Salaniponi, F.M.L. 2002. Moderate to severe malnutrition in patients with tuberculosis is a risk factor associated with early death. *Transactions of the Royal Society of Tropical Medicine and Hygiene*. 96(3):291–294. DOI: 10.1016/S0035-9203(02)90103-3.

Zhang, J., Hayes, S., Sadler, B.M., Minto, I., Brandt, J., Piscitelli, S., Min, S. & Song, I.H. 2015. Population pharmacokinetics of dolutegravir in HIV-infected treatment-naive patients. *British Journal of Clinical Pharmacology*. 80(3):502–514. DOI: 10.1111/bcp.12639.

Appendix A: NONMEM scripts

Final NONMEM scripts for results presented in **Chapter 4**

```
;; 1. Based on: 207
;; 2. Description: 2cmp,FFM, ASAQ_CL + AL_CL (1433)
; Two compartment model of Dolutegravir
; Settings for the memory of NONMEM
$SIZES      PD=-1000 LVR=-150 LTH=-200 MAXFCN=10000000 LNP4=
-150000
$PROBLEM    DOLACT
$INPUT      ID DAT2=DROP DAY TIME PKPOINT=DROP VPCTIME AMT DV OCC
 MDV
            EVID ARM RX SQS SEX AGE WT HT FLAG=DROP OLDPKPOINT=
            DROP TAG=DROP WHAT=DROP

; IGNORE=@ will skip any line starting with any non-numerical
character
$DATA      Dolact_final_dataset_2020.csv IGNORE=@

$ABBREVIATED PROTECT ;TO PROTECT YOUR CODE AGAINST UNDEFINED
OPERATIONS (ALWAYS CHECK YOUR FUNCTIONS)

$SUBROUTINE ADVAN13 TRANS1 TOL=9 ; TOL is the precision to solve
differential equations

$MODEL      NCOMPARTMENTS=3 ;2 ; 4
            COMP=(ABS DEFDOSE) COMP=(CENTRAL DEFOBSERVATION)
            COMP=(PERI1)


;-------------------------------------------------------------------
-------
$PK
; ------------ Between Subject variability
-----------------------------

BSVCL    = ETA(1)
BSVV     = ETA(2)
BSVKA    = ETA(3)
BSVBIO   = ETA(4)
BSVV3    = ETA(21)
BSVQ     = ETA(22)

;-------------- Between Occasion
variability-----------------------------
BOVCL    = 0
BOVKA    = 0
BOVMTT   = 0
BOVBIO   = 0
BOVCL    = 0

;OCCASION
1-------------------------------------------------------------------
--
IF (OCC==1) THEN
```

```
42      BOVCL  = ETA(5)
43      BOVKA  = ETA(9)
44      BOVMTT = ETA(13)
45      BOVBIO = ETA(17)
46  ENDIF
47
48  ;OCCASION 2-------------------------------------------------------------
    --
49  IF (OCC==2) THEN
50      BOVCL  = ETA(6)
51      BOVKA  = ETA(10)
52      BOVMTT = ETA(14)
53      BOVBIO = ETA(18)
54  ENDIF
55
56  ;OCCASION 3-------------------------------------------------------------
    ---
57  IF (OCC==3) THEN
58      BOVCL  = ETA(7)
59      BOVKA  = ETA(11)
60      BOVMTT = ETA(15)
61      BOVBIO = ETA(19)
62  ENDIF
63
64  ;OCCASION 4-------------------------------------------------------------
    ----
65  IF (OCC==4) THEN
66      BOVCL  = ETA(8)
67      BOVKA  = ETA(12)
68      BOVMTT = ETA(16)
69      BOVBIO = ETA(20)
70  ENDIF
71
72
73  ; -------------- Calculation of Fat-free Mass
74  ; These formulas require WT in KG and HT in m !!!
75
76  ; Conversion from cm to m
77  HTM = HT/100
78
79  IF (SEX.EQ.0) THEN  ; female
80      WHSMAX=37.99
81      WHS50=35.98
82  ELSE        ;males
83      WHSMAX=42.92
84      WHS50=30.93
85  ENDIF
86  HTM2 = HTM**2
87  FFM = (WHSMAX*HTM2*WT)/(WHS50*HTM2+WT)
```

```
88   FAT = WT-FFM
89
90   ; ------- Typical values of covariates
91   ;TVWT   = 59.1 ;Median weight in my population
92   ;TVFAT = 11.406
93   TVFFM = 48.6015
94
95
96   ;--------- Allometric scaling and covariates
97   ;ALLMCL_WT = (WT/TVWT)**0.75
98   ;ALLMV_WT = (WT/TVWT)
99
100  ;ALLMCL_FAT = (FAT/TVFAT)**0.75
101  ;ALLMV_FAT = (FAT/TVFAT)
102
103  ALLMCL_FFM = (FFM/TVFFM)**0.75
104  ALLMV_FFM = (FFM/TVFFM)
105
106  ;----------------------covariates----------------------------------
     ------------
107  ASAQ_CL = 1 ;covariate effect of Artesunate/Amodiaquine on
     clearance
108  If(RX.EQ.3) ASAQ_CL = THETA(11)
109
110  AL_CL = 1  ;covariate effect of Artemether/Lumefantrine on
     clearance
111  If(RX.EQ.2) AL_CL = THETA(12)
112
113  ;---------Typical
     values-------------------------------------------------------
114  TVCL = THETA(1) * ALLMCL_FFM * ASAQ_CL * AL_CL
115  TVV  = THETA(2) * ALLMV_FFM
116  TVKA = THETA(3)
117  TVBIO = THETA(4)
118  TVMTT = THETA(7)
119  TVNN  = EXP(THETA(8))
120  TVV3  = THETA(9)* ALLMV_FFM
121  TVQ   = THETA(10)* ALLMCL_FFM
122
123  ;-----------Define
     parameters-------------------------------------------
124  CL   = TVCL*EXP(BSVCL+BOVCL)     ; CLEARANCE
125  V    = TVV*EXP(BSVV)             ; CENTRAL VOL.
126  KA   = TVKA*EXP(BSVKA+BOVKA)     ; ABS. RATE CONSTANT
127  BIO = TVBIO*EXP(BSVBIO+BOVBIO) ; BIOAVAILABILITY
128  MTT = TVMTT*EXP(BOVMTT)         ; MTT TIME
129  NN   = TVNN                      ; Number of transit compartments
130  V3   = TVV3*EXP(BSVV3)           ; PERIPH VOL
131  Q    = TVQ*EXP(BSVQ)             ; INTER COMPT CL
132
133  ;-----------re-parameterization-----------------------------------
     ---
```

```
134
135   K = CL/V     ;(rate constant of elimination)
136   K23 = Q/V    ; (rate constant from central to peripheral 1)
137   K32 = Q/V3   ;(rate constant from peripheral 1 to central)
138
139
140   ;------------- Transit compartment absorption
141   F1=0 ; I need to set bioavailability in compartment 1 to 0 for
      this implementation of the transit compartment absorption
142
143   KTR = (NN+1)/MTT ; The number of actual transit compartments is
      NN+1, so this number can never be 0
144
145   IF (NEWIND/=2.OR.EVID>=3) THEN ; new individual, or reset event
146       ; The values read here will be stored in TDOS and PD in this
          very PK call.
147       TNXD=TIME ; Time of the dose
148       PNXD=AMT ; Amount. If it's zero, the DE is deactivated.
149   ENDIF
150
151   TDOS=TNXD ; This will either save here the temporary values if
      it's a new individual...
152   PD=PNXD ; ...or the values which were read one record ahead
      during the execution of the previous record.
153
154   IF(AMT>0) THEN ; This reads one record ahead and stores the data
      to be used when running the following record
155   ; IF(AMT.GT.0.AND.ALAG1.EQ.0) THEN ; Use this INSTEAD if there
      is ALAG, as it will also checks if the ALAG is not 0. Note that
      you normally do not want to include both ALAG and transit, this
      is a very exceptional case
156       TNXD=TIME
157       PNXD=AMT
158   ENDIF
159
160   ; Uncomment this if you have ALAG or if you use ADDL
161   ; IF (DOSTIM>0) THEN ; This will account for the ADDL or lagged
      doses. It will overwrite the time, if it a non-event record
162   ;   TNXD=DOSTIM
163   ;   PNXD=AMT
164   ; ENDIF
165
166   ; To speed up the computation, I calculate here all the
      non-time-varying quantities used in $DES
167   PIZZA = LOG(BIO*PD*KTR + 0.00001) - GAMLN(NN+1)  ; without
      +0.00001, it won't work with ETAs in bioavailability
168
169
170   $DES
171
172   TEMPO = T-TDOS ; this is time after dose for the transit, it
      should always be >= 0
```

```
173   KTT = 0
174   TRANSIT = 0
175   IF(PD.GT.0.AND.TEMPO.GT.0) THEN ; This happens only id PD>0, so
      only if a dose has been detected
176       KTT = KTR*(TEMPO)
177       TRANSIT = EXP(PIZZA+NN*LOG(KTT)-KTT)
178   ENDIF
179   DADT(1) = TRANSIT -KA*A(1)
180   DADT(2) = KA*A(1)- K*A(2)- K23*A(2)+ K32*A(3)
181   DADT(3) = K23*A(2)- K32*A(3)
182
183
184   ;-----------------------------------------------------------------
      -----------------------------------------------------------------
      ----------------------
185
186   $ERROR
187
188   IPRED=A(2)/V
189
190   LLOQ = 0.01 ; DEFINE YOUR OWN LLOQ HERE
191   IMPUTED_BLQ = LLOQ/2
192
193   PROP = IPRED*THETA(5)
194   ADD = THETA(6)            ;+(LLOQ*0.2)
195
196   ;IF (ICALL/=4.AND.BLQ==1) THEN
197   ;ADD = ADD+(LLOQ/2)
198   ;ENDIF
199   ; BLQ==1 are the BLQ samples kept in the fit. When you have a
      serires, keep the last one before the cmax and the first one
      after the cmax.
200
201   ; BLQ==2 are the remaining BLQ samples in series, which I want
      to disergard, but yet include for diagnostic purposes
202   ;IF (ICALL/=4.AND.BLQ==2) THEN
203       ;PROP = 0
204       ;ADD = 10000000000 ; Using this large error has the same
          effect as ignoring, expect the record is still there, so I
          can use it in VPCs.
205   ;ENDIF
206
207   W = SQRT(ADD**2+PROP**2)
208
209   ; Protective code
210   IF (W.LE.0.000001) W=0.000001
211
212   IRES=DV-IPRED
213   IWRES=IRES/W
214
215   Y = IPRED + W*ERR(1)
216
```

```
217  ; For simulation, like in case of VPC
218  IF (ICALL==4.AND.Y<=LLOQ) THEN
219      Y = IMPUTED_BLQ ; All BLQ values in simulation get imputed
         to LLOQ/2. This also prevents negative values
220  ;ENDIF
221
222  ; To calculate time after dose.
223  IF(AMT>0) THEN
224      TIMEDOSE = TIME
225      AMOUNTDOSE = AMT
226  ENDIF
227
228  TAD = TIME-TIMEDOSE
229
230  VARCL  = BSVCL + BOVCL
231  VARBIO = BSVBIO + BOVBIO
232  VARAUC = BSVBIO + BOVBIO - BSVCL - BOVCL
233
234
235  ;-------------RETRIEVE AMOUNT IN EACH COMPARTMENT----------------
236  AA1 = A(1)
237  AA2 = A(2)
238  AA3 = A(3)
239
240  ;-----------------------------------------------------------------
241  $THETA  (0,0.714,90)     ; 1 CL [L/h]
242  $THETA  (0,13.3,800)     ; 2 V [L]
243  $THETA  (0,1.62,5)       ; 3 KA [1/h]
244  $THETA  1 FIX            ; 4 BIO
245  $THETA  (0,0.05,0.5)     ; 5 PROPORTIONAL ERROR []
246  $THETA  (0,0.19,10)      ; 6 ADDITIVE ERROR [mg/L]
247  $THETA  (0,1.17,3)       ; 7 MTT
248  $THETA  (0,3.45,5)       ; 8 NN [LOG]
249  $THETA  (0,5.62,800)     ; 9 V3 [L]
250  $THETA  (0,0.84,90)      ; 10 Q [L/h]
251  $THETA  (0,1.28,10)      ; 11 ASAQ_CL
252  $THETA  (0,1.1,10)       ; 12 AL_CL
253  ;-----------------------------------------------------------------
     -------------
254  $OMEGA  BLOCK(1)
255   0.0744  ;   1 BSV CL
256  $OMEGA  BLOCK(1) FIX
257   0  ;    2 BSV V
258  $OMEGA  BLOCK(1) FIX
259   0  ;   3 BSV KA
260  $OMEGA  BLOCK(1) FIX
261   0  ;  4 BSV BIO
262  ;-----------------------------------------------------------------
     -------------
263  $OMEGA  BLOCK(1) FIX
264   0  ;    5 BOVCL
265  $OMEGA  BLOCK(1) SAME
```

```
$OMEGA  BLOCK(1) SAME
$OMEGA  BLOCK(1) SAME
;----------------------------------------------------------------------
----------------
$OMEGA  BLOCK(1)
 0.813  ;     9 BOVKA
$OMEGA  BLOCK(1) SAME
$OMEGA  BLOCK(1) SAME
$OMEGA  BLOCK(1) SAME
;----------------------------------------------------------------------
-----------------
$OMEGA  BLOCK(1)
 0.371  ;  13 BOVMTT
$OMEGA  BLOCK(1) SAME
$OMEGA  BLOCK(1) SAME
$OMEGA  BLOCK(1) SAME
;----------------------------------------------------------------------
------------------
$OMEGA  BLOCK(1)
 0.047  ;  17 BOVBIO
$OMEGA  BLOCK(1) SAME
$OMEGA  BLOCK(1) SAME
$OMEGA  BLOCK(1) SAME
;----------------------------------------------------------------------
------------------
$OMEGA  BLOCK(1) FIX
 0  ;    21 BSVV3
$OMEGA  BLOCK(1) FIX
 0  ;     22 BSVQ
;----------------------------------------------------------------------
------------------
$SIGMA  1  FIX
;----------------------------------------------------------------------
----------------------------------------------------------------------
------------------
$ESTIMATION MSFO=run207a.msf MAXEVAL=9999 PRINT=1 METHOD=1 INTER
            NOABORT NSIG=3 SIGL=9 ; RULES for precision
            SIGL=<TOL AND NSIG=<SIGL/3
            NONINFETA=1 ETASTYPE=1 ; REPEAT ;


;As the model becomes more complex, you can use MATRIX=S and
then remove the $COVARIANCE step completely when the model is
too complex to obtain precisions
$COVARIANCE PRINT=E ; MATRIX=S
$TABLE      WRESCHOL FILE=sdtab207a.csv ID OCC TIME TAD VPCTIME
AA1
            AA2 AA3 ;AA4
            Y DV PRED RES WRES IPRED IRES IWRES CWRES CWRESI OBJI
            NOPRINT NOAPPEND ONEHEADER FORMAT=,
$TABLE      FILE=patab207a.csv ID OCC CL V KA BIO MTT NN BSVCL
BSVV V3
```

```
306                 Q ;V4 Q2 BSVBIO BSVMTT BSVV3 BSVQ BSVV4 BSVQ2
307                 BSVKA BOVCL BOVKA BOVBIO BOVMTT VARCL VARBIO VARAUC
308                 NOPRINT NOAPPEND ONEHEADER FORMAT=,
309   $TABLE        FILE=cotab207a.csv ID OCC WT HT AGE FFM FAT NOPRINT
310                 NOAPPEND ONEHEADER FORMAT=,
311   $TABLE        FILE=catab207a.csv ID OCC SEX SQS ARM RX NOPRINT
      NOAPPEND
312                 ONEHEADER FORMAT=,
313   $TABLE        FILE=mytab207a.csv ID OCC TIME TAD VPCTIME Y DV AA1
      AA2
314                 AA3 ;AA4
315                 PRED RES WRES IPRED IRES IWRES CWRES CWRESI OBJI CL V
                     KA
316                 BIO MTT BSVCL BSVV V3 Q ;V4 Q2,BSVBIO BSVMTT BSVV3
                    BSVQ BSVV4 BSVQ2
317                 BSVKA BOVCL BOVKA BOVBIO BOVMTT VARCL VARBIO VARAUC
                    SEX WT
318                 RX HT AGE FFM FAT NOPRINT NOAPPEND ONEHEADER FORMAT=,
319
320
```

Final NONMEM scripts for results presented in **Chapter 5**

```
;; 1. Based on: 094
; One compartment model of Dolutegravir
; Settings for the memory of NONMEM
$SIZES      PD=-1000 LVR=-150 LTH=200 MAXFCN=10000000 LNP4=-150000
$PROBLEM    DTG_RIFAMPICIN_RADIO_VIIV
$INPUT      ID DAT2=DROP TIME AMT DV OCC MDV EVID VPCTIME WT HT
AGE
            SEX STUDY PHASE PANEL PANELB RIF RBN BID DOSE RACE
            ARM GROUP STDSEX
            WHAT=DROP

$DATA      vivrad_final2021.csv IGNORE=@

$SUBROUTINE ADVAN4 TRANS1

;---------------------------------------------------------------
$PK
;-----------Defining Between Subject variability --------------

BSVCL   = ETA(1)
BSVV    = ETA(2)
BSVKA   = ETA(3)
BSVBIO  = ETA(4)
BSVV3   = ETA(5)
BSVQ    = ETA(6)

;------------Defining Between Occasion variability---------------
BOVKA = 0
BOVLAG = 0
BOVBIO = 0

;OCCASION 1-----------------------------------------------------
IF (OCC==1) THEN
BOVKA = ETA(7)
BOVLAG= ETA(15)
BOVBIO = ETA(23)
ENDIF

;OCCASION 2
IF (OCC==2) THEN
BOVKA = ETA(8)
BOVLAG = ETA(16)
BOVBIO = ETA(24)
ENDIF

;OCCASION 3
IF (OCC==3) THEN
BOVKA = ETA(9)
BOVLAG = ETA(17)
BOVBIO = ETA(25)
ENDIF

```

```
51   ;OCCASION 4
52   IF (OCC==4) THEN
53   BOVKA = ETA(10)
54   BOVLAG = ETA(18)
55   BOVBIO = ETA(26)
56   ENDIF
57
58   ;OCCASION 5
59   IF (OCC==5) THEN
60   BOVKA = ETA(11)
61   BOVLAG = ETA(19)
62   BOVBIO = ETA(27)
63   ENDIF
64
65   ;OCCASION 6
66   IF (OCC==6) THEN
67   BOVKA = ETA(12)
68   BOVLAG = ETA(20)
69   BOVBIO = ETA(28)
70   ENDIF
71
72   ;OCCASION 7
73   IF (OCC==7) THEN
74   BOVKA = ETA(13)
75   BOVLAG = ETA(21)
76   BOVBIO = ETA(29)
77   ENDIF
78
79   ;OCCASION 8
80   IF (OCC==8) THEN
81   BOVKA = ETA(14)
82   BOVLAG = ETA(22)
83   BOVBIO = ETA(30)
84   ENDIF
85
86   ; -------------- Calculation of Fat-free Mass -----------------
87   ; These formulas require WT in KG and HT in m !!!
88   ; Conversion from cm to m
89   HTM = HT/100
90
91   IF (SEX.EQ.0) THEN  ; female
92       WHSMAX = 37.99
93       WHS50  = 35.98
94   ELSE                ; males
95       WHSMAX = 42.92
96       WHS50  = 30.93
97   ENDIF
98
99   HTM2 = HTM**2
100  FFM  = (WHSMAX*HTM2*WT)/(WHS50*HTM2+WT)
101  FAT  = WT-FFM
102
```

```
103  ; ------- Typical values of covariates--------------------------
104  TVWT    = 70 ;Median weight of 70KG
105  ;TVFAT = 23.98
106  ;TVFFM = 59.10
107  ;--------- Allometric scaling and covariates
108  ALLMCL_WT = (WT/TVWT)**0.75
109  ALLMV_WT  = (WT/TVWT)
110
111  ;ALLMCL_FAT = (FAT/TVFAT)**0.75
112  ;ALLMV_FAT  = (FAT/TVFAT)
113
114  ;ALLMCL_FFM = (FFM/TVFFM)**0.75
115  ;ALLMV_FFM  = (FFM/TVFFM)
116
117  ;---------------------- Effect of Rifampicin on Clearance--------
118  RIF_CL=1
119  IF (RIF.EQ.1) RIF_CL= THETA(10) ;CO-ADMINISTRATION OF RIFAMPICIN
120
121  ;----------------------Effect of Rifabutin  on Clearance---------
122  RBN_CL=1
123  IF (RBN.EQ.1) RBN_CL= THETA(11) ;CO-ADMINISTRATION OF RIFABUTIN
124
125  ;---------------------Food Effect(STUDY) on Bioavailability------
126  STUDY_BIO=1
127  IF (STUDY.EQ.2) STUDY_BIO = THETA(13) ;FOOD EFFECT(STUDY) on BIO
128
129  ;----------------------RIFABUTIN EFFECT on VOLUME----------------
130  RBN_V = 1
131  IF (RBN.EQ.1) RBN_V= THETA(14) ;CO-ADMINISTRATION OF RIFABUTIN
     on VOLUME
132
133  ;----------------------EFFECT OF MALE GENDER ON ABSORPTION RATE
     CONSTANT-----
134  SEX_KA=1
135  IF (SEX.EQ.1) SEX_KA = THETA(15)
136
137
138  ;--------- Typical values of the fixed parameters
     --------------------------
139  TVCL = THETA(1) * ALLMCL_WT * RIF_CL * RBN_CL
140  TVV  = THETA(2) * ALLMV_WT * RBN_V
141  TVKA = THETA(3) * SEX_KA
142  TVBIO = THETA(4)* STUDY_BIO
143
144  IF (STUDY.EQ.1) TVLAG = THETA(7)    ; Estimate lag for ViiV study
145  IF (STUDY.EQ.2) TVLAG = THETA(12)   ; Estimate lag for RADIO study
146
147  TVV3  = THETA(8) * ALLMV_WT
148  TVQ   = THETA(9) * ALLMCL_WT
149
150  ;-----------Define parameters
     ---------------------------------------------
```

```
151
152   CL   = TVCL*EXP(BSVCL)                ; CLEARANCE
153   V    = TVV*EXP(BSVV)                  ; VOLUME CENTRAL COMPARTMENT
154   KA   = TVKA*EXP(BSVKA+BOVKA)          ; ABSORPTION RATE CONSTANT
155   BIO  = TVBIO*EXP(BSVBIO+BOVBIO)       ; BIOAVAILABILITY
156   LAG  = TVLAG*EXP(BOVLAG)              ; LAG TIME
157   V3   = TVV3*EXP(BSVV3)                ; PERIPHERAL VOLUME
158   Q    = TVQ*EXP(BSVQ)                  ; INTER_COMPARTMENTAL
      CLEARANCE
159
160   ;-------------
      re-parameterization-----------------------------------------------
161   K = CL/V      ;(rate constant of elimination)
162   K23 = Q/V     ;(rate constant from central to peripheral 1)
163   K32 = Q/V3    ;(rate constant from peripheral 1 to central)
164
165   ALAG1 = LAG
166
167   F1 = BIO
168
169   S2 = V
170
171   ;-------------------------------------------------------------------
      -------------
172
173   $ERROR
174   IPRED=A(2)/V
175   ;LLOQ = 0.03 ; DEFINE YOUR OWN LLOQ HERE
176   ;IMPUTED_BLQ = LLOQ/2
177
178   ; DEFINE LLOQ for VIIV study
179   IF (STUDY==1) THEN
180   LLOQ = 0.02
181   ENDIF
182
183   ;DEFINE LLOQ for RADIO studyv
184   IF (STUDY==2) THEN
185   LLOQ = 0.05
186   ENDIF
187
188   PROP = IPRED*THETA(5)
189   ADD = THETA(6)+(LLOQ*0.2)
190
191   W = SQRT(ADD**2+PROP**2)
192
193   ; Protective code
194   IF (W.LE.0.000001) W=0.000001
195
196   IRES  = DV-IPRED
197   IWRES = IRES/W
198
199   Y = IPRED + W*ERR(1)
```

```
;-------------------------------------------------------------------
-------
; To prevent simulation (ICALL==4) of negative values. It set a
positive lower bound for Y, so that VPCs in the log-scale can be
plotted
IF (ICALL==4.AND.Y<=0.000001) Y=0.000001

; To calculate time after dose.
IF(AMT.GT.0) THEN
    TIMEDOSE = TIME
    AMOUNTDOSE = AMT

ENDIF

TAD = TIME-TIMEDOSE
;-----------------RETRIEVE AMOUNT IN EACH
COMPARTMENT----------------
AA1 = A(1)
AA2 = A(2)
AA3 = A(3)

;-------------------------------------------------------------------
----
$THETA  (0,1.03,90)      ; 1 CL [L/h]
$THETA  (0,12.7,800)     ; 2 V [L]
$THETA  (0,1.61,5)       ; 3 KA [1/h]
$THETA  1 FIX            ; 4 BIO
$THETA  (0,0.0883,0.5)   ; 5 PROPORTIONAL ERROR []
$THETA  (0,0.0318,1)     ; 6 ADDITIVE ERROR [mg/L]
$THETA  (0,0.185,3)      ; 7 VIIV_LAG
$THETA  (0,3.85,800)     ; 8 V3 [L]
$THETA  (0,0.883,90)     ; 9 Q [L/h]
$THETA  (0,2.44,10)      ; 10 RIF_CL
$THETA  1 FIX            ; RBN_CL
$THETA  (0,0.984,10)     ; 12 RADIO_LAG
$THETA  (0,1,10) FIX     ; 13 STUDY_BIO
$THETA  (0,1,10) FIX     ; 14 RBN_V
$THETA  (0,0.57,10)      ; 15 SEX_KA
;-----------------------------------------------------------------
$OMEGA  BLOCK(1)
 0.0637  ;   1 BSV CL
$OMEGA  BLOCK(1) FIX
 0  ;    2 BSV V
$OMEGA  BLOCK(1) FIX
 0  ;   3 BSV KA
$OMEGA  BLOCK(1) FIX
 0  ;  4 BSV BIO
$OMEGA  BLOCK(1) FIX
 0  ;    5 BSVV3
$OMEGA  BLOCK(1) FIX
 0  ;     6 BSVQ
;-------------------------------------------------------------------
```

```
247  $OMEGA  BLOCK(1)
248   0.304  ;     7 BOVKA
249  $OMEGA  BLOCK(1) SAME
250  $OMEGA  BLOCK(1) SAME
251  $OMEGA  BLOCK(1) SAME
252  $OMEGA  BLOCK(1) SAME
253  $OMEGA  BLOCK(1) SAME
254  $OMEGA  BLOCK(1) SAME
255  $OMEGA  BLOCK(1) SAME
256  ;-----------------------------------------------------------------
     --
257  $OMEGA  BLOCK(1)
258   0.21   ;  15 BOVLAG
259  $OMEGA  BLOCK(1) SAME
260  $OMEGA  BLOCK(1) SAME
261  $OMEGA  BLOCK(1) SAME
262  $OMEGA  BLOCK(1) SAME
263  $OMEGA  BLOCK(1) SAME
264  $OMEGA  BLOCK(1) SAME
265  $OMEGA  BLOCK(1) SAME
266  ;-----------------------------------------------------------------
     ---
267  $OMEGA  BLOCK(1)
268   0.187  ;  23 BOVBIO
269  $OMEGA  BLOCK(1) SAME
270  $OMEGA  BLOCK(1) SAME
271  $OMEGA  BLOCK(1) SAME
272  $OMEGA  BLOCK(1) SAME
273  $OMEGA  BLOCK(1) SAME
274  $OMEGA  BLOCK(1) SAME
275  $OMEGA  BLOCK(1) SAME
276  ;-----------------------------------------------------------------
     ---
277  $SIGMA  1  FIX
278  ;-----------------------------------------------------------------
     ---
279  $ESTIMATION MSFO=run095.msf MAXEVAL=9999 PRINT=1 METHOD=1 INTER
280              NOABORT NSIG=3 NONINFETA=1 ETASTYPE=1
281
282  $COVARIANCE PRINT=E ;MATRIX=S
283  $TABLE      WRESCHOL ID OCC TIME TAD VPCTIME AA1 AA2
284              Y DV PRED RES WRES IPRED IRES IWRES CWRES CWRESI OBJI
285              NOPRINT NOAPPEND ONEHEADER FILE=sdtab095.csv FORMAT=,
286  $TABLE      ID OCC CL V KA BIO BOVKA BOVBIO BOVLAG
287              ALAG1 BSVCL BSVV BSVKA BSVBIO NOPRINT NOAPPEND
                 ONEHEADER
288              FILE=patab095.csv FORMAT=,
289  $TABLE      ID WT HT AGE FFM FAT NOPRINT NOAPPEND ONEHEADER
290              FILE=cotab095.csv FORMAT=,
291  $TABLE      ID OCC RIF RBN SEX AMT BID RACE GROUP STUDY ARM DOSE
     PHASE
```

```
292                NOPRINT NOAPPEND ONEHEADER FILE=catab095.csv FORMAT=,
293   $TABLE       ID OCC PHASE PANEL PANELB GROUP TIME TAD VPCTIME Y DV
294                AA1 AA2 ALAG1 PRED RES WRES IPRED IRES IWRES CWRES
                   CWRESI
295                OBJI CL V KA BIO BSVCL BSVV BSVKA BSVBIO BOVKA BOVBIO
296                BOVLAG SEX AMT DOSE BID WT HT RIF AGE RACE ARM PHASE
                   PANEL PANELB
297                STUDY RBN FFM FAT NOPRINT NOAPPEND ONEHEADER
298                FILE=mytab095.csv FORMAT=,
299
300
```

Final NONMEM scripts for results presented in **Chapter 6**

```
;; 1. Based on: 190
; One compartment model of Dolutegravir + Rifabutin effect
; Settings for the memory of NONMEM
$SIZES      PD=-1000 LVR=-150 LTH=200 MAXFCN=10000000 LNP4=-150000
$PROBLEM    DTG_RIFAMPICIN_RADIO_VIIV
$INPUT      ID DAT2=DROP TIME AMT DV OCC MDV EVID VPCTIME WT HT
AGE
            SEX STUDY PHASE RIF RBN BID DOSE RACE ARM GROUP WHAT=
            DROP
; IGNORE=@ will skip any line starting with any non-numerical
character
$DATA      vivrad_all_0819.csv IGNORE=@

$SUBROUTINE ADVAN4 TRANS1 ; 2 compartments

;-------------------------------------------------------------------
--
$PK
;----------- Between Subject variability
---------------------------

BSVCL    = ETA(1)
BSVV     = ETA(2)
BSVKA    = ETA(3)
BSVBIO   = ETA(4)
BSVV3    = ETA(5)
BSVQ     = ETA(6)

;---------------------------------Defining Between OCC
variability-----
BOVKA = 0
BOVLAG = 0
BOVBIO = 0

;OCCASION 1
IF (OCC==1) THEN
BOVKA = ETA(7)
BOVLAG= ETA(15)
BOVBIO = ETA(23)
ENDIF

;OCCASION 2
IF (OCC==2) THEN
BOVKA = ETA(8)
BOVLAG = ETA(16)
BOVBIO = ETA(24)
ENDIF

;OCCASION 3
IF (OCC==3) THEN
BOVKA = ETA(9)
BOVLAG = ETA(17)
```

```
47   BOVBIO = ETA(25)
48   ENDIF
49
50   ;OCCASION 4
51   IF (OCC==4) THEN
52   BOVKA = ETA(10)
53   BOVLAG = ETA(18)
54   BOVBIO = ETA(26)
55   ENDIF
56
57   ;OCCASION 5
58   IF (OCC==5) THEN
59   BOVKA = ETA(11)
60   BOVLAG = ETA(19)
61   BOVBIO = ETA(27)
62   ENDIF
63
64   ;OCCASION 6
65   IF (OCC==6) THEN
66   BOVKA = ETA(12)
67   BOVLAG = ETA(20)
68   BOVBIO = ETA(28)
69   ENDIF
70
71   ;OCCASION 7
72   IF (OCC==7) THEN
73   BOVKA = ETA(13)
74   BOVLAG = ETA(21)
75   BOVBIO = ETA(29)
76   ENDIF
77
78   ;OCCASION 8
79   IF (OCC==8) THEN
80   BOVKA = ETA(14)
81   BOVLAG = ETA(22)
82   BOVBIO = ETA(30)
83   ENDIF
84
85   ; -------------- Calculation of Fat-free Mass -------------------
86   ; These formulas require WT in KG and HT in m !!!
87
88   ; Conversion from cm to m
89   HTM = HT/100
90
91   IF (SEX.EQ.0) THEN  ; female
92       WHSMAX = 37.99
93       WHS50  = 35.98
94   ELSE                ; males
95       WHSMAX = 42.92
96       WHS50  = 30.93
97   ENDIF
98
```

```
HTM2 = HTM**2
FFM  = (WHSMAX*HTM2*WT)/(WHS50*HTM2+WT)
FAT  = WT-FFM

; ------- Typical values of covariates--------------------------
TVWT   = 70 ;70KG individual
;TVFAT = 23.98
;TVFFM = 59.10
;--------- Allometric scaling and covariates
ALLMCL_WT = (WT/TVWT)**0.75
ALLMV_WT  = (WT/TVWT)

;ALLMCL_FAT = (FAT/TVFAT)**0.75
;ALLMV_FAT  = (FAT/TVFAT)

;ALLMCL_FFM = (FFM/TVFFM)**0.75
;ALLMV_FFM  = (FFM/TVFFM)

;---------------------Rifampicin EFFECT on CLEARANCE-----
RIF_CL=1
IF (RIF.EQ.1) RIF_CL= THETA(10) ; CO-ADMINISTRATION OF RIF

 ;---------------------Rifabutin EFFECT on CLEARANCE------------
RBN_CL=1
IF (RBN.EQ.1) RBN_CL= THETA(11) ; CO-ADMINISTRATION OF RBN

 ;---------------------Study EFFECT on BIO----------------------
STUDY_BIO=1
IF (STUDY.EQ.2) STUDY_BIO = THETA(13)

;---------------------Rifabutin EFFECT on Volume---------------
RBN_V = 1
IF (RBN.EQ.1) RBN_V= THETA(14) ; CO-ADMINISTRATION OF RBN

;-----------------sex on ka-------------------------------------
SEX_KA=1
IF (SEX.EQ.1) SEX_KA = THETA(15)


;--------- Typical values of the fixed parameters --------------
TVCL = THETA(1) * ALLMCL_WT * RIF_CL * RBN_CL
TVV  = THETA(2) * ALLMV_WT * RBN_V
TVKA = THETA(3) * SEX_KA
TVBIO = THETA(4)* STUDY_BIO

IF (STUDY.EQ.1) TVLAG = THETA(7)
IF (STUDY.EQ.2) TVLAG = THETA(12)

TVV3  = THETA(8) * ALLMV_WT
TVQ   = THETA(9) * ALLMCL_WT
```

```
151  ;-----------Define parameters ------------------------------
152
153  CL  = TVCL*EXP(BSVCL)                ; CLEARANCE
154  V   = TVV*EXP(BSVV)                  ; VOLUME CENTRAL COMPARTMENT
155  KA  = TVKA*EXP(BSVKA+BOVKA)          ; ABSORPTION RATE CONSTANT
156  BIO = TVBIO*EXP(BSVBIO+BOVBIO)       ; BIOAVAILABILITY
157  LAG = TVLAG*EXP(BOVLAG)              ; LAG TIME
158  V3  = TVV3*EXP(BSVV3)                ; PERIPH VOL
159  Q   = TVQ*EXP(BSVQ)                  ; INTER COMPT CL
160
161  ;-------------
     re-parameterization-----------------------------------
162
163  K = CL/V    ;(rate constant of elimination)
164  K23 = Q/V   ;(rate constant from central to peripheral 1)
165  K32 = Q/V3  ;(rate constant from peripheral 1 to central)
166
167  ALAG1 = LAG
168
169  F1 = BIO
170
171  S2 = V
172
173  ;-------------------------------------------------------------------
     -
174
175  $ERROR
176  IPRED=A(2)/V
177
178  ; DEFINE LLOQ for VIIV study
179  IF (STUDY==1) THEN
180  LLOQ = 0.02
181  ENDIF
182
183  ;DEFINE LLOQ for RADIO studyv
184  IF (STUDY==2) THEN
185  LLOQ = 0.05
186  ENDIF
187
188  PROP = IPRED*THETA(5)
189  ADD = THETA(6)+(LLOQ*0.2)
190
191  W = SQRT(ADD**2+PROP**2)
192
193  ; Protective code
194  IF (W.LE.0.000001) W=0.000001
195
196  IRES  = DV-IPRED
197  IWRES = IRES/W
198
199  Y = IPRED + W*ERR(1)
200  ;-------------------------------------------------------------------
```

```
---
; To prevent simulation (ICALL==4) of negative values. It set a positive lower bound for Y, so that VPCs in the log-scale can be plotted
IF (ICALL==4.AND.Y<=0.000001) Y=0.000001

; To calculate time after dose.
IF(AMT.GT.0) THEN
    TIMEDOSE = TIME
    AMOUNTDOSE = AMT

ENDIF

TAD = TIME-TIMEDOSE
;--------------------RETRIEVE AMOUNT IN EACH COMPARTMENT-----------------
AA1 = A(1)
AA2 = A(2)
AA3 = A(3)

;-----------------------------------------------------------------------
--
$THETA  (0,1.03,90)      ; 1 CL [L/h]
$THETA  (0,13.3,800)     ; 2 V [L]
$THETA  (0,1.63,5)       ; 3 KA [1/h]
$THETA  1 FIX            ; 4 BIO
$THETA  (0,0.0885,0.5)   ; 5 PROPORTIONAL ERROR []
$THETA  (0,0.0352,1)     ; 6 ADDITIVE ERROR [mg/L]
$THETA  (0,0.205,3)      ; 7 VIIV_LAG
$THETA  (0,3.52,800)     ; 8 V3 [L]
$THETA  (0,0.675,90)     ; 9 Q [L/h]
$THETA  (0,2.43,10)      ; 10 RIF_CL
$THETA  1 FIX            ; RBN_CL
$THETA  (0,0.986,10)     ; 12 RADIO_LAG
$THETA  (0,1,10) FIX     ; 13 STUDY_BIO
$THETA  (0,0.669,10)     ; 14 RBN_V
$THETA  (0,0.62,10)      ; 15 SEX_KA
;-----------------------------------------------------------------------
----
$OMEGA  BLOCK(1)
 0.0629  ;   1 BSV CL
$OMEGA  BLOCK(1) FIX
 0  ;    2 BSV V
$OMEGA  BLOCK(1) FIX
 0  ;   3 BSV KA
$OMEGA  BLOCK(1) FIX
 0  ;  4 BSV BIO
$OMEGA  BLOCK(1) FIX
 0  ;    5 BSVV3
$OMEGA  BLOCK(1) FIX
 0  ;     6 BSVQ
;-----------------------------------------------------------------------
```

```
---------
$OMEGA  BLOCK(1)
 0.368  ;     7 BOVKA
$OMEGA  BLOCK(1) SAME
$OMEGA  BLOCK(1) SAME
$OMEGA  BLOCK(1) SAME
$OMEGA  BLOCK(1) SAME
$OMEGA  BLOCK(1) SAME
$OMEGA  BLOCK(1) SAME
$OMEGA  BLOCK(1) SAME
;-----------------------------------------------------------------
-----------
$OMEGA  BLOCK(1)
 0.22  ;  15 BOVLAG
$OMEGA  BLOCK(1) SAME
$OMEGA  BLOCK(1) SAME
$OMEGA  BLOCK(1) SAME
$OMEGA  BLOCK(1) SAME
$OMEGA  BLOCK(1) SAME
$OMEGA  BLOCK(1) SAME
$OMEGA  BLOCK(1) SAME
;-----------------------------------------------------------------
----------------
$OMEGA  BLOCK(1)
 0.185  ;  23 BOVBIO
$OMEGA  BLOCK(1) SAME
$OMEGA  BLOCK(1) SAME
$OMEGA  BLOCK(1) SAME
$OMEGA  BLOCK(1) SAME
$OMEGA  BLOCK(1) SAME
$OMEGA  BLOCK(1) SAME
$OMEGA  BLOCK(1) SAME
;-----------------------------------------------------------------
---------------------
$SIGMA  1  FIX
;-----------------------------------------------------------------
----------------------
$ESTIMATION MSFO=run190a.msf MAXEVAL=9999 PRINT=1 METHOD=1 INTER
            NOABORT NSIG=3 NONINFETA=1 ETASTYPE=1 ; REPEAT

$COVARIANCE PRINT=E
$TABLE      WRESCHOL ID OCC TIME TAD VPCTIME AA1 AA2
            Y DV PRED RES WRES IPRED IRES IWRES CWRES CWRESI OBJI
            NOPRINT NOAPPEND ONEHEADER FILE=sdtab190a.csv FORMAT=,
$TABLE      ID OCC CL V KA BIO BOVKA BOVBIO BOVLAG
            ALAG1 BSVCL BSVV BSVKA BSVBIO NOPRINT NOAPPEND
            ONEHEADER
            FILE=patab190a.csv FORMAT=,
$TABLE      ID WT HT AGE FFM FAT NOPRINT NOAPPEND ONEHEADER
            FILE=cotab190a.csv FORMAT=,
$TABLE      ID OCC RIF RBN SEX AMT BID RACE GROUP STUDY ARM DOSE
PHASE
```

```
292                NOPRINT NOAPPEND ONEHEADER FILE=catab190a.csv FORMAT=,
293   $TABLE       ID OCC PHASE GROUP TIME TAD VPCTIME Y DV
294                AA1 AA2 ALAG1 PRED RES WRES IPRED IRES IWRES CWRES
                   CWRESI
295                OBJI CL V KA BIO BSVCL BSVV BSVKA BSVBIO BOVKA BOVBIO
296                BOVLAG SEX AMT DOSE BID WT HT RIF AGE RACE ARM PHASE
                   STUDY
297                RBN FFM FAT NOPRINT NOAPPEND ONEHEADER FILE=
                   mytab190a.csv
298                FORMAT=,
299
300
```

Final NONMEM scripts for results presented in **Chapter 7**

```
;; 1. Based on: run360
;; 2. Description: run360_get AUC
; ADVANCE_Dolutegravir pk and genetics_mixture
; One compartment model of Dolutegravir
; Settings for the memory of NONMEM
$SIZES      PD=-1000 LVR=-150 LTH=-200 MAXFCN=10000000 LNP4=
-150000
$PROBLEM    ADVANCE intense

$INPUT      ID  DAT2=DROP   TIME DV AMT VPCTIME BLQ SS  II  MDV
EVID OCC COUNTRY
            INSPA SEX AGE   WT  HT  DOSE SPARSE GENO GENOTYPECODE
            =DROP GENOTYPE=DROP
            RANID=DROP WHAT=DROP PKWEEK=DROP WHATSAMP=DROP
            SPECIMENDATE=DROP SPECIMENTIME=DROP
            DTGNGML=DROP DTGMGL=DROP SPECIMENID=DROP VID=DROP GRP
            =DROP  PID2=DROP FID=DROP

$DATA      finaljoint2_dec2021.csv IGNORE=@


;IGNORE=(week.GT.2) ;IGNORE=(PROBLEM.GT.0)
IGNORE=(OCC.GT.2)DATASET_FILE.csv IGNORE=@ ;IGNORE=(PROBLEM.GT.0)
;$ABBREVIATED COMRES=2
$SUBROUTINE ADVAN5 TRANS1 ;TOL=9  ATOL=12 ; TOL is the precision
to solve differential equations
$ABB DERIV2=NO

$MODEL        NCOMPS=8 ; NUMBER OF COMPARTMENTS (ABSORPTION
COMPATMENT (DEFINED AS FIRST ONE) AND CENTRAL COMPARTMENT
DEFIEND AS 2ND COMPARTMENT
              COMP=(TRANSIT1,DEFDOSE) ;1 GUT TRANIST 1 (F1 is
              associated with first compartment)
                    COMP=(TRANSIT2)    ;2 GUT TRANIST 2
                    COMP=(TRANSIT3)    ;3 GUT TRANIST 3
                    COMP=(TRANSIT4)    ;4 GUT TRANIST 4
                    COMP=(TRANSIT5)    ;5 GUT TRANIST 5
              COMP=(ABS)               ;6 GUT ABS
              COMP=("CENTRAL",DEFOBS) ;7 CENTRAL CMT
              COMP=(PERI1)             ;8 PERIPHERAL CMT

;-----------------mixture modelling (3-subpop mixture);
; Wild type, Heterozygous, Homozygous
;Sim_start
$MIX
NSPOP=3       ; number of subpopulations (genotypes)

P(1) = THETA(13)  ; probability of SPOP 1, wildtype
P(2) = THETA(14)  ; probability of SPOP 2, Heterozygous
P(3) = THETA(15)  ; probability of SPOP 3, Homozygous
;Sim_end

```

```
$PK
; ------------ Between Subject variability
-----------------------------

BSVCL    = ETA(1)
BSVV     = ETA(2)
BSVKA    = ETA(3)
BSVBIO   = ETA(4)
BSVV3    = ETA(5)
BSVQ     = ETA(6)


;Defining Between OCC
variability-----------------------------------------
BOVKA = 0
BOVMTT = 0
BOVBIO = 0

;OCCASION 1
IF (OCC==1) THEN
BOVKA = ETA(7)
BOVMTT = ETA(11)
BOVBIO = ETA(15)
ENDIF

;OCCASION 2
IF (OCC==2) THEN
BOVKA = ETA(8)
BOVMTT = ETA(12)
BOVBIO = ETA(16)
ENDIF

;OCCASION 3
IF (OCC==3) THEN
BOVKA = ETA(9)
BOVMTT = ETA(13)
BOVBIO = ETA(17)
ENDIF

;OCCASION 4
IF (OCC==4) THEN
BOVKA = ETA(10)
BOVMTT = ETA(14)
BOVBIO = ETA(18)
ENDIF

; -------------- Calculation of Fat-free Mass
----------------------------
; These formulas require WT in KG and HT in m !!!

; Conversion from cm to m
HTM = HT  ;/100
```

```
92
93   IF (SEX.EQ.0) THEN  ; female
94       WHSMAX = 37.99
95       WHS50  = 35.98
96   ELSE                ; males
97       WHSMAX = 42.92
98       WHS50  = 30.93
99   ENDIF
100
101  HTM2 = HTM**2
102  FFM  = (WHSMAX*HTM2*WT)/(WHS50*HTM2+WT)
103  FAT  = WT-FFM
104
105
106  ; ------- Typical values of
     covariates--------------------------------------
107  TVWT  = 73.1 ;Median weight in my population
108  TVFAT = 25.44
109  TVFFM = 47.12
110  ;--------- Allometric scaling and covariates
111  ;ALLMCL_WT = (WT/TVWT)**0.75
112  ;ALLMV_WT  = (WT/TVWT)
113
114  ;ALLMCL_FAT = (FAT/TVFAT)**0.75
115  ;ALLMV_FAT  = (FAT/TVFAT)
116
117  ALLMCL_FFM = (FFM/TVFFM)**0.75
118  ALLMV_FFM  = (FFM/TVFFM)
119
120  ;---------mixture-----------------------------------------------------
     -----------
121
122  GENETICS = GENO
123
124  ;Sim_start
125  IF(GENO.GT.4 .AND. MIXNUM.EQ.1) GENETICS = 1
126  IF(GENO.GT.4 .AND. MIXNUM.EQ.2) GENETICS = 2
127  IF(GENO.GT.4 .AND. MIXNUM.EQ.3) GENETICS = 3
128  ;Sim_end
129
130  ;---------Typical values of
     clearance--------------------------------------
131  IF (GENETICS.EQ.1) TVCL_GENO = 1         ;TVCL for subpopulation
     1 (Wildtype)
132  IF (GENETICS.EQ.2) TVCL_GENO = THETA(11) ;TVCL for subpopulation
     2 (Heterozygous)
133  IF (GENETICS.EQ.3) TVCL_GENO = THETA(12) ;TVCL for subpopulation
     3 (homozygous)
134
135
136  ;--------- Typical values of the fixed parameters
     ----------------------------
```

```
TVCL = THETA(1) * ALLMCL_FFM * TVCL_GENO
TVV  = THETA(2) * ALLMV_FFM
TVKA = THETA(3)
TVBIO = THETA(4)
TVMTT = THETA(7)
TVV3  = THETA(8) * ALLMV_FFM
TVQ   = THETA(9) * ALLMCL_FFM
TVNN  = THETA(10)

;-----------------------------------------------------------------------------
CL  = TVCL*EXP(BSVCL)            ; CLEARANCE
V   = TVV*EXP(BSVV)              ; VOLUME CENTRAL COMPARTMENT
KA  = TVKA*EXP(BSVKA+BOVKA)      ; ABSORPTION RATE CONSTANT
BIO = TVBIO*EXP(BSVBIO+BOVBIO)   ; BIOAVAILABILITY
MTT = TVMTT*EXP(BOVMTT)          ; MTT TIME
V3  = TVV3*EXP(BSVV3)            ; PERIPH VOL
Q   = TVQ*EXP(BSVQ)
NN  = TVNN                      ; Number of transit compartments

;-----------re-parameterization-----------------------------------
---------------
F1  = BIO
KTR = (NN+1)/MTT
K12 =   KTR   ;Rate between transit CMT
K23 =   KTR   ;Rate between transit CMT
K34 =   KTR   ;Rate between transit CMT
K45 =   KTR   ;Rate between transit CMT
K56 =   KTR   ;Rate between transit CMT
K67 =   KA
K70 =  CL/V  ;(rate constant of elimination)
K78 =  Q/V   ;(rate constant from central to peripheral 1)
K87 =  Q/V3  ;(rate constant from peripheral 1 to central)
;S7  =  V

;-----------------------------------------------------------------------------
--------------------
$ERROR

IPRED=A(7)/V

LLOQ = 0.03
CENS_THR = LLOQ  ;CENS_THR =0.3*LLOQ    ; check the readme section

PROP = IPRED*THETA(5)
ADD = THETA(6)+(LLOQ*0.2)

; For CENS==1 (i.e. first CENSORED value in a series, which was
imputed to CENS_THR/2), we add extra additive error on the
concentrations,
; since the value in DV has been imputed and therefore more
uncertain.
```

```
IF (ICALL/=4.AND.BLQ==1) THEN
    ADD = ADD +(CENS_THR*0.5)
ENDIF

NO_FIT = 0
; For CENS==2 (i.e. the trailing CENSORED values in a series that were imputed to CENS_THR/2), we don't want these to influence the fit,
; we only want them for simulation-based diagnostics such as the VPC.
; So we define a separate error structure for these points. It has no proportional component
; (PROP = 0, as we would not want these points to affect our estimate of proportional error)
; and a FIXED and HUGE additive component (ADD = 1000000000, large with respect to the readings of concentration),
; so that the values do not affect the fit. It's also a good idea to repeat the diagnostic plots without the CENS=2 points

IF (ICALL/=4.AND.BLQ==2) THEN
    PROP = 0
    ADD = 10000000000
    NO_FIT = 1
ENDIF


W = SQRT(ADD**2+PROP**2)

; Protective code
IF (W.LE.0.000001) W=0.000001

IRES=DV-IPRED
IWRES=IRES/W

Y = IPRED + W*ERR(1)

; To prevent simulation (ICALL==4) of negative values. It set a positive lower bound for Y, so that VPCs in the log-scale can be plotted
IF (ICALL==4.AND.Y<=CENS_THR) Y = CENS_THR/2


; To calculate time after dose.
IF(AMT>0) THEN
    TIMEDOSE = TIME
    AMOUNTDOSE = AMT
ENDIF

TAD = TIME-TIMEDOSE

AUC_INF = AMOUNTDOSE*BIO/CL

```

```
;-------------------------------------------------------------------
------------
;Sim_start
MIX_POP = MIXEST
MIX_PROB = MIXP
;Sim_end

;-------------------------------------------------------------------
---------------

VARCL  = BSVCL ;+ BOVCL
VARBIO = BSVBIO + BOVBIO
VARAUC = BSVBIO + BOVBIO - BSVCL ;- BOVCL

;------------------RETRIEVE AMOUNT IN EACH COMPARTMENT------
AA1 = A(6) ; ABS CMT
AA2 = A(7) ; CENTRAL CMT
AA3 = A(8)

CONC_MOD = A(7)/V
;-------------------------------------------------------------------
----

$THETA
(0, 0.786,90)    ; 1 CL [L/h]
(0, 10.5,800)    ; 2 V [L]
(0, 1.67,5)      ; 3 KA [1/h]
(1) FIX          ; 4 BIO
(0, 0.0752,0.5) ; 5 PROPORTIONAL ERROR []
(0, 0.18,10)     ; 6 ADDITIVE ERROR [mg/L]
(0, 0.18,3)      ; 7 MTT
(0, 3.77,800)    ; 8 V3 [L]
(0, 1.29,90)     ; 9 Q [L/h]
(5) FIX          ; 10 NN
(-0.99, 0.892,10)    ; 11 HETERO
(-0.99, 0.741,10)    ; 12 HOMOZY
(0, 0.33,1) FIX      ; 13 Wild_PROB
(0, 0.5,1) FIX       ; 14 HETE_PROB
(0, 0.17,1) FIX      ; 15 HOMO_PROB

;---------------------------------BSV---------------------------
----------
$OMEGA  BLOCK(1)
 0.0781 ;    1 BSV CL
$OMEGA  BLOCK(1) FIX
 0    ;     2 BSV V
$OMEGA  BLOCK(1) FIX
 0   ;    3 BSV KA
$OMEGA  BLOCK(1) FIX
 0    ;    4 BSV BIO
$OMEGA  BLOCK(1) FIX
 0    ;     5 BSVV3
```

```
$OMEGA  BLOCK(1) FIX
 0  ;      6 BSVQ
;----------------------------------------BOV----------------------
-------------
$OMEGA  BLOCK(1)
 0.368 ;     7 BOVKA
$OMEGA  BLOCK(1) SAME
$OMEGA  BLOCK(1) SAME
$OMEGA  BLOCK(1) SAME
;---------------------------------------------------------------------
---------------
$OMEGA  BLOCK(1)
 3.38 ;  11 BOVMTT
$OMEGA  BLOCK(1) SAME
$OMEGA  BLOCK(1) SAME
$OMEGA  BLOCK(1) SAME
;---------------------------------------------------------------------
----------------
$OMEGA  BLOCK(1)
 0.15 ;  15 BOVBIO
$OMEGA  BLOCK(1) SAME
$OMEGA  BLOCK(1) SAME
$OMEGA  BLOCK(1) SAME
;---------------------------------------------------------------------
----------------

$SIGMA 1 FIX
;---------------------------------------------------------------------
----------------
;Sim_start

$ESTIMATION MSFO=run361.msf MAXEVAL=0 PRINT=1 METHOD=1 INTER
NOABORT NSIG=3 SIGL=9 ; RULES for precision SIGL=<TOL AND
NSIG=<SIGL/3
NONINFETA=1 ETASTYPE=1 ; REPEAT ;
;As the model becomes more complex, you can use MATRIX=S and
then remove the $COVARIANCE step completely when the model is
too complex to obtain precisions
;$COVARIANCE PRINT=E ; MATRIX=S
$TABLE WRESCHOL ID OCC TIME TAD VPCTIME AA1 AA2 CONC_MOD
AA3 Y DV PRED RES WRES IPRED IRES IWRES CWRES CWRESI OBJI
NOPRINT NOAPPEND ONEHEADER FILE=sdtab361.csv FORMAT=,
$TABLE ID OCC CL V KA MTT NN AUC_INF
BIO BOVKA BOVBIO BOVMTT BSVCL BSVV BSVKA BSVBIO
VARBIO SPARSE INSPA EVID MDV NOPRINT NOAPPEND ONEHEADER FILE=
patab361.csv
FORMAT=,
$TABLE ID OCC WT HT FFM FAT AGE NOPRINT NOAPPEND
ONEHEADER FILE=cotab361.csv FORMAT=,
$TABLE ID OCC SEX GENO GENETICS NOPRINT NOAPPEND ONEHEADER FILE=
catab361.csv
FORMAT=,
```

```
$TABLE ID OCC TIME TAD VPCTIME Y DV AA1 AA2 BOVKA
BOVBIO BOVMTT PRED RES WRES IPRED IRES IWRES CWRES CWRESI
OBJI CL SPARSE V KA BIO BSVCL BSVV BSVKA AUC_INF
BSVBIO SEX GENO EVID MDV GENETICS INSPA MIX_POP MIX_PROB WT AGE
BLQ NOPRINT
NOAPPEND ONEHEADER FILE=mytab361.csv FORMAT=,
;Sim_end
```

Final NONMEM scripts for results presented in **chapter 8**

```
;; 1. Based on: run383
;Tenofovir PK
;Using general linear model (advan5) to implement transit ABSORPTION
;each tranist is hard coded, much faster when compared with ADVAN6, or 13
;Settings for the memory of NONMEM
$SIZES      PD=-1000 LVR=-150 LTH=-200 MAXFCN=10000000 LNP4=-150000
;-------------------------------------------------------------------
$PROBLEM    Two absorption routes for TAF
;-------------------------------------------------------------------
;you need to drop CMT data item
$INPUT      ID DAT2=DROP TIME VPCTIME DV AMT CMT OCC ADDL II MDV EVID VID
            RX RX2 WT HT SEX GENTEST BLQTFV CENS OUT REMOVE MODPRED CRCL ABOVE4
           TFVNGML=DROP DVNGML=DROP WEEKONRX=DROP TFV_CONC=DROP DOSEDATE=DROP DOSETIME=DROP
           VPCTIMEBIG=DROP RANID RXCODE=DROP LABID=DROP SPECIMENID=DROP RECEIVEDDATE=DROP
           SGSID=DROP VISITDATE=DROP CHECKDATE=DROP CHECK2=DROP TFV_CON_WK24=DROP
           CRTCLEA_WK24=DROP TFV_CONC_WK48=DROP CRTCLEA_WK48=DROP TFV_CONC_WK36=DROP
           CRTCLEA_WK36=DROP TAGCWRESI=DROP TAGCWRES=DROP

;-------------------------------------------------------------------

$DATA       TFV_sparsepk_ADDL_220303.csv IGNORE=@
            IGNORE=(REMOVE.EQ.1) ;IGNORE=(ABOVE4.EQ.1)
            IGNORE=(BLQTFV.EQ.1)


;-------------------------------------------------------------------
$SUBROUTINE ADVAN5 TRANS1 ;TOL=9 ATOL=9 ;SSTOL=6 SSATOL=6
$ABBREVIATED DERIV2=NO ; Prevents  the computation of second derivatives,which are needed only for the Laplacian method.
;----------------------------------------------------
$MODEL

NCOMPARTMENTS=5                              ; NUMBER OF COMPARTMENTS (ABSORPTION COMPATMENT (DEFINED AS FIRST ONE)
             COMP=(DEPOT1,DEFDOSE)           ;1.Dosing compartment for TDF
             COMP=(DEPOT2)                   ;2.Dosing compartment for TAF
             COMP=(CENTRAL DEFOBSERVATION)   ;3.Central compartment
```

```
35              COMP=(PERI1)                    ;4.Peripheral
                compartment 1
36              COMP=(TRANSIT1)                 ;5.This is the
                "cells" compartment (transit, doesnt have a volume)
37
38  $PK
39  ;Defining ETA's
40  ;BETWEEN SUBJETS VARIABILITY---------------------------------------
41  BSVCL  = ETA(1)
42  BSVV   = ETA(2)
43  BSVKA  = ETA(3)
44  BSVBIO = ETA(4)
45  BSVV3  = ETA(5)
46  BSVQ   = ETA(6)
47  BSVKS  = ETA(7)
48
49  ;Defining Between OCC VARIABILITY-----------------------------
50
51  BOVCL           = 0
52  BOVBIO_TDF      = 0
53  BOVKA_TDF       = 0
54  BOVLAG          = 0
55  BOVFFAST        = 0
56  BOVKA_TAF       = 0
57  BOVLAG2_TAF     = 0
58  BOVBIO_TAF      = 0
59
60  ;OCCASION 1
61  IF (OCC==1) THEN
62      BOVCL           = ETA(8)
63      BOVBIO_TDF      = ETA(10)
64      BOVKA_TDF       = ETA(12)
65      BOVLAG          = ETA(14)
66      BOVFFAST        = ETA(16)
67      BOVKA_TAF       = ETA(18)
68      BOVLAG2_TAF     = ETA(20)
69      BOVBIO_TAF      = ETA(22)
70  ENDIF
71
72  ;OCCASION 2
73  IF (OCC==2) THEN
74      BOVCL           = ETA(9)
75      BOVBIO_TDF      = ETA(11)
76      BOVKA_TDF       = ETA(13)
77      BOVLAG          = ETA(15)
78      BOVFFAST        = ETA(17)
79      BOVKA_TAF       = ETA(19)
80      BOVLAG2_TAF     = ETA(21)
81      BOVBIO_TAF      = ETA(23)
82  ENDIF
83
84  ; Calculation of Fat-free
```

```
      Mass-------------------------------------------------------
 85   ; These formulas require WT in KG and HT in m !!!
 86   ; Conversion from cm to m
 87   HTM = HT;/100      ;my height is already in meters
 88   ;HTM = HEIGHT
 89
 90   IF (SEX.EQ.0) THEN  ; female
 91       WHSMAX=37.99
 92       WHS50=35.98
 93   ELSE         ;males
 94       WHSMAX=42.92
 95       WHS50=30.93
 96   ENDIF
 97   HTM2 = HTM**2
 98   FFM = (WHSMAX*HTM2*WT)/(WHS50*HTM2+WT)
 99   FAT = WT-FFM
100
101   ; Typical values of
      covariates-------------------------------------------------------
102   TVWT = 70
103   TVFAT = 22.4
104   TVFFM = 56.1
105
106   ;Allometric scaling and
      covariates-----------------------------------------------------
107
108   ALLMCL_WT = (WT/TVWT)**(0.75)
109   ALLMV_WT = (WT/TVWT)
110
111   ALLMCL_FAT = (FAT/TVFAT)**(0.75)
112   ALLMV_FAT = (FAT/TVFAT)
113
114   ALLMCL_FFM = (FFM/TVFFM)**(0.75)
115   ALLMV_FFM = (FFM/TVFFM)
116
117   PER_FAT = (FAT/WT)*(100)
118
119
120   ;---------Typical values-----------------------------------------
121
122   TVCL      = THETA(1)*ALLMCL_WT       ;Clearance Typical Value
      WITH ALLOMETRIC SCALING
123   TVV       = THETA(2)*ALLMV_WT        ;Volume Typical Value WITH
      ALLOMETRIC SCALLING
124   TVKA_TDF  = THETA(3)                 ;KA of TDF_ARM
125   TVKA_TAF  = THETA(10)                ;KA of TAF_ARM
126   TVBIO_TDF = THETA(4)                 ;Bioavailabiliy of tfv that
      gets to the blood stream for the TDF_ARM (FIX to 1)
127   TVBIO_TAF = THETA(11)                ;Bioavailabiliy of tfv that
      gets to the blood stream for the TAF_ARM (estimate relaive to 1)
128   TVLAG     = THETA(7)                 ;Absorption lag time of
      DEPOT1
```

```
129   TVLAG2_TAF = THETA(12)                ;Absorption lag time of
      DEPOT2
130   TVV3       = THETA(8)*ALLMV_WT        ;Peripheral Volume
131   TVQ        = THETA(9)*ALLMCL_WT       ;Inter-compartmental
      clearance
132
133   ;------SLOWER ABSORPION COMPONENTS FOR TAF
      ARM-----------------------------------------------------
134
135   TVFFAST    = THETA(13)            ;fracion of bioavailability
      readily absorbed, fraction must be between 0 and 1
136   TVKS_HALF = THETA(14)*24          ;halflife of transfer of drug
      from cells to central compartment
137   TVKS       = LOG(2)/TVKS_HALF     ;KS typical value in days
138
139
140   ;------Logit transform FFAST so we can add variability on
      it,remember it must be maintained between 0 and 1 -----------------
141
142   LOGITTVFFAST = LOG(TVFFAST/(1-TVFFAST))      ;logit of TVFFAST
143   LOGITFFAST   = LOGITTVFFAST + (BOVFFAST)     ;add variability in
      the logit space for FFAST
144   FRACFAST     = 1/(1+EXP(-LOGITFFAST))        ;Then turn logit
      back to normal space. This is the fracion absorbed quickly
145   FRACSLOW     = 1-FRACFAST                    ;This is the fracion
      absorbed slowly
146
147   ;-----------Define
      parameters-----------------------------------------------------------
      --------
148   CL       = TVCL * EXP(BOVCL+BSVCL)           ; CLEARANCE
149   V        = TVV * EXP(BSVV)                   ; CENTRAL VOL.
150   V3       = TVV3 * EXP(BSVV3)                 ; PERIPH VOL
151   Q        = TVQ * EXP(BSVQ)                   ; INTER COMPT CL
152   LAG      = TVLAG * EXP(BOVLAG)               ; LAG TIME of
      KA_TDF
153   LAG2     = TVLAG2_TAF * EXP(BOVLAG2_TAF)     ; LAG TIME of KA_TAF
154   KS       = TVKS*EXP(BSVKS)                   ; KS in days
155
156   ;-------KA,BIO parameter per
      ARM-----------------------------------------------------
157
158   KA_TAF = TVKA_TAF * EXP(BSVKA + BOVKA_TAF)            ; KA_TAF
159   KA_TDF = TVKA_TDF * EXP(BSVKA + BOVKA_TDF)            ; KA_TDF
160
161   BIO_TAF = TVBIO_TAF * EXP(BSVBIO + BOVBIO_TAF)   ; BIO_TDF arm,
      goes to F1 (DEPOT1)
162   BIO_TDF = TVBIO_TDF * EXP(BSVBIO + BOVBIO_TDF)    ; BIO_TAF arm,
      goes to F2 (DEPOT2
163
164   ;---------Reparametrarize_rate
      constants-----------------------------------------------------------
```

```
      -----------
165   F1   = BIO_TDF
166   F2   = BIO_TAF
167   ALAG1 = LAG
168   ALAG2 = LAG2
169   K13 =    KA_TDF               ; TDF rate of absorpion between
      DEPOT1 and central CMT
170   K34 =    Q/V                  ; Rate between Central to
      Peripheral CMT
171   K43 =    Q/V3                 ; Rate between Peripheral to
      Central CMT
172   K23 =    KA_TAF * FRACFAST    ; TAF rate OF absorption from
      DEPOT2 direcl to central CMT
173   K25 =    KA_TAF * FRACSLOW    ; TAF rate OF absorption from
      DEPOT2 to the "CELLS compartment" should also be equal to KA
174   K53 =    KS                   ; Rate between Cells and Central
      compartment  ; The cells are represented by transit compartment
175   K30 =    CL/V                 ; Actual elimination
176
177
178   ;;;-----------Initialize
      compartments-----------------------------------------------------
179   A_0(1) = 1E-12
180   A_0(2) = 1E-12
181   A_0(3) = 1E-12
182   A_0(4) = 1E-12
183   A_0(5) = 1E-12
184
185   ;;;---------------------------------------------------------------
      ------------------------
186
187   $ERROR
188
189   IPRED=A(3)/V
190
191   LLOQ = 0.0005
192
193   CENS_THR = LLOQ  ;CENS_THR =0.3*LLOQ    ; check the readme section
194
195   PROP = IPRED*THETA(5)
196
197   ADD = THETA(6)+(LLOQ*0.2)
198
199
200   ; For CENS==1 (i.e. first CENSORED value in a series, which was
      imputed to CENS_THR/2), we add extra additive error on the
      concentrations,
201   ; since the value in DV has been imputed and therefore more
      uncertain.
202   IF (ICALL/=4.AND.CENS==1) THEN
203       ADD = ADD +(CENS_THR*0.5)
204   ENDIF
```

```
205
206   NO_FIT = 0
207   ; For CENS==2 (i.e. the trailing CENSORED values in a series
      that were imputed to CENS_THR/2), we don't want these to
      influence the fit,
208   ; we only want them for simulation-based diagnostics such as the
      VPC.
209   ; So we define a separate error structure for these points. It
      has no proportional component
210   ; (PROP = 0, as we would not want these points to affect our
      estimate of proportional error)
211   ; and a FIXED and HUGE additive component (ADD = 1000000000,
      large with respect to the readings of concentration),
212   ; so that the values do not affect the fit. It's also a good
      idea to repeat the diagnostic plots without the CENS=2 points
213
214   IF (ICALL/=4.AND.CENS==2) THEN
215       PROP = 0
216       ADD = 10000000000
217       NO_FIT = 1
218   ENDIF
219
220
221   W = SQRT(ADD**2+PROP**2)
222
223   ; Protective code
224   IF (W.LE.0.000001) W=0.000001
225
226   IRES=DV-IPRED
227   IWRES=IRES/W
228
229   Y = IPRED + W*ERR(1)
230
231   ; To prevent simulation (ICALL==4) of negative values. It set a
      positive lower bound for Y, so that VPCs in the log-scale can be
      plotted
232   IF (ICALL==4.AND.Y<=CENS_THR) Y = CENS_THR/2
233
234
235   ; To calculate time after dose.
236   IF(AMT>0) THEN
237       TIMEDOSE = TIME
238       AMOUNTDOSE = AMT
239   ENDIF
240
241   TAD = TIME-TIMEDOSE
242
243   ;---------------calculate variability in
      AUC-----------------------------------------------
244   ;VARCL  = BSVCL + BOVCL
245   ;VARBIO = BSVBIO + BOVBIO
246   ;VARABS = BOVKA + BSVKA - BOVLAG ;-BSVMTT - BOVMTT
```

```
247
248   VARAUC = BSVBIO + BOVBIO_TDF - BSVCL - BOVCL                ;TDF
      arm
249   IF(RX.EQ.2)VARAUC = BSVBIO + BOVBIO_TAF - BSVCL - BOVCL     ;TAF
      arm
250   ;------------- calculate AUC
      -----------------------------------------------------------------
251
252   AUC_INF_BIO = AMOUNTDOSE*BIO_TDF/CL                         ;TDF
      arm
253   IF(RX.EQ.2) AUC_INF_BIO = AMOUNTDOSE*BIO_TAF/CL             ;TAF
      arm
254
255
256   ;----------------------------------------RETRIEVE AMOUNT IN
      EACH COMPARTMENT-----------
257   AA1 = A(1) ; DEPOT1
258   AA2 = A(2) ; DEPOT2
259   AA3 = A(3) ; CENTRAL CMT
260   AA4 = A(4) ; PERIPHERAL CMT
261   AA5 = A(5) ; CELLS CMT
262   ;-----------------------------------------------------------------
      ------------------
263   ;initialization-of-theta(S)-------------------------------------
      ---------------
264
265   $THETA
266   (0, 44.7,250)    ; 1 CL [L/h]
267   (20, 378,4000)   ; 2 V [L]
268   (0, 3.04,100)    ; 3 KA_TDF [1/h]
269   (1) FIX          ; 4 BIO_TDF
270   (0, 0.119,50)    ; 5 PROP []
271   (0) FIX          ; 6 ADD [mg/L]
272   (0) FIX          ; 7 LAG1
273   (0, 356,10000)   ; 8 V3 [L]
274   (0, 157,900)     ; 9 Q [L/h]
275   (0, 1.45,10)     ; 10 KA_TAF [1/h]
276   (0, 0.822)       ; 11 BIO_TAF
277   (0, 0,25) FIX    ; 12 LAG2_TAF
278   (0, 0.324,0.99) ; 13 FRACFAST_TAF
279   (1, 6.83,200) FIX ; 14 KS_HALF [days]
280
281   $OMEGA BLOCK(1) 0.0404 ;1  BSVCL
282   $OMEGA  BLOCK(1) FIX
283    0    ;     2 BSVV
284   $OMEGA  BLOCK(1) FIX
285    0    ;    3 BSVKA
286   $OMEGA  BLOCK(1) FIX
287    0    ;    4 BSVBIO
288   $OMEGA  BLOCK(1) FIX
289    0    ;    5 BSVV3
290   $OMEGA  BLOCK(1) FIX
```

```
 0   ;   6 BSVQ
$OMEGA  BLOCK(1) FIX
 0   ;   7 BSVKS

;----------BOV---------------------------------------------------
-----------------------
$OMEGA  BLOCK(1) FIX
 0  ;    8 BOVCL
$OMEGA  BLOCK(1) SAME
;---------------------------------
$OMEGA  BLOCK(1)
 0.0569 ;   10 BOVBIO_TDF
$OMEGA  BLOCK(1) SAME
;---------------------------------
$OMEGA  BLOCK(1)
 1.31 ; 12 BOVKA_TDF
$OMEGA  BLOCK(1) SAME
;---------------------------------
$OMEGA  BLOCK(1) FIX
 0   ;  14 BOVLAG
$OMEGA  BLOCK(1) SAME
;---------------------------------
$OMEGA  BLOCK(1) FIX
 0   ; 16 BOVFFAST
$OMEGA  BLOCK(1) SAME
;---------------------------------
$OMEGA  BLOCK(1)
 0.439 ; 18 BOVKA_TAF
$OMEGA  BLOCK(1) SAME
;---------------------------------
$OMEGA  BLOCK(1) FIX
 0   ;  20 BOVLAG2_TAF
$OMEGA  BLOCK(1) SAME
;---------------------------------
$OMEGA  BLOCK(1) FIX
 0   ; 22 BOVBIO_TAF
$OMEGA  BLOCK(1) SAME
;-----------------------------------------------------------------

$SIGMA 1 FIX
;-----------------------------------------------------------------
--

$ESTIMATION MSFO=run384.msf MAXEVAL=9999 PRINT=1 METHOD=1 INTER
NOABORT NSIG=3 NONINFETA=1 ETASTYPE=1 ; REPEAT

$COVARIANCE PRINT=E ; MATRIX=S

;---------------------------------------------------------
$TABLE WRESCHOL ID OCC TIME VPCTIME TAD AA1 AA2 AA3 AA4 AA5 Y DV
PRED
RES WRES IPRED IRES IWRES CWRESI CWRES OBJI NOPRINT
```

```
340  NOAPPEND ONEHEADER FORMAT=, FILE=sdtab384.csv
341  ;------------------------------------------------------------------
     -----
342  $TABLE ID OCC CL V KA_TDF KA_TAF KS ALAG1 ALAG2 V3 Q BSVCL BSVV
343  BSVKA BSVBIO BOVFFAST BSVV3 BSVQ BOVLAG BOVBIO_TAF BOVLAG2_TAF
     BOVCL BOVKA_TDF
344  BOVKA_TAF BOVBIO_TDF BSVKS FRACSLOW FRACFAST VARAUC
345  NOPRINT NOAPPEND ONEHEADER FORMAT=, FILE=patab384.csv
346  ;------------------------------------------------------------------
     -
347  $TABLE ID OCC WT HT FFM CRCL FAT NOPRINT NOAPPEND ONEHEADER
348  FORMAT=, FILE=cotab384.csv
349  ;------------------------------------------------------------------
     -----
350  $TABLE ID OCC SEX RX NOPRINT NOAPPEND ONEHEADER FORMAT=,
351  FILE=catab384.csv
352  ;------------------------------------------------------------------
     -------------
353  $TABLE ID OCC TIME AMT VPCTIME TAD AA1 AA2 AA3 AA4 AA5 Y DV PRED
     RES WRES
354  IPRED IRES IWRES CWRESI CWRES OBJI VARAUC AUC_INF_BIO MODPRED CL
     V F1 F2 KA_TDF KA_TAF KS
355  FRACSLOW FRACFAST ALAG1 ALAG2 V3 Q BSVCL BSVV
356  BSVKA BOVKA_TDF BOVKA_TAF BSVBIO BOVBIO_TAF BOVLAG2_TAF BSVV3
     BSVQ BOVCL BOVBIO_TDF
357  BOVLAG BSVKS WT HT FFM FAT RANID ;VARCL VARBIO VARAUC
358  SEX RX NOPRINT NOAPPEND ONEHEADER FORMAT=,
359  FILE=mytab384.csv
360
```